FINAL REPORT

CHARACTERIZATION OF THE ADSORPTION OF WATER VAPOR AND CHLORINE ON MICROCRYSTALLINE SILICA

by

Jean Ann Skiles and James P. Wightman

Prepared for

National Aeronautics and Space Administration

February, 1979

Grant NSG-1389

NASA-Langley Research Center
Hampton, Virginia 23665
Space Applications and Technology Division
Dr. Gerald L. Pellett

Department of Chemistry
Virginia Polytechnic Institute and State University
Blacksburg, Virginia 24061

TABLE OF CONTENTS

Chapter Page

LIST OF TABLES

LIST OF FIGURES

Figure Page

Figure Page

CHAPTER I

INTRODUCTION

The NASA Space Shuttle uses a solid rocket propellant composed of an ammonium perchlorate oxidizer, powdered aluminum and other additives contained in a polybutadiene binder (1). The predicted exhaust composition of the propellant is: 30.2% Al_2O_3, 20.9% HCl, 9.4% H_2O, 24.2% CO, 3.4% CO_2, 2.5% H_2, 8.7% N_2 and 0.6% $FeCl_3$ (2). The predicted exhaust composition of HCl was based upon the presence of chlorine atoms in the exhaust effluent. These chlorine atoms may react to form HCl or Cl_2. Of the total chlorine produced, 95% results in HCl and 5% in Cl_2 (3).

During the launch phase of the space shuttle, considerable ground debris, which contains principally silica, is swept upwards into the atmosphere. Water vapor from the atmosphere and gaseous exhaust products could adsorb onto the silica surface. Hydrogen chloride gas or molecular chlorine could also adsorb onto the silica and be removed from the atmosphere.

The objective of this research was to study the adsorption of water and chlorine on Min-U-Sil, a model silica. The characterization of water adsorption on silica is necessary to an understanding of how hydrogen chloride interacts with silica. The adsorption was studied as a function of outgas temperatures of silica and as a function of the isotherm temperature. Related studies performed included: characterization of the silica structure by infrared analysis, X-ray diffraction and differential scanning calorimetry,

surface area determinations, characterization of the sample surface by electron spectroscopy for chemical analysis (ESCA), and determinations of the heat of immersion in water of silica. In addition, the silica was examined with a scanning electron microscope.

CHAPTER II

REVIEW OF THE LITERATURE

A. Structures of Silica

Silicon dioxide or silica is a chemical compound with 46.72% silicon and 53.28% oxygen by weight. Sixty percent of the earth's crust is composed of silica, which occurs in three polymorphic forms and also in combination with three other oxides as silicates. If molten silica is supercooled or solid silica is heated until it softens, it becomes a random arrangement of polymorphic chains; this form of silica is amorphous and vitreous. The presence of silica, an acidic compound, in biological processes is limited and predominately found in primitive life such as horsetail plants and diatoms (4).

The crystalline, polymorphic forms of natural silica are quartz, tridymite and cristobalite. In each case, the silicon atom is at the center of a tetrahedron and surrounded by four oxygen atoms via single, ionic bonds as shown in Figure 1. Each oxygen ion is centered between two silicon ions and is therefore shared in the adjacent tetrahedron. Quartz and tridymite, which are shown in Figure 2, exist as helices and have optical isomers. In comparison, cristobalite, shown in Figure 3, is characterized by silicons in a diamond shape with oxygen atoms equidistant from the silicon atom.

Quartz is the most common natural silica and is thermodynamically stable below 1,143K. The surface energy is 980 mJ/m^2 (7); the interfacial surface energy between quartz and water is 416 mJ/m^2 (4) and the heat of wetting of quartz in water is 564 ± 16 mJ/m^2 (8). It is

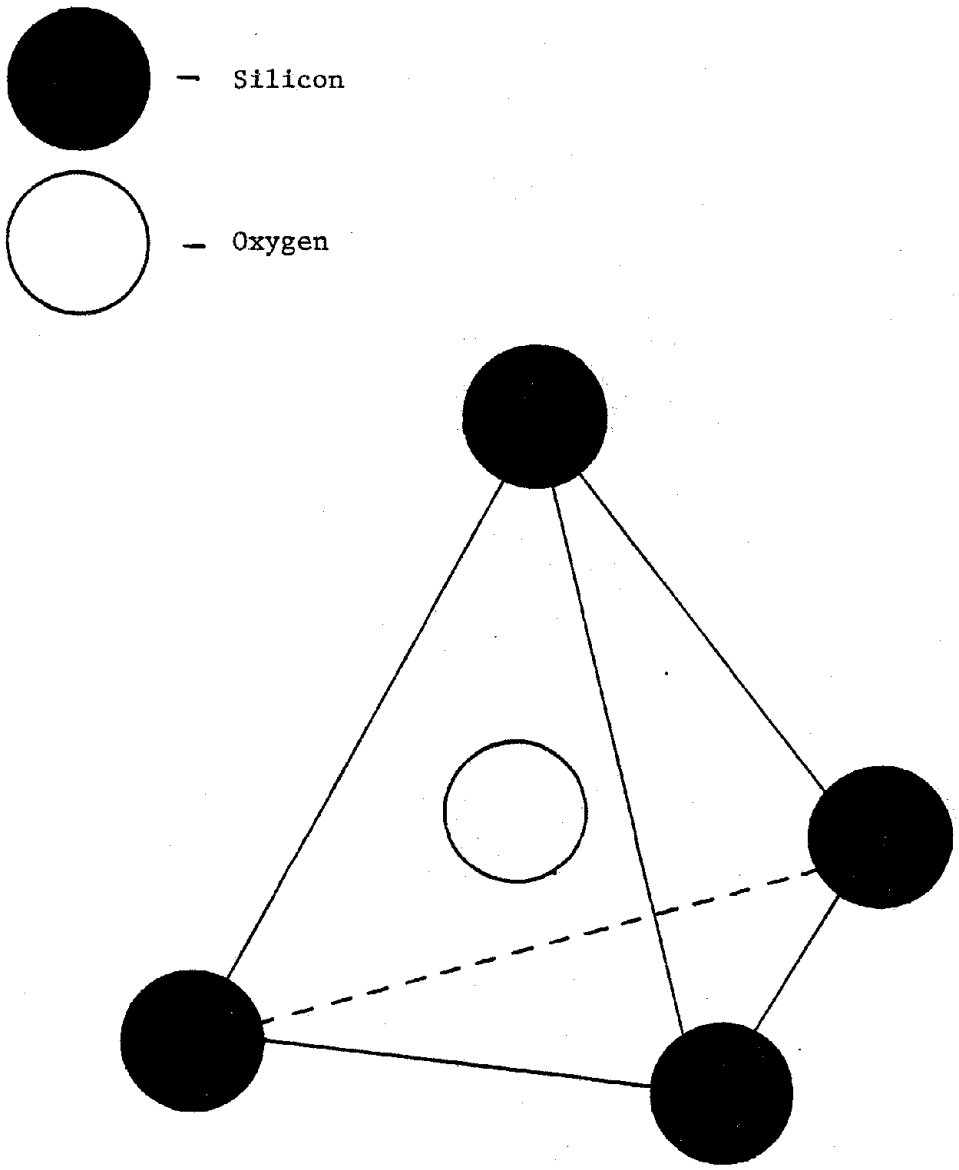

Figure 1. The Tetrahedral Structure of Silica (5).

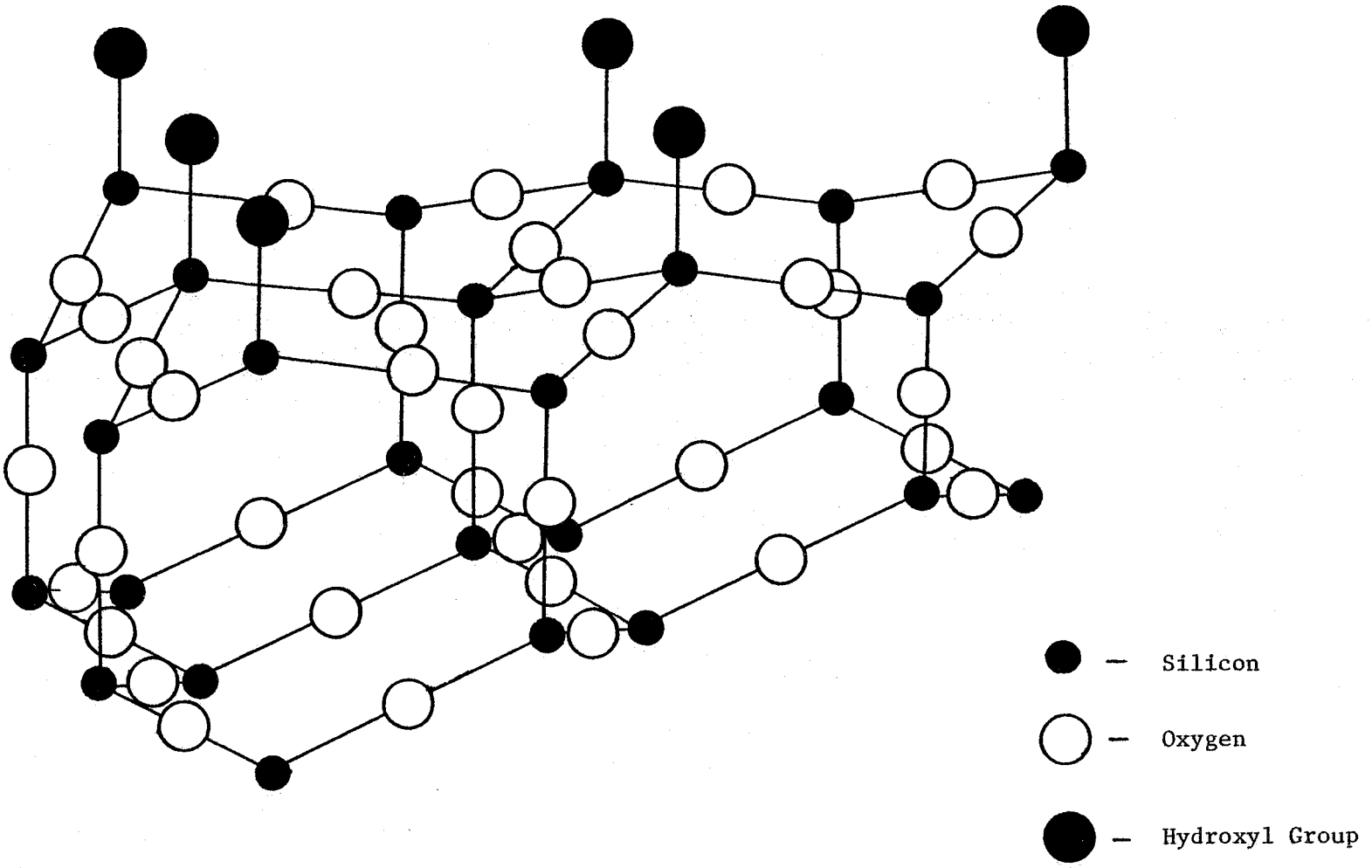

Figure 2. Structure of B-Tridymite (4).

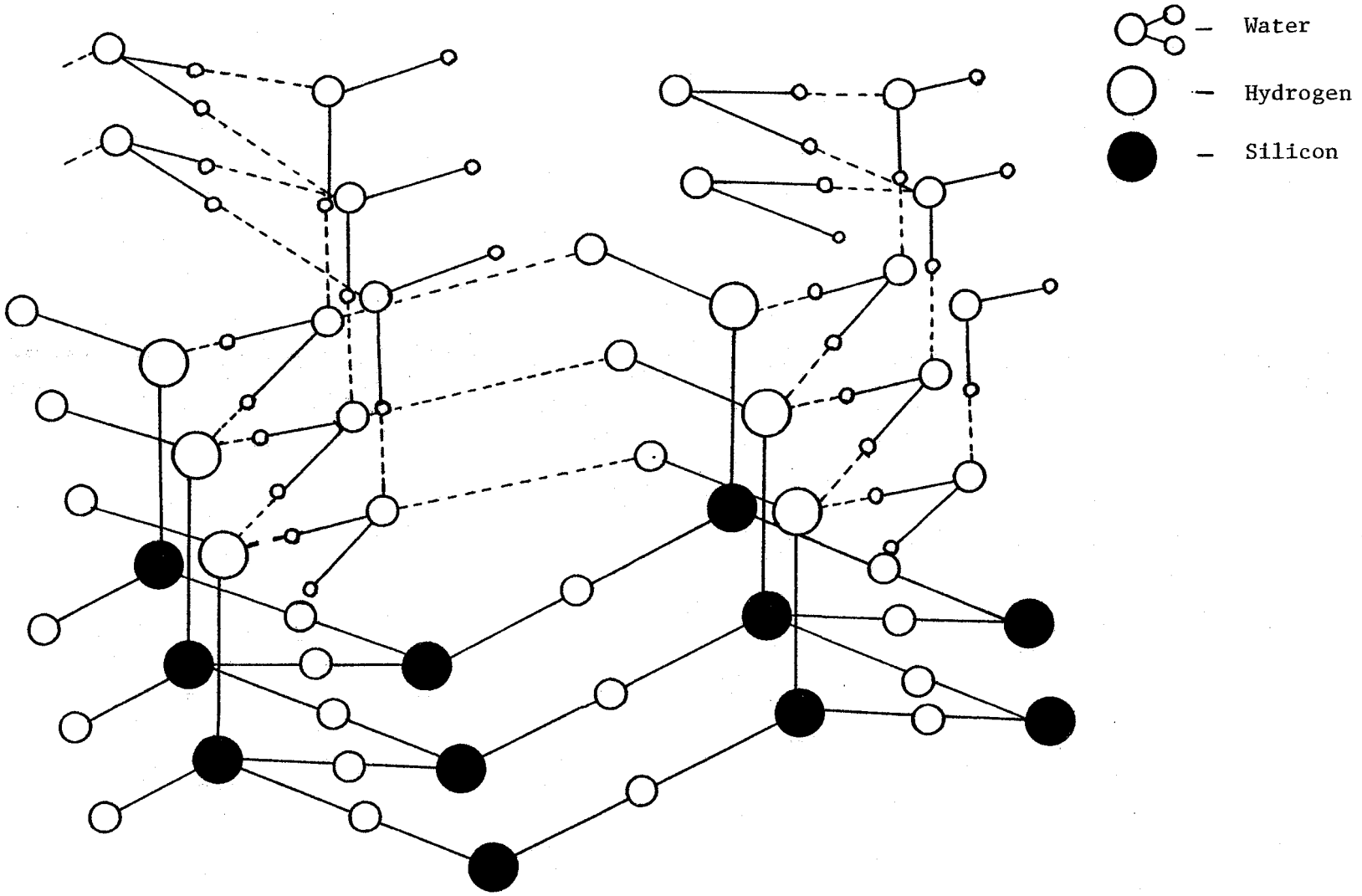

Figure 3. Adsorption Layers of Water on the Surface of α-Cristobalite (6).

only slightly soluble in H_2O; Gardner (9) has calculated that the solubility of quartz in water at 298-303K is .093% for three millimicron particles.

Iler (10) has described the amorphous layer surrounding crystalline quartz and its removal procedure. When quartz is ground, an amorphous, surface layer of about .3 microns in thickness is formed on 3 to 15 micron quartz particles. Upon cleaning the quartz surface, Iler reported that investigators have measured quartz solubility in water as 11 ppm. or .0011% of unspecified particle size.

B. Characterization of the Silica Surface.

Irrespective of its polymorphic form, the reactivity of silica is dependent upon its surface properties. The bulk is a Si-O-Si formation which is terminated at the surface, and the silicon valencies are maintained by either formation of silanol or siloxane bonds. Because of the strain associated with the siloxane bond, the formation of silanol groups is a preferred configuration. Various values have been reported for the total number of silanol groups per 100 A^2. These values range from approximately 5 hydroxyls per $100A^2$ (11) to 8 hydroxyls per $100A^2$ (4,12) for porous silicas. The upper end of the range was determined by calculating the area covered by each hydroxyl group from crystal structure data (4). The number of surface silanols reported for Cab-O-Sil, an amorphous silica, was approximately 1.70 OH groups/$100A^2$ using gravimetric analysis (13). Whalen (14) reported 5 hydroxyls per $100A^2$ for a quartz powder with

a particle size of 1 μm and a nitrogen BET surface area of 4.0 m^2/g. Experimentally determined silanol coverages are not definitive, and this may be attributed to the experimental techniques used and/or the reactivity of the different silica surfaces. The extent of physical adsorption on silicas surface is dependent upon the silanol coverage as indicated by Young (15). Young reported that the amount of water physically adsorbed was directly related to the number of surface hydroxyl groups.

In addition, surface reactivity is characterized by the types of silanols present on the surface (16). There are four types of silanol coverages for silica in addition to the siloxane linkages as shown in Figure 4. These silanols are described as:

1.) silanols with physically adsorbed water,

2.) geminal silanols,

3.) bound and reactive silanols, and

4.) free silanols.

The amount of each type of silanol coverage is dependent upon the particular silica surface structure. Moreover the surface structure of silica remains controversial and is not definitive (17).

It was shown that considerably more adsorption of hydrocarbons or water occurs on a silica surface treated to contain only free hydroxyl groups than a treated silica surface which contained only siloxane linkages (13). Silica which had not been pretreated and contained the different types of silanols displayed preferential water adsorption on the H-bonded silanol groups (13,18). The dif-

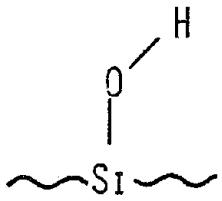

FREE

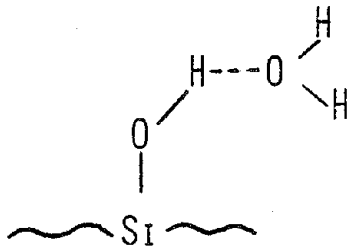

ADSORBED WATER

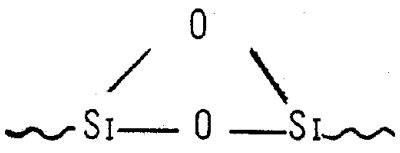

SILOXANE

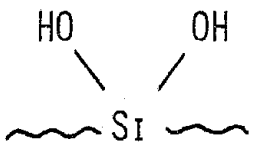

GEMINAL

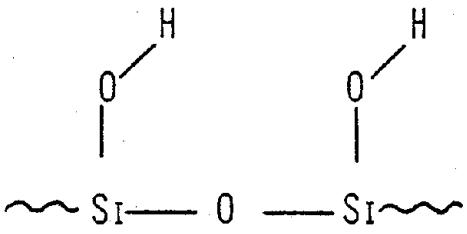

REACTIVE

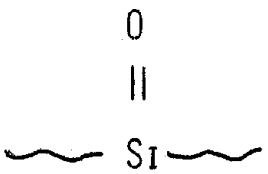

STRUCTURE A

Figure 4. Silica Surface Structures.

ference in reactivity of surface silanols could account for the stepwise, multilayer adsorption of water vapor reported on silica from 403 to 423K (6). The authors suggest that there are adsorption sites which have different rates of adsorption.

It is apparent that there are distinct differences in the reactivity of the types of silanol groups to adsorbates. Moreover, the number of silanols representing a reactive surface site can vary. Hair and Wertl (13) have shown that geminal pairs appear to act like a single site for non-hydrocarbon compounds. Therefore, one adsorbate molecule could adsorb on each pair.

Steric factors also need to be considered in silicas surface reactivity. The bulkier the group attached to the surface silanols, the lower the extent of surface substitutions (20).

Another factor which affects chemical and physical adsorption on silica is temperature. All forms of silica were relatively unreactive with chlorine, bromine, hydrogen, most acids and metals at room temperature (21). Heating silica in chlorine gas at 973-1,223K (22) or in carbon tetrachloride at 623-873K (23) chlorinated the surface with complete dehydroxylation.

C. Water Adsorption on Silica

Whereas high temperatures are necessary for chlorination of silica, high temperatures impede physical adsorption of water by dehydroxylation of the silica gel surface. Physical adsorption of water occurred more readily on a silica gel that had silanols on the

surface than silica gel which was exposed to high temperatures and was anhydrous. Rehydration of a silica surface upon exposure to water vapor occurred slowly (4).

The temperature which results in dehydroxylation of the silica surface is not definitive. It has been suggested that below 423K loss of physically adsorbed water occurred (11,12). Unger (24) has reported that silanol concentration decreased slightly until 573K and between 573K and 773K, a radical decrease in the silanol concentration occurred. The author stated that the decreased silanols resulted from condensation of bound hydroxyl groups to form siloxane linkages. Heating silica gel above 873K may induce structural deformations with a decrease in surface area (4).

In comparison with silica gels, quartz has a relatively small surface area and a semi-amorphous surface region; however, it has been suggested that the surface structure of quartz is analogous to silica gel (25). Moreover, quartz and silica gel share similar dehydration properties. Irreversible water adsorption occurred on quartz outgassed at temperatures greater than 423K, and rehydration of the quartz surface at room temperature was not complete at low relative pressures (26,27).

A model for water physisorbed on an amorphous silica with a decreased, predetermined percentage of surface silanols after high outgassing temperatures has been proposed (28,29). The adsorbed water may be assuming a stretched state over the silica surface, which is reasonable since the silanols are not closely packed on the surface.

A model for water physisorbed on an amorphous silica, Cab-O-Sil, has been proposed (13). Isotherm data obtained at 295K indicated an adsorption plateau at 0.5 molecules/100A^2 and another plateau at 1.6 molecules/100A^2. The authors conjectured that the first plateau represented the first layer of water which hydrogen bonded on the H-bonded silanol surface. The second plateau represented the second layer of physically adsorbed water (Figure 5).

The molar heats of adsorption were calculated for the stepwise adsorption of water vapor on Porasil F, an α-cristobalite (6). A heat of adsorption of 104.6 kJ/mol and an entropy less than solid water were determined for water molecules adsorbed in the first layer. The molar heat of adsorption for the second layer formation was 66.9kJ/mol and the third water layer formation was 39.7 kJ/mol. The authors suggested that the high isosteric heat and the differential entropy value calculated for the first water layer formation indicated that the water molecules were in a more localized state. The third water layer formation may be in a more liquid state.

Like cristobalite, indications of the immobility associated with the adsorbed water phase on quartz have been determined (26).

D. Heat of Immersion Data for Silica in Water

Heat of immersion data for quartz in water provided thermodynamic information on the energy changes involved in the water molecule-hydroxyl group interaction. Heats of immersion were determined for quartz exposed to specific pressures of water vapor and it was determined that the heat of immersion varied with coverage.

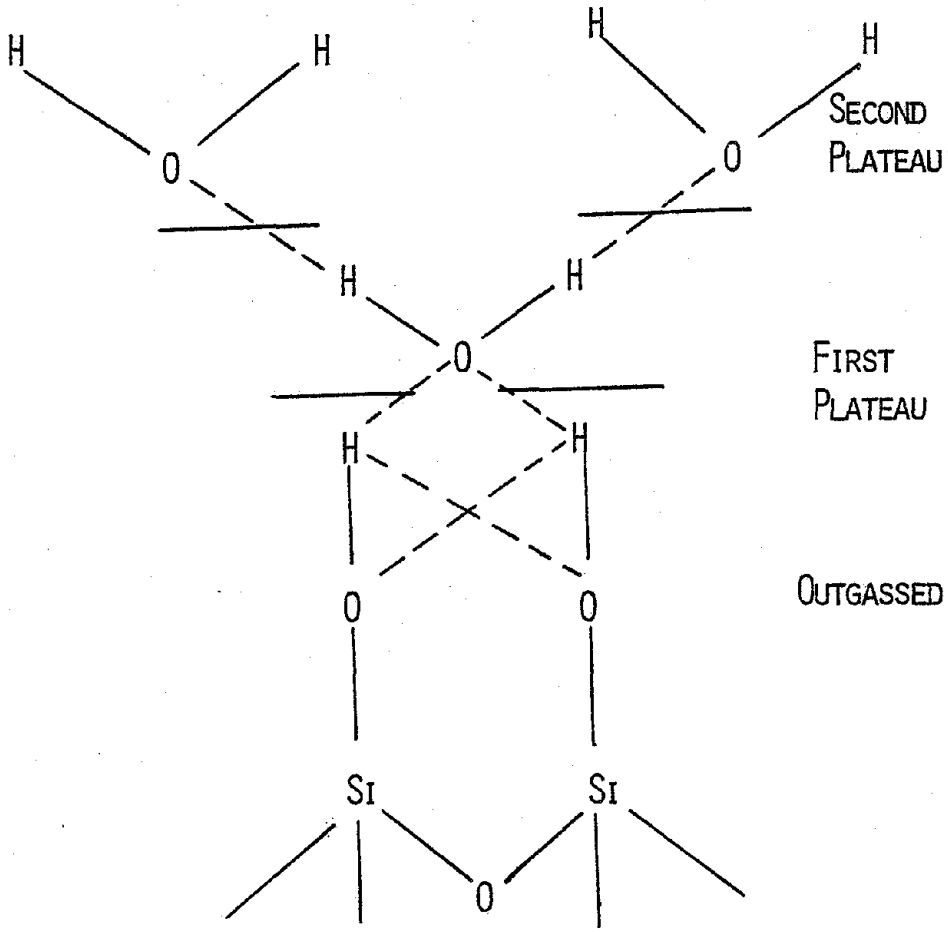

Figure 5. A Model of Water Adsorption on Silica (13).

A drastic minimum in the heat of immersion at a surface coverage of 0.38 indicated that a first layer water molecule could be locally associated with 29 $\mathring{A}^2$ of solid surface (26).

Spherical, clean quartz particles of $\leq$ 5 μm in diameter outgassed at 383K and with a BET nitrogen surface area of 7.5 m^2/g produced a heat of immersion of 310 mJ/m^2 (26).

The marked dependence of the heat of immersion upon particle size has been investigated. Energies associated with bound H_2O molecules range from 9623 J/mol to 15,062 J/mol for quartz $\leq$ 5 μm to a more crystalline structure of 20-40 μm, respectively (30). Whalen (26) reported that a great variation in particle size for a quartz sample resulted in higher immersion heats because of the increased crystalline order in the larger particles (20-40 micron) of the sample. Likewise small particles (5 micron or less) exhibit lower heats of immersion due to a decreased crystal order (31). As much as 48% of < 5 μm particles may be non-crystalline with respect to the α-β quartz transition as determined by thermal analysis (30). A decrease in crystalline order for the smaller quartz particles resulted not only in a lower surface energy but also in a lower free energy change upon adsorption. An extrapolated value of 209 mJ/m^2 was reported for the free energy change of water vapor adsorbed on quartz with a surface area of 5.5 m^2/g (32).

Whalen (26) reported that heat of immersions in water for quartz with a surface area of 5.5 m^2/g varied with the outgassing temperature. The outgassing temperature was maintained for $\geq$ 3 days or until the

system pressure was 5×10^{-6} torr (6.7×10^{-4} Pa). The heats of immersion for quartz, which had not previously been exposed to water, were determined on samples outgassed at 383K and 523K. The heats of immersion were approximately 310 mJ/m^2 and 420 mJ/m^2, respectively. The heat of immersion for quartz samples, which were outgassed and exposed to specific amounts of water vapor prior to immersion were also studied. For outgassings at 383K, a minimum at $P/P_o = 0.05$ of 200 mJ/m^2 was observed. A general trend of decreasing heats of immersion with increasing P/P_o was observed except for a slight upward inflection at $P/P_o = 0.60$ corresponding to approximately 150 mJ/m^2. Heats of immersion for quartz samples outgassed at 523K did not show a minimum at $P/P_o = 0.05$, but did exhibit an upward inflection at $P/P_o = 0.75$. Whalen proposed two explanations for the lack of a corresponding minimum in the heat of immersion at $P/P_o = 0.05$ for samples outgassed at 523K as compared to outgassing at 383K. The sites available on silica for H_2O interaction at a 383K outgassing may not be available at a 523K outgassing. On the other hand, the interaction of silica and H_2O at these silica sites may be prevented because of the altered surface structure due to outgassing temperatures of 523K.

Investigators (32,33) have reported that heats of immersion increased, attained a maximum value, and then decreased with increasing outgassing temperature of the quartz. A correlation of the high heats of immersion with the gradual, endothermic loss of physically adsorbed water at lower outgassing temperatures was made. Likewise,

the endothermic loss of silanols at higher outgassing temperatures was attributed to the decreasing heat of immersion since dehydroxylated SiO_2 surfaces do not rehydrate rapidly (33).

Whalen (30) compared heats of immersion for a quartz sample of $\leq$ 5 μm with an amorphous layer and a quartz sample of 20-40 μm without the amorphous surface layer for pretreatment outgassing temperatures of 383, 473, 573, and 673K. He concluded that the two quartz samples showed comparable heats of immersions below a pretreatment temperature of 573K. Consequently bound water loss below 573K cannot be attributed to the amorphous region of the quartz sample of $\leq$ 5 μm. It was subsequently shown that the loss of hydroxyl groups for pretreatment temperatures greater than 573K was due to an amorphous region on the quartz surface. Makrides and Hackerman (31) suggested that grinding quartz crystals to decrease particle size may alter the spacing of surface hydroxyl groups in the amorphous layer. The result of this changed surface of quartz may be an alteration in the heat of wetting data.

Correlations of the heat of immersion study for quartz $\leq$ 5 μm and isotherm adsorption studies provided an explanation for heat of immersion data (30) obtained for quartz. Water adsorption-desorption studies at 383, 473, 573 and 673K outgassing pretreatment temperatures for quartz showed that there was irreversibly bound water loss for quartz exposed to pretreatment temperatures greater than 523K. As pretreatment temperatures were increased from 523K to 673K, the amount of water adsorbed decreased. Vapor desorption studies showed

that replacement of bound water for quartz outgassed at 383K and 473K was possible but for 573K and 673K replacement of bound water was not possible. The heat of immersion maximum was reached at an outgassing temperature of 523K and then declined upon approach of 723K. The maximum in heat of immersion was obtained prior to the irreversible loss of bound silanol molecules on the surface according to isotherm data.

More recent adsorption work by Whalen (14) indicated that outgassing quartz at temperatures greater than 473K resulted in surface structural changes, which impeded rehydroxylation. During a 24 hour period water adsorption on quartz increased under constant water vapor pressure and desorption was slow. Two models of the silica surface upon evacuation at 473-573K have been postulated (34,35) as structure A and the siloxane linkage indicated in Figure 4. Crystallographic data indicated the siloxane linkage was less probable than structure A (19); however, experiments (36) have supported the possible existence of the siloxane linkage.

Ranges of heats of wetting can be associated with surface areas of the silica. Heats of wetting were shown to decrease with an increase in the specific surface area (31). Values for heats of wetting between 450-750 mJ/m^2 correspond to surface areas < $3m^2/g$. Whereas heats of wetting between 100-250 mJ/m^2 were for powders and silica gels with surface areas less than 100 m^2/g.

Egorov, Krasil'nikov and Sysoev (37) have observed the same trend of decreasing heats of wetting with increasing specific areas for

silica gels. In addition, they observed a decrease in the number of hydroxyl groups per area with increasing surface area. Therefore large heats of wetting for small surface areas may be associated with a greater number of hydroxyl groups for silica gels. Since gels and powders show similar heats of wetting values and trends, a decrease in heats of wetting for powders with increased surface area may indicate a decrease in hydroxyl groups.

E. Chlorination of the Silica Surface

Models for water adsorption on silica are based primarily on the assumption that hydrogen bonding of water occurs on the silanol surface. Because of the π-bonding interaction between the unshared electrons on the oxygen atom of silica and an empty d orbital on the silicon atom, electrons are drawn away from the oxygen. This increases the positive character of the hydrogen and insures hydrogen bonding with the water molecule (18). Because of this π-bonding interaction, covalent bond formation with the surface silicon atom at room temperature is not possible for chlorine.

The reactivity of molecular chlorine with silica has been investigated (38). The formation of the Si-Cl bond was dependent upon weakening the Si-O bond by subjecting silica to high temperatures and to the chlorine gas in the presence of a reducing agent such as carbon. The activation energy for the reaction was reported as 217.96 kJ/mol.

Surface hydroxyls can be partially replaced on silica gels and porous glass if silica is refluxed with sulfuryl chloride (18,34). The reaction proceeds as follows with the HCl and SO_2 removed as gaseous byproducts:

$$2\text{-}\overset{|}{\underset{|}{Si}}\text{-OH} + SO_2Cl_2 \rightarrow 2\text{-}\overset{|}{\underset{|}{Si}}\text{-Cl} + 2HCl + SO_2 \qquad [1]$$

Hair and Hertl (39) reacted Cab-O-Sil, an amorphous silica with a surface area of 160 m^2/g, with Cl_2 in a controlled temperature furnace. The chlorination of the silica surface at 673K was monitored by infrared analysis. Chlorination was measured by observation of the decrease of the freely vibrating hydroxyl band at 3747 cm^{-1}, which was the only reactive group present after outgassing at 1,073K. Absorbance of Si-Cl at 650-550 cm^{-1} and 550-425 cm^{-1} cannot be observed because of interference from silica absorbance bands (40). About 10% of the hydroxyls was removed by an initial fast reaction. This was attributed to direct chlorine substitution onto the silica surface. The remainder of the reaction at 24.0 torr (3199.7 Pa) of chlorine with Cab-O-Sil at 673K was a relatively slow reaction. After approximately 19 hours only 60% of the surface was chlorinated. The reaction was not followed to completion; Hair and Hertl concluded that the reaction order was between 1.0 and 2.0.

It must be noted that chlorosiloxanes such as Si_2OCl_6 are not stable molecules and readily hydrolyze to silica and the hydrogen halide (34,35,41). Therefore, it was important that chlorination of silica and reaction studies occurred under vacuum conditions in the preceding experiments.

F. ESCA and AES Studies of Silica

Surface analysis of silica has been performed using ESCA (electron spectroscopy for chemical analysis) and AES (Aujer electron spectroscopy) to determine the valence states of the surface elements.

An ESCA study of a small particle SiO_2 surface revealed a change of the valence electrons with dehydration temperatures of 523, 673 and 973K. The study revealed that the removal of silanols resulted in a decrease in the negative charge on the oxygen of the siloxane bond and a change in the covalent Si-O bond (42).

Salmerón and Baró (43) examined an oxidized silicon surface and reported chemical shifts of silicon in the Auger spectrum due to decomposition of the Si-O bond from electron beam bombardment at 2500 eV. The sample was etched with a HNO_3 and HF solution and heated to 773K prior to electron bombardment. A peak at 78 eV was reported for silicon in the first Auger scan. Successive scans of one minute intervals showed increased kinetic energies in the 70-100 eV range. The authors suggested that the increase in energy was due to production of either elemental silicon or a less oxidized complex compound SiO_x where $x < 2$. This explanation was supported by the appearance of a peak at 91eV with successive scans, which corresponded to the $L_{2,3}VV$ Auger peak of a clean silicon surface.

The appearance of two peaks, silicon at 78 eV due to oxidized silicon and silicon at 92eV due to elemental silicon, have been reported in Auger spectroscopy (44,45). Salmerón and Baró (43) con-

tended that the presence of free available oxygen in conjunction with the electron beam resulted in complex oxidation states of silicon and therefore a single silicon peak in their study.

The effect of oxidation of silicon by ESCA has been studied (46). Two Si 2p (99 eV) peaks due to elemental silicon and silicon dioxide were reported for a Si crystal oxidized in air. Peak separation increased as the ratio of the areas of elemental silicon to silicon oxide peaks decreased. A separation of 3.4 eV correlated with a ratio of $\approx$ 4. When peak separation measured 5 eV due to an energy shift of the oxide peak, the ratio of elemental silicon to oxidized silicon was approximately zero. The decrease in the ratio resulted from the increased oxidation of the silicon surface. The ESCA data indicated that an elemental silicon peak and a silicon oxide peak can be observed. The effects of available oxygen may result in a decrease in the elemental silicon peak.

CHAPTER III

EXPERIMENTAL

A. Adsorbents

A nonporous, white, microcrystalline quartz, Min-U-Sil 5, was supplied by the Penn Glass Company. The average particle size was $\leq$ 5 microns. Min-U-Sil from two shipments dated June 1971 and March 1972 was used as received for some experiments.

For other experiments, silica was subjected to an etching treatment described by Iler (10) to remove the amorphous surface layer. The effects of this chemical treatment on adsorption were studied. Twenty grams of Min-U-Sil were treated with 100 ml of 9-15% HF for 15 minutes to dissolve about 25% of the silica by cleaving Si-O-Si bonds. The HF solution was filtered using a 600 ml-90M KIMAX ceramic frit of medium coarseness. The sample was washed once with 200 ml of 0.1N NaOH solution and rinsed ten times with deionized water to remove the fluoride and rehydrate the surface.

Surface characterization studies were conducted on two samples of ground debris collected near launch complex 40 at the NASA-Kennedy Space Center. NASA #2 was collected 73° and 701 meters from launch complex 40. NASA #4 was collected 180° and 2926 meters from launch complex 40.

B. Characterization of the Adsorbent

1. Infrared Analysis

Transmission infrared analysis of silica was conducted on a Perkin-Elmer Model 283 Spectrophotometer. Two types of sample preparations of silica were performed in an effort to obtain a sample which had the optimum thickness for IR analysis.

Pellets of KBr and silica in a 100:1 ratio were prepared using a WILKS Mini-Press. A torque was exerted for 5 minutes on 0.050 grams of the KBr and silica mixture. A spectrum of the sample was obtained with the sample remaining in the Mini-Press and a Mini-Press with a KBr pellet was placed in the reference beam. Desiccant was placed in the sample compartment of the spectrophotometer during the IR work.

Slurries of untreated silica in deionized water were placed upon NaCl crystals for IR analysis in an attempt to minimize sample thickness. Various concentrations of the slurries were studied to obtain the optimum light transmission and decrease light scattering. The concentration of the slurries were:

1. 0.5g silica/ml of H_2O,
2. 0.05g silica/ml of H_2O, and
3. 0.005g silica/ml of H_2O.

A clean crystal was placed in the reference beam during all IR analyses of the slurries on NaCl crystals.

2. X-Ray Diffraction and Differential Scanning Calorimetry

A Diano-XRD 8000 diffractometer using Cu K_α radiation and a graphite monochromator was used to determine the X-ray patterns for the untreated and the etched silica.

Differential scanning calorimetry was used to characterize the silica. The instrument used was a DuPont 990 thermal analyzer. A 0.96 mg sample of silica was heated from 313K to 893K in a nitrogen flow of 75 ml/min and the thermograms of the sample were recorded.

3. Scanning Electron Microscopy (SEM) and Energy Dispersive X-Ray Analysis (EDAX)

The following samples were examined using SEM:

1. untreated silica,
2. untreated silica outgassed at 373K for 2 hours and exposed to approximately 40 torr (5.3×10^3 Pa) of Cl_2 gas at 303K,
3. untreated silica outgassed at 673K for 2 hours and exposed to approximately 40 torr (5.3×10^3 Pa) of Cl_2 gas at 303K, and
4. etched silica.

An Advanced Metals Research Corporation Model 900 scanning electron microscope operating at 20KV was used for the analysis. All samples were mounted on nonconducting copper tape and were treated with a

thin film of Au/Pd alloy to prevent charging of the sample surface, which decreases photographic clarity.

EDAX, or energy dispersive X-ray analysis, was obtained for NASA samples #2 and #4 using an International Model 707A unit attached to the microscope. Untreated silica samples outgassed at 373K and 673K respectively and then exposed to Cl_2 gas at 303K were analyzed for chlorine. Analysis of Na with EDAX in the etched silica was determined to ascertain that all Na had been removed upon completion of the etching process.

C. Surface Area Measurements

1. Procedures

Surface areas of the samples were determined on a Micrometrics Model 2100D Orr surface-Area Pore-Volume Analyzer using low temperature adsorption of dry nitrogen from Airco. Approximately 2 grams of a sample were outgassed at 373K or 673K for 2 hours or 15 minutes at an ultimate pressure of $< 5 \times 10^{-4}$ torr ($<6.7 \times 10^{-2}$ Pa). Helium dead space measurements of the sample bulb using Airco helium were conducted prior to the nitrogen adsorption measurements. All measurements were made based upon instructions in the Micrometrics Manual (MIC P/N 210/4280/00, 5 September 1974).

2. Calculations

The BET equation (47) used in calculating the surface area of the nonporous solids is

$$P/V(P_0-P) = 1/V_mC + (C-1)/V_mC(P/P_0) \quad [2]$$

where V_m is the monolayer volume expressed in STP cc of adsorbate per gram of adsorbent, V is the volume in STP cc of adsorbate per gram of adsorbent at each pressure, P, and P_0 is the saturation vapor pressure at the adsorption temperature. The constant, C, is related to the heat of adsorption and is characteristic of the gas/solid system.

A plot of $P/V(P_0-P)$ vs. P/P_0 allowed the determination of V_m, the monolayer volume expressed in STP cc per gram of adsorbent by the equation

$$V_m = 1/(m+y) \quad [3]$$

where m and y are the slope and y-intercept of the plot, respectively. The surface area, SA, is expressed in m^2/g obtained by

$$SA = V_m(NA)(S)/VO(W) \quad [4]$$

where V_m is as previously defined, NA is Avogadro's number (6.02×10^{23} molecules/mole), and S is the cross sectional area of an adsorbate molecule. Values for S of 16.2×10^{-20} and 10.4×10^{-20} m^2/molecule were used (48) for nitrogen and water in the surface area determinations respectively. The VO is the STP molar volume (22400 cc/mole) and W is the sample weight in grams.

Calculations of the surface area were made using a linear least squares computer program written in BASIC and run on a PDP-8 computer.

The program is listed in Appendix I.

D. Adsorption Measurements

1. System

Adsorption measurements of chlorine gas and water on samples were conducted in a constant volume apparatus with glass stopcocks lubricated with Apiezon N as shown in Figure 6. The system was maintained at a pressure of 1×10^{-5} torr (1.33×10^{-3} Pa) by means of a mercury diffusion pump (DP) and a mechanical pump (MP). The pressure was measured with a McLeod gauge (MG). The mercury diffusion pump was accessed to the apparatus via stopcock (S1). Helium contained in a reservoir bulb (HB) was used for dead volume measurements and was accessed to the system through a stopcock (S2). Bulb (WB) and its associated stopcock (S3) was used for storing water and introducing water vapor into the system. Chlorine gas was stored in bulb (RC) and introduced into the system by stopcock (S4). A chlorine reservoir bulb (CB) with its stopcock (S5) replenished the chlorine supply for bulb (RC). The sample bulb (SB) was sealed to the system vacuum line (SL) with Apiezon W wax, and introduction of adsorbate onto the sample was controlled by stopcock (S6). Stopcock (S7) connected the system vacuum line to the main vacuum line (ML).

Pressures were measured by a MKS Baratron gauge (BG) which is a differential capacitance manometer. The output was displayed on a Baratron meter type 144 (BM) with a precision of 0.5 torr (66.66 Pa)

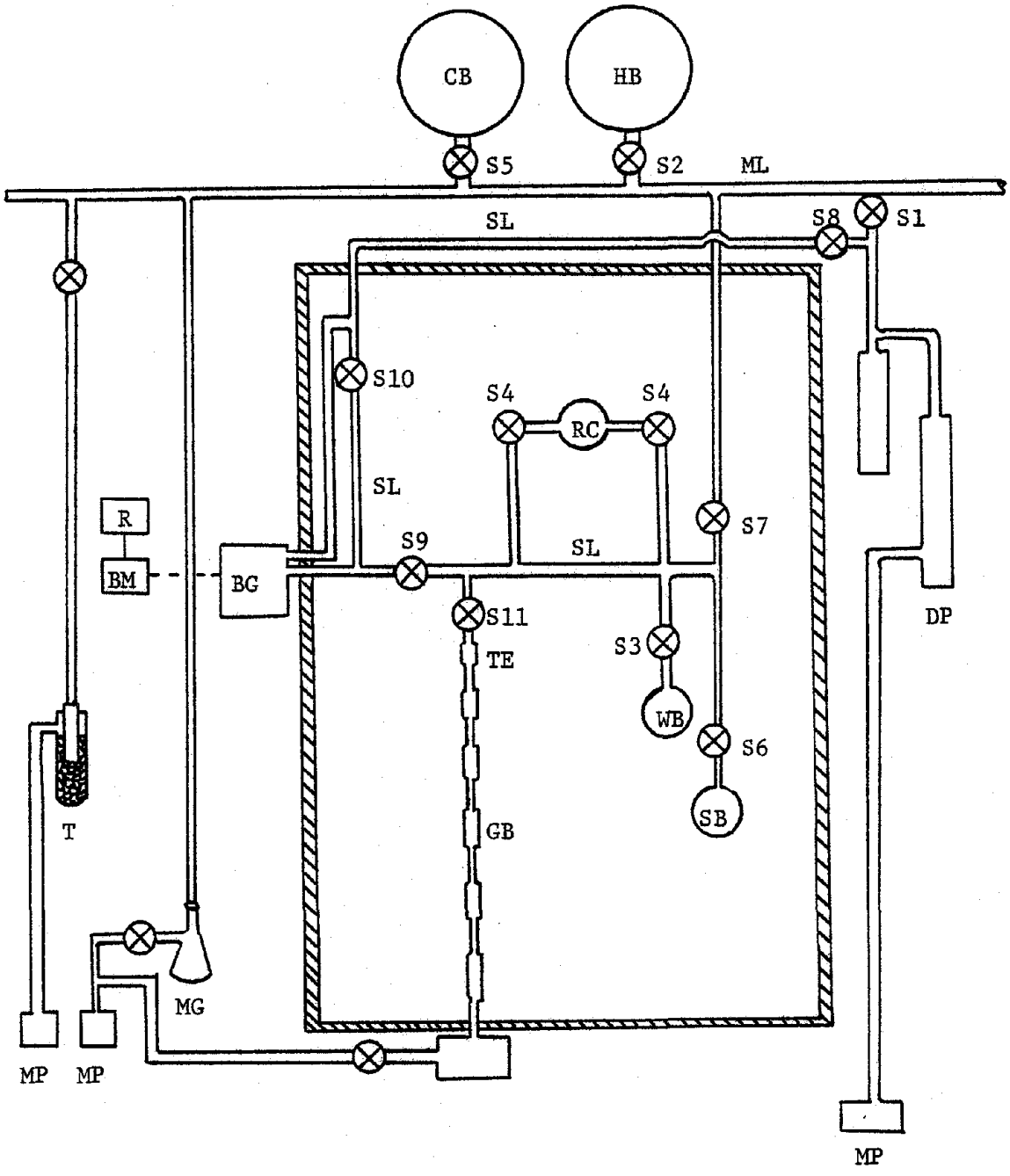

Figure 6. Schematic Diagram of the Adsorption Apparatus

and recorded on a Hewlett Packard Mosley 680 strip chart recorder (R).

Stopcocks (S8) and (S9) provided a method to isolate a specific region of the vacuum line. The cross member stopcock (S10) allowed isolation of a portion of the vacuum line. A gas buret (GB) consisting of calibrated bulbs containing mercury was used to regulate the volume of the apparatus. Stopcock (S11) at the top of the bulbs was used to isolate the bulb volume from the adsorption apparatus when necessary.

Adsorption of water vapor on silica was measured at 303K, 313K and 323K. Adsorption measurements were obtained within 10% of saturation water pressures at each temperature. It was important that the apparatus be maintained at a constant temperature to prevent condensation of water on the walls of the system. A uniform temperature was maintained by constructing a thermostated air encasement. Heat was supplied by a 100 watt tungsten light bulb for the 303K adsorption studies; a 500 watt tungsten light bulb was used for the 313K and 323K adsorption studies. The cooling unit was a supply of water circulated through a coil. A rotary fan placed in front of the coil circulated air in the air bath. This thermostated system was used for all water and chlorine adsorption studies.

2. Procedures

The chosen sample was outgassed on the vacuum line at a designated temperature for two hours and within 8 hours of the adsorption study. Forty five minutes prior to pressure measurements, the thermostat in the air bath was set.

Before measuring the helium dead volume of the sample bulb at the designated temperature, the pressure of the system was checked via the McLeod gauge with all stopcocks opened except for the adsorbate stopcocks. Stopcocks (S8) and (S9) were then closed and the cross member (S10) was opened to zero the Baratron meter. For the water studies, stopcock (S11) was opened with the level of mercury in the bulbs preset to level TE. For the chlorine studies, stopcock (S11) was closed. Stopcocks (S7), (S8) and (S9) were opened, stopcocks (S1), (S6) and (S10) were closed and helium was introduced to the system vacuum line. Stopcock (S7) was then closed and the obtainment of an equilibrium pressure was monitored on the Baratron meter and recorder. Stopcock (S6) was then opened and the helium pressure upon equilibration with the sample was recorded. Evacuation of the helium from the sample bulb and system vacuum line resulted upon opening stopcocks (S1) and (S7).

Upon completion of the dead volume measurements, the pressure of the system was rechecked and the Baratron meter rezeroed. Stopcocks (S1), (S8) and (S9) were then opened for the H_2O adsorption measurements. Stopcock (S11) was opened with the level of the Hg preset to fill all the bulbs to level TE. Stopcocks (S6), (S7) and (S10) were closed. The first dose of water, which was approximately 10 torr (1.33×10^3 Pa), was introduced to the system and the equilibrium pressure recorded. The sample stopcock was opened and the first adsorbate dose was allowed to reestablish an equilibrium pressure which was recorded. Approximately 10 adsorbate doses, or 20

pressure readings, were obtained for one adsorption study. Water vapor was evacuated from the system vacuum line using the procedure described for helium evacuation.

When the adsorbate used was Cl_2, the procedures for Cl_2 adsorption on the sample paralleled the procedures for H_2O adsorption except that stopcock (S11) remained closed. Approximately ten Cl_2 doses were introduced first to the system vacuum line and then to the sample bulb at 303K. Because of the corrosive nature of chlorine gas, the mercury diffusion pump was closed off from the system line by closing stopcocks (S1) and (S8). The gas was then pumped via a mechanical pump (MP) through a trap containing potassium hydroxide pellets (T).

3. Calculations

The number of moles of adsorbate adsorbed by the solid was determined by using the ideal gas equation and the difference of the final and initial pressures for each dose of adsorbate introduced into the system.

Calculations of the number of moles of gas adsorbed on the solid for the first designated adsorbate pressure were determined by the following three equations:

$$1.\quad P_1(V_s) = n_i RT \qquad [5]$$

$$2.\quad P_2(V_s+V_{sb}) = n_f RT \qquad [6]$$

$$3.\quad n_s = n_i - n_f \qquad [7]$$

where P_1 is the initial adsorbate pressure and P_2 is the equilibrium pressure of adsorbate, n_i is the initial number of adsorbate moles in the system, n_f is the final number of adsorbate moles, V_s is the dead volume of the system, V_{sb} is the dead volume of the sample bulb, T is the temperature of the air bath and n_s is the number of moles adsorbed on the surface.

Adsorption calculations for the second designated adsorbate pressure and all proceeding pressures introduced to the system are based on the following equations, which account for the number of moles of adsorbate in the sample bulb prior to that dose:

1. $P_2(V_{sb}) = n_{is}RT$ [8]
2. $P_3(V_s) = n_iRT$ [9]
3. $P_4(V_s+V_{sb}) = n_fRT$ [10]
4. $n_s = n_{is}+n_i-n_f$ [11]

where n_{is} is the number of moles in the sample bulb prior to the second adsorbate pressure dose introduced to the system, P_3.

Calculations of the number of moles of adsorbate per gram of solid and per square meter of solid were executed by computer analysis using a PDP-8 computer and flexible minidisk. The software for the computer analysis consisted of translating the ideal gas equation into BASIC as shown in Appendix II. Prior to execution of the program, sample weight, temperature of the air bath, volume measurements of the system and the sample bulb and the surface area of the sample were entered into the memory of the computer.

E. Microcalorimetry

1. Procedures

Heat of immersion studies of Min-U-Sil in water were conducted on a Setaram, Calvet MS 70 microcalorimeter. The microcalorimeter had two matched pairs of cells, which allowed assembly of four samples. During a heat of immersion study, the matched cell served as a reference.

Pyrex sample bulbs 2.7 cm long and 0.63 cm wide were used. Approximately 0.7 cm of the total length was a narrow tip designed to break upon impact. Approximately 0.5 grams of sample was placed in the sample bulb and was then outgassed at about 1×10^{-5} torr (1.33×10^{-3} Pa) at a specified temperature for two hours and sealed off under vacuum. The sample bulb was fitted onto a metal breaker rod and cleaned with acetone. A pyrex cylinder which contained 2 ml of deionized water was inserted in a metal cylinder and attached to the sample bulb.

The sample bulb was inserted into the calorimetric cell and upon attainment of steady state, the metal breaker rod was depressed. The area of the exothermic peak was monitored by a paper readout. Approximately sixty minutes after bulb breaking, the immersion heat was completed.

Heat of immersion studies for silica in deionized water were conducted at 310K for the following samples:

1. untreated silica outgassed at 373K for two hours,
2. untreated silica outgassed at 673K for two hours,
3. etched silica outgassed at 373K for two hours, and
4. etched silica outgassed at 673K for two hours.

The heats of immersion in deionized water of empty bulbs outgassed at 373K and 673K respectively were determined also.

2. Calculations

The heat of immersion was determined by

$$\Delta H = S \times C/W \qquad [12]$$

where S is the sensitivity, C is the number of counts, W is the sample weight and ΔH is the heat of immersion. The sensitivity in joules/count for a microcalorimeter cell was determined by

$$S = I^2Rt/C \qquad [13]$$

A known current (I) was applied for a specific time interval (t); by knowing the resistance (R), the heat evolved in joules/count was determined. The counts (C) represent the integrated area for the heat of immersion of the sample and are displayed via a printout from the microcalorimeter.

Amplification of the sensitivity is controlled by variation of the number of thermocouples. A PS amplification setting utilizes 124 thermocouples whereas a GS amplification setting utilizes 496 thermocouples. For each thermocouple setting, a range of sensitivities is available from X100 to X1000, where X100 allows the greatest sensitivity. Heat of immersion studies were conducted at a sensitivity of GS X100 for the untreated Min-U-Sil outgassed at 373K. All other studies were conducted using a sensitivity of PS X100.

F. Electron Spectroscopy for Chemical Analysis (ESCA)

1. Procedures

ESCA (electron spectroscopy for chemical analysis) was used to characterize elements within 50 Å of the solid surface. A DuPont 650 electron spectrometer was used. The sample is bombarded with X-rays from a magnesium target in an analyzer chamber maintained at approximately 1×10^{-7} torr (1.33×10^{-5} Pa). The energy of the incident Mg K_α X-ray is 1253.6 eV.

When X-rays strike a sample, photoelectrons of the element within about 50 Å of the surface are ejected from the sample. The kinetic energy of the photoelectrons is measured. By knowing the kinetic energy of the photoelectrons, KE, the work function of the spectrometer, ϕ, and the energy of the X-ray beam, $h\nu$, the binding energy of the photoelectrons, BE, can be determined from the equation

$$BE = h\nu - KE - \phi \qquad [14]$$

ESCA was used in the analysis of the following silica samples:

1. untreated silica,
2. etched silica, and
3. silica outgassed at 373K and exposed to approximately 40 torr (5.3×10^3 Pa) of chlorine gas at 303K.

The ESCA analysis of untreated Min-U-Sil washed with 0.01M NaCl or 1M NaCl was studied to determine the presence of cationic (Na^+) and/or anionic (Cl^-) adsorption on untreated Min-U-Sil. The 0.01M and 1M NaCl was prepared using NaCl crystals from Allied Chemical Code 2232 (99.5% purity) and deionized water. Ten ml of the respective NaCl solution was equilibrated with approximately 1 gram of Min-U-Sil for 1 hour with intermittent stirring. The solution was filtered using a 30ml-30F KIMAX, ceramic frit. After filtering the sample, it was heated at 383K for 1 hour and then covered and stored. The samples were prepared within 8 hours of the ESCA study.

An ESCA study of the valence states of chlorine in NaCl, $KClO_4$, and $NaClO_3$ was made. The $KClO_4$ was Baker Analyzed Reagent Lot 5163. Sodium chlorate, $NaClO_3$, was Baker Analyzed Reagent Lot 21349.

All samples analyzed were mounted on a round brass probe with an area of 30 mm^2 using double stick transparent tape.

2. Calculations

The binding energy of a surface element was determined by measuring the distance from the beginning of the peak to the midpoint of the peak measured along the base. The distance was converted to eV by multiplying it by the scan speed (2 V/cm); the quantity was then subtracted from the starting binding energy of the scan to obtain the elemental binding energy. All elemental binding energies were measured relative to carbon where the energy of the 1s photoelectron was taken to be 284 eV (47,50). The difference between the experimental and the reference carbon binding energy, designated ϕ, was subtracted from all elemental binding energies.

Calculations of the atomic fractions of the surface elements were based upon peak intensity. The intensity of the peak, I, was determined from multiplying the peak height by the selected scanning sensitivity in cps/cm. Values of I were divided by σ, the elemental cross section of the orbital state associated with the elemental binding energy. Elemental cross sections were obtained from the literature values (50): $S_1$2s is 0.855, Na2s is 0.390, C1s is 1.00, O1s is 2.85, and C12p 1/2 and 2p 3/2 are 0.810 and 1.564 respectively. The atomic fraction of the surface element, A.F., was then determined by

$$\text{A.F.} = \frac{I/\sigma}{\sum_i I/\sigma} \qquad [15]$$

A Na Auger (NaA) peak was detected on some sample surfaces. The atomic fraction of sodium present was determined by using the photoelectric cross section of Na 2s. The intensity of the Na 2s peak was calculated by first determining the ratio of the intensity of Na A:Na 2s, which 11.5, for $Na_2B_4O_7$. By knowing this ratio and the intensity of the Na A on the sample, the intensity and the atomic fraction of the Na 2s was determined. This method was used in the determination of the atomic fraction of Na 2s for all ESCA results where the Na A was detected.

CHAPTER IV

RESULTS AND DISCUSSION

A. SEM and EDAX Studies of Silica

A scanning electron microscopy (SEM) photomicrograph (5000X) of untreated silica is shown in Figure 7, and illustrates the crystallinity of the sample. Etched silica, and silica samples outgassed at 373K and 673K and exposed to 40 torr (5332.8 Pa) of chlorine vapor in the adsorption apparatus were photographed at the same magnification. No differences in the surface could be detected as a result of the etching process, outgassing temperature or exposure to chlorine.

The energy dispersive X-ray analysis (EDAX) of silica showed that there was no sodium. The EDAX of silica samples outgassed at 373K and 673K after exposure to chlorine gas showed no trace of chlorine on the sample.

B. X-Ray Diffraction Studies and Differential Scanning Calorimetry of Silica

X-ray diffraction patterns were obtained on both untreated silica and etched silica. The measured d spacing, or the tetrahedral spacing, in a crystallographic direction for untreated silica was 4.29 Å for the 101 plane and 3.35 Å for the 100 plane. The measured spacing between atoms for etched Min-U-Sil was 4.25 Å and 3.35 Å. Literature values (51) of 4.26 Å and 3.34 Å for quartz verified that

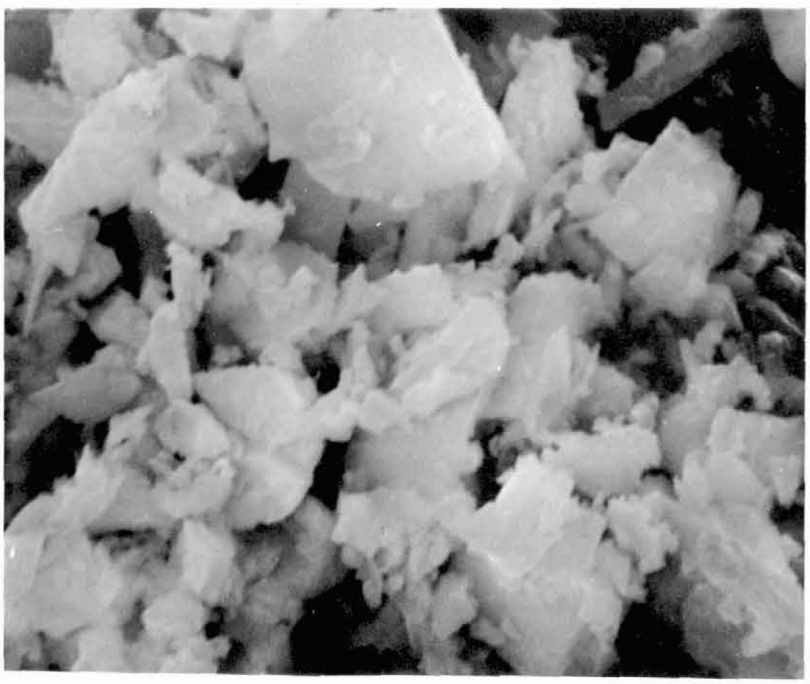

Figure 7. SEM Photomicrograph of Microcrystalline Silica (5000X).

both untreated silica and etched silica were α-quartz.

Thermograms of untreated silica further supported the conclusion that Min-U-Sil was quartz. An exothermic peak at approximately 808K observed in the thermogram is characteristic of α-quartz (35).

C. Infrared Analysis

A spectrum of silica in a KBr pellet (1:100 ratio) is shown in Figure 8. A similar spectrum was obtained for a slurry of 0.005 grams of silica per one ml of deionized water placed on a NaCl crystal. For both spectra, absorption peaks were detected at 1170, 1080, 800, 780, 690, 510, 460, 395, and 370 cm^{-1}. These peaks are comparable to reported literature values for quartz (52). Neither spectrum indicated the absorbance of free surface hydroxyls at the reported value of free surface hydroxyls at the reported value of 3749 cm^{-1} (18). A broad absorption band at 3500 cm^{-1} attrabuted to physically adsorbed water (18) was also not evident. The low surface area of silica may have prevented detection of surface hydroxyl groups.

D. Nitrogen BET Surface Area Measurements

Figure 9 shows the BET plot for nitrogen adsorption at 77K on silica outgassed at 373K. Based upon the slope and the intercept of the plot, the surface area of silica was determined from a nitrogen area of 16.2 $Å^2$ per molecule (48).

Table I indicates the mean surface area for samples outgassed 2 hours at a designated temperature. The number in brackets indicates

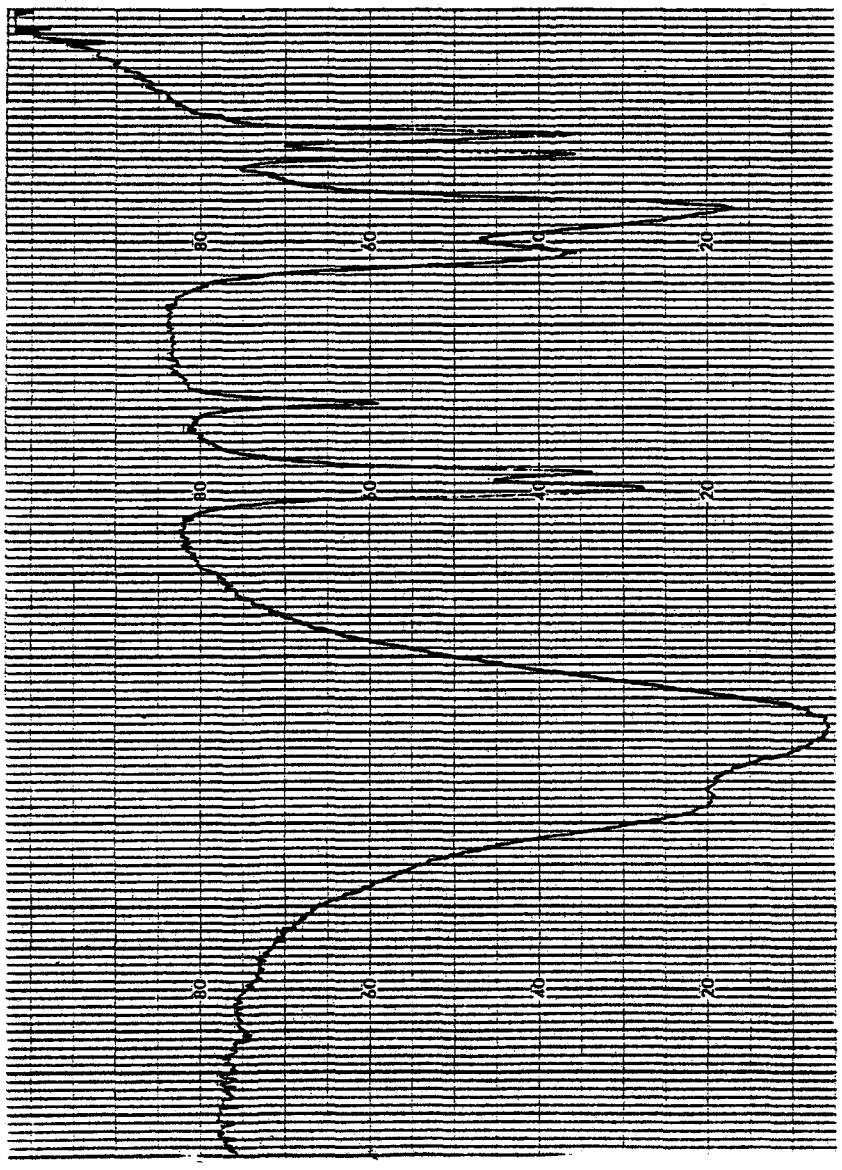

Figure 8. Infrared Spectrum of Silica in a KBr Pellet.

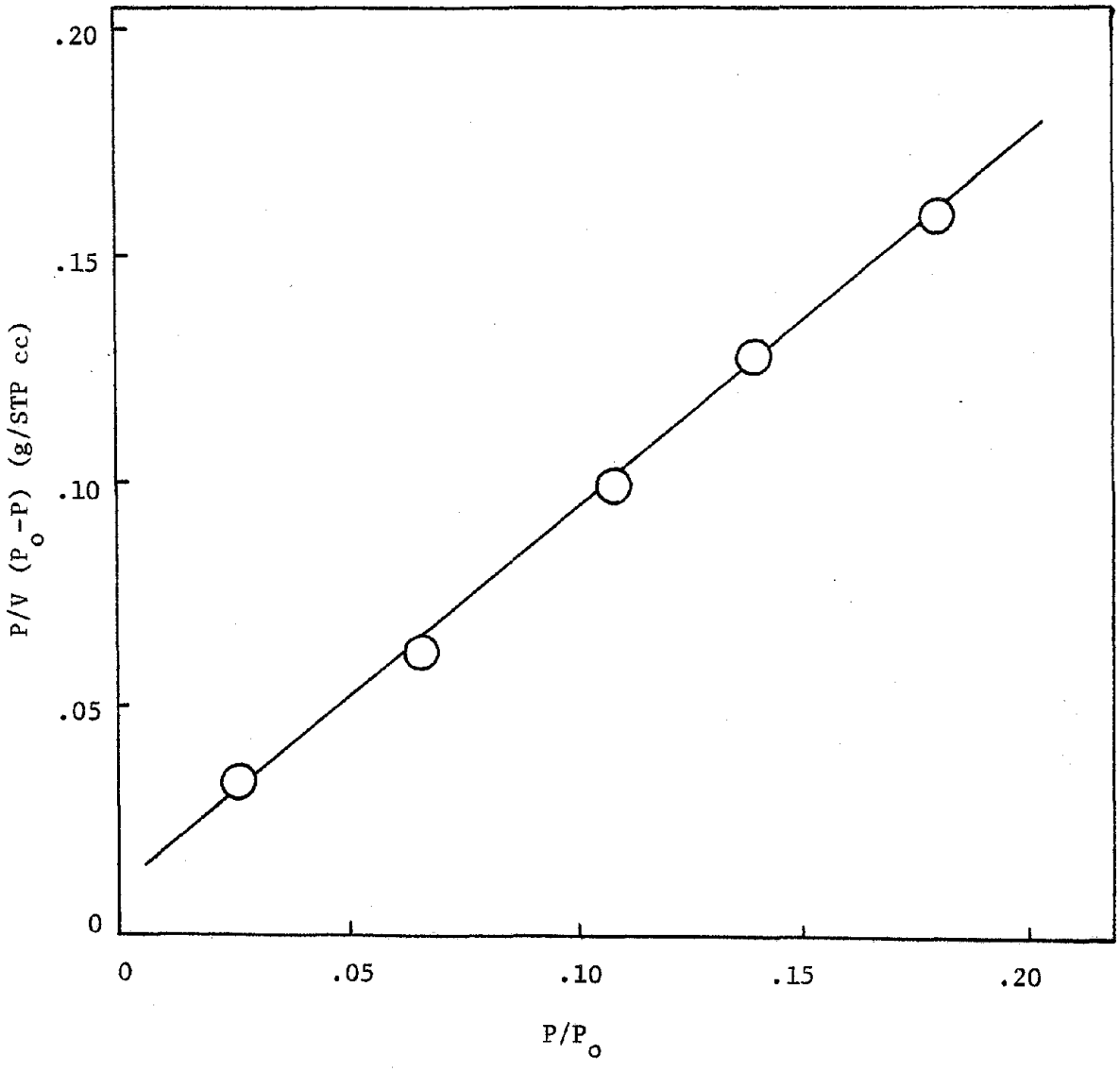

Figure 9. BET Plot for Nitrogen Adsorption at 77K on Silica Outgassed at 373K.

TABLE I

Nitrogen BET Surface Area Measurements

Sample	Outgassing Temperature (K)	Surface Area (m^2/g)
Silica 1971 2	373	5.08
Silica 1971 2	673	5.23
Silica 1972 2	373	5.04
Silica 1972 2	673	5.41
Etched Silica 4	373	2.93
Etched Silica 4	673	3.33
NASA #2 1	373	0.35
NASA #4 1	373	0.14

the number of surface area determinations. The similarity in the surface areas for the two sample lots outgassed at the same temperature indicates that the surface areas of the silica from the sample lots were similar. Particle size in the two sample lots was ≤ 5 microns; similarity in the surface area measurements indicates a similar particle size distribution.

Increasing the outgassing temperature of silica from 373K to 673K increased the surface area measurements of silica by 5%. The increase in the surface area of silica outgassed at 673K instead of 373K may be within experimental error, since only 2 surface area determinations were made for each sample lot at each outgassing temperature.

The surface area of etched silica obtained from 3 batch preparations, and outgassed at 373K, was 42% less than silica outgassed at 373K. The etching treatment hydroxylates the surface and counteracts condensation (35). Therefore, more surface hydroxyls per $\mathring{A}^2$ would be expected on etched silica than untreated silica. The increased number of hydroxyls on etched silica may decrease the packing density of nitrogen molecules and contribute to the decreased surface area. Calculations (53) indicate that increased surface hydroxylation may affect the packing density of nitrogen on a silica surface. As nitrogen coverage approaches monolayer coverage on a hydroxylated silica gel, the entropy of adsorption for the nitrogen molecule decreases. This decreased entropy of adsorption may decrease the packing density of the nitrogen molecule and hence decrease the surface area of the silica.

The surface area of etched silica increased by 14% whereas the surface area of untreated silica increased by 5% upon outgassing at 673K. The greater increase in surface area for etched silica than for untreated silica upon increasing the outgassing temperature from 373 to 673K may be attributed to greater surface dehydroxylation of the etched silica. Since the etched surface is believed to be more hydroxylated than the untreated silica, outgassing at 673K would result in greater surface dehydroxylation of etched silica. Calculations (53) indicate that as the nitrogen coverage on a dehydroxylated silica gel approaches monolayer coverage, the entropy of adsorption for the nitrogen molecule increases. Therefore, the increased entropy of adsorption may increase the packing density of the nitrogen molecule and hence increase the surface area of the etched silica outgassed at 673K.

Outgassing silica at 373K for .25 hour instead of 2 hours results in surface areas of 4.94 m^2g^{-1}. The outgassing time at 373K does not appear to be critical in surface area measurements.

NASA #2 and NASA #4 samples had a drastically reduced surface area when compared to silica. The smaller surface area resulted in part from the larger particle size of the sample and also from the chemical heterogeneity of the NASA samples.

In summary, an increase in surface area of 5% for silica when the outgassing temperature was increased from 373K to 673K may be due to experimental error. The etching process reduced the surface area of silica outgassed at 373K by 42%. A 14% increase in the sur-

face area of etched silica occurred upon increasing the outgassing temperature to 673K. The etching process and the outgassing temperature of 673K may alter the silica surface and hence the packing density of the nitrogen molecule. The outgassing time is insignificant to surface area determinations of silica. The surface area of NASA #2 and #4 were less than the surface area of silica.

E. Water Adsorption on Untreated Silica

The isotherms for water adsorption at 302K for silica received June 1971 and March 1972 are shown in Figure 10. All adsorption data is listed in Appendix III. The number of moles of water vapor adsorbed increased as the equilibrium pressure increased. The data from this graph was replotted in a comparison plot (54) in Figure 11. The slope was 1.24 and indicates approximately a 20% increase in adsorbance for silica received June 1971. A y-intercept of approximately zero indicates that the surface adsorption characteristics of the two sample lots are similar.

A BET plot for water adsorption at 303K on silica shown in Figure 12 was based upon the water adsorption isotherms for silica received June 1971 and outgassed at 373K. The surface area of silica was determined as 2.8 m^2/g based upon a water cross sectional area of 10.4×10^{-20} $Å^2$/molecule. A surface area of 5.06 m^2/g was previously determined for silica from the BET plots for nitrogen adsorption. The ratio of the water and nitrogen surface areas of silica indicates that the hydrophobic character of silica is approximately 50%.

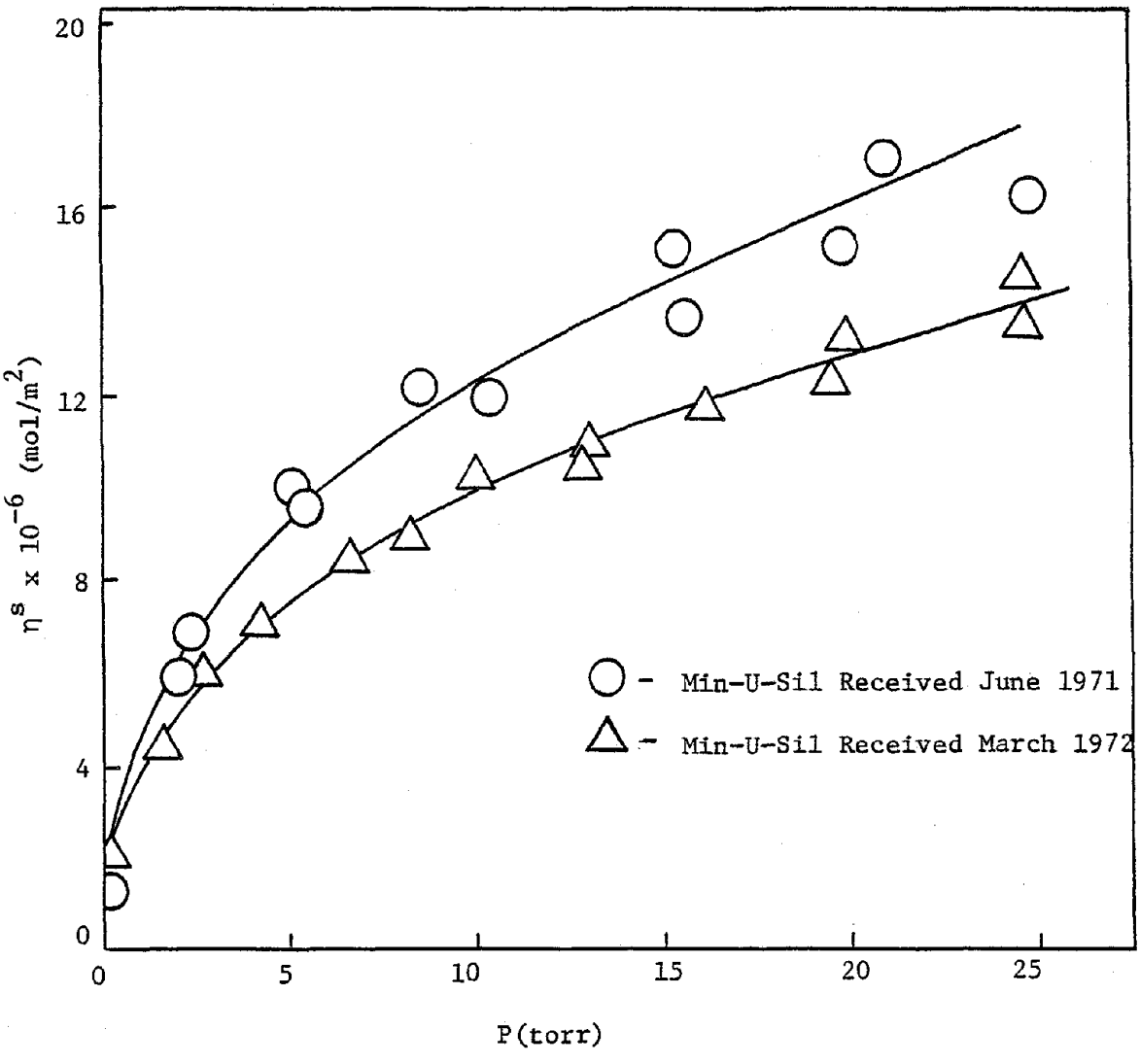

Figure 10. A Comparison of Water Adsorption Isotherms at 302K for Silica Outgassed at 373K from Two Sample Lots.

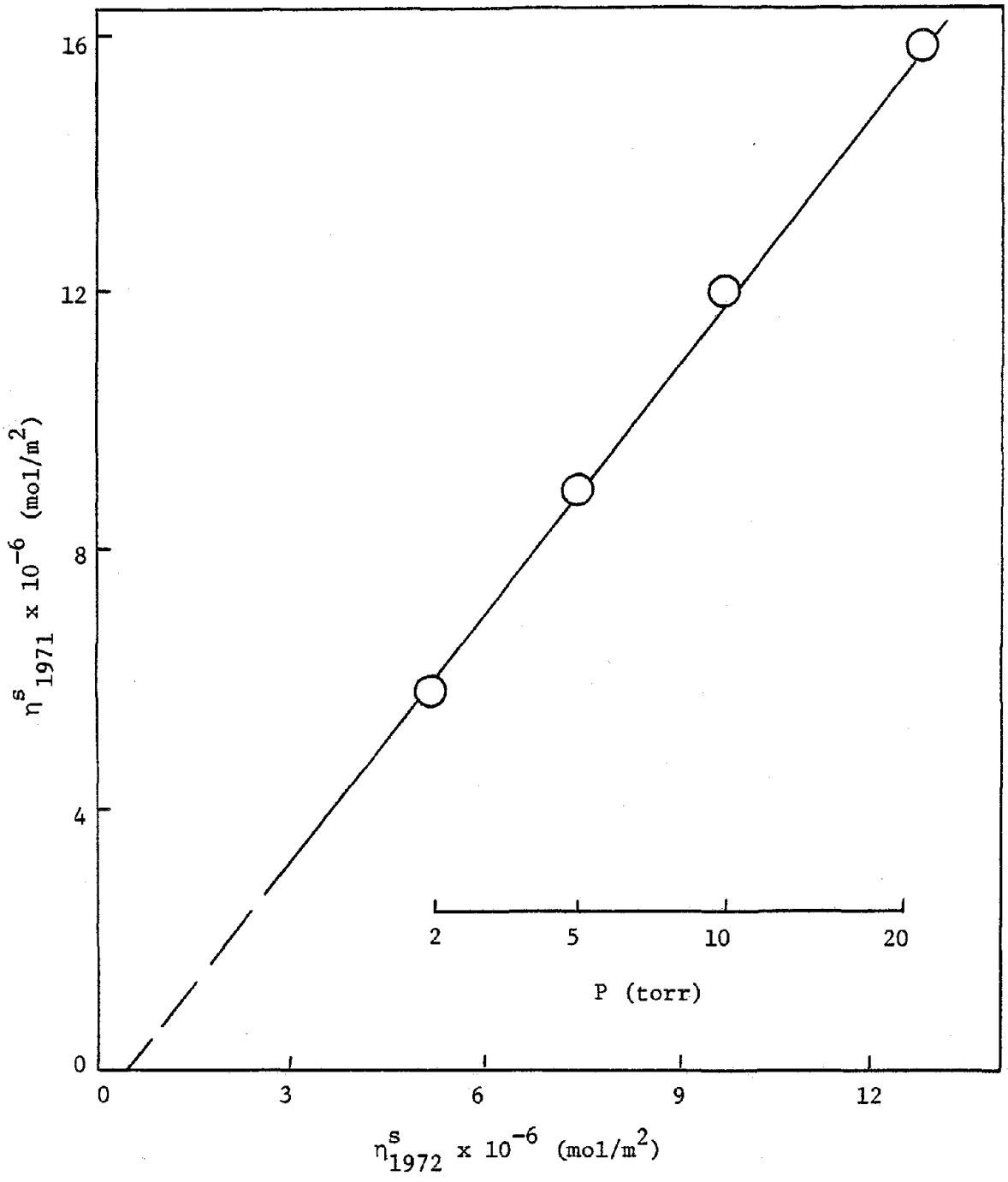

Figure 11. A Comparison Plot of Water Adsorption at 302K for Silica Outgassed at 373K from Two Sample Lots.

Appendix IV contains the adsorption data and calculations for water adsorption on empty sample bulbs. Approximately 0.8% and 0.4% of the water vapor was adsorbed by an empty sample bulb outgassed for 2 hours at 373K and 673K respectively. Thus, water vapor adsorption on the sample bulb was a negligible variable in determining the water adsorption isotherms for silica.

Adsorption isotherms at 302, 313, and 322K for water vapor on silica outgassed at 373K are depicted in Figure 13. It can be noted that water vapor adsorption studies at a specified temperature are reproducible. Statistical analysis of the adsorption data using the F test shows a 95% or greater confidence level that all isotherms at a given temperature represent data points from the same population. An F test calculation is shown in Appendix V. At any given water vapor pressure, the amount of water vapor adsorbed decreased as the temperature increased. At higher temperatures, more kinetic energy is provided for water molecules to desorb from the surface.

The effect of repeated outgassings of silica at 373K on water adsorption at 302K appears to be negligible as shown in Figure 14. The effect of repeated outgassings of silica at 373K on water adsorption at 312K is also negligible as indicated by the adsorption data for experiments #13, #14 and #15 in Appendix III. Outgassing at 373K does not alter the surface structure and apparently removes only physically adsorbed water, which can be replaced (30).

The time interval prior to the adsorption study did not affect the reproducibility of the adsorption work. A sample was outgassed

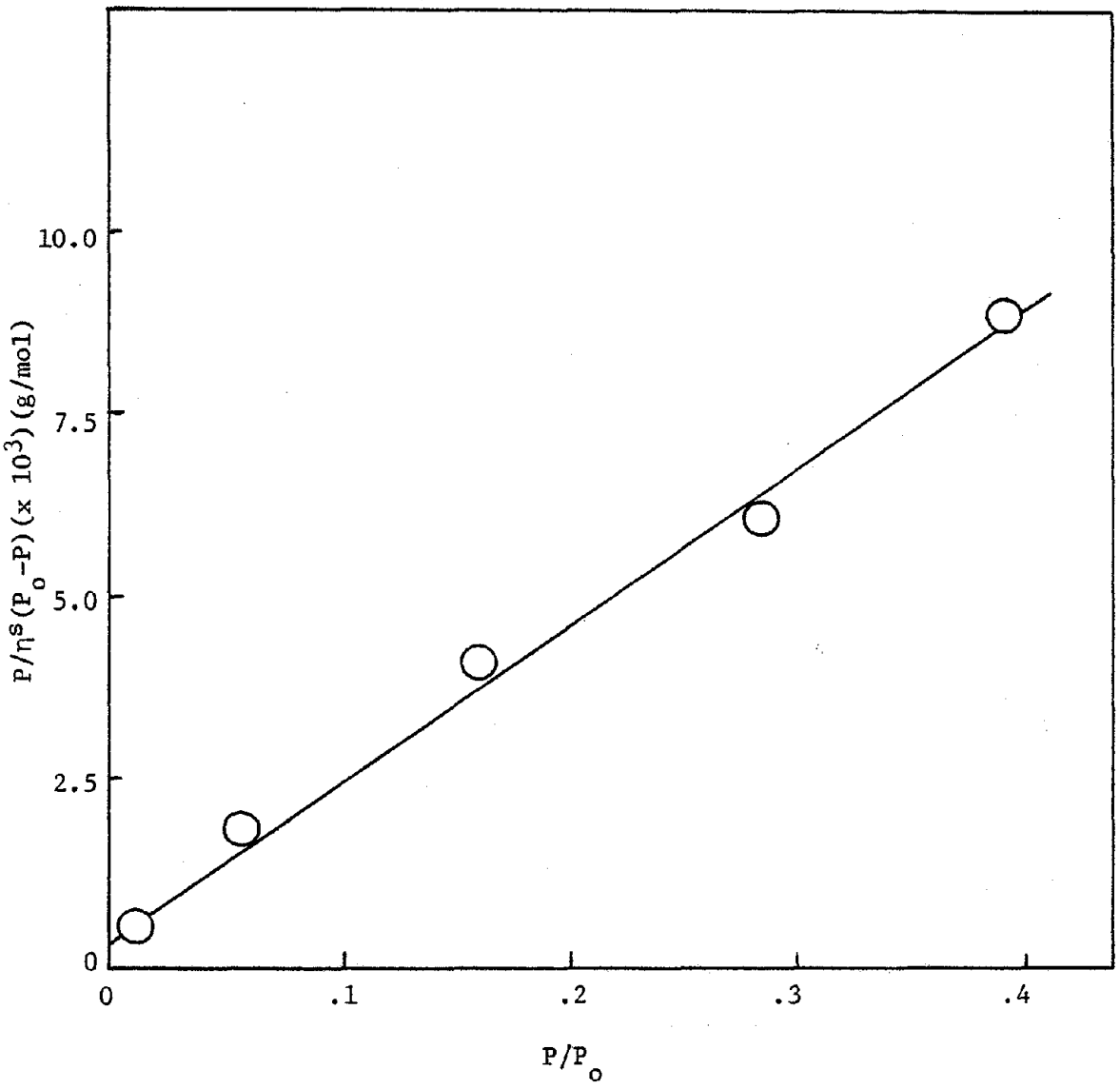

Figure 12. BET Plot for Water Adsorption at 303K on Silica Outgassed at 373K.

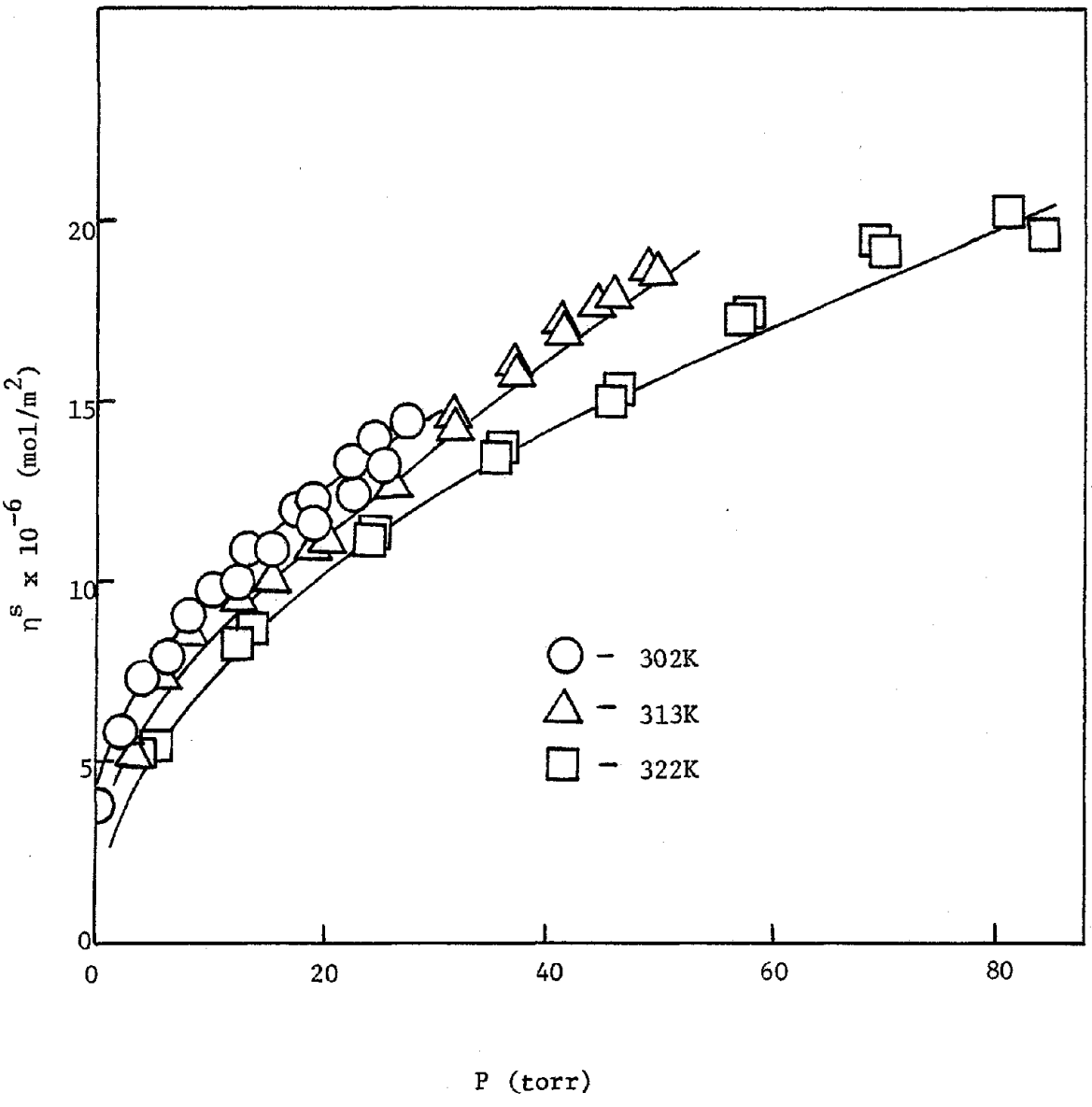

Figure 13. Adsorption Isotherms at 302, 313, and 322K for Water on Silica Outgassed at 373K.

three times at 373K and remained *in vacuo* one month prior to the adsorption study. The adsorption isotherm reproduced the isotherm of a sample outgassed at 373K two times and exposed to water vapor within eight hours of the outgassing treatment. The adsorption data for the above described experiments are in Appendix III.

The water adsorption isotherms at 302K in Figure 14 were used to test the Polanyi model (55). A comparison of the predicted water vapor adsorption at 313K and 322K with experimental results is shown in Figure 15 and a sample calculation is in Appendix VI. It can be noted that the Polanyi model predicts less adsorption at 313K and 322K than was experimentally determined. The lack of correlation between the experimentally determined isotherms at 313K and 322K and the corresponding Polanyi model is not explained.

Adsorption isotherms at 302, 312 and 322K for silica outgassed at 673K are depicted in Figure 16 and surprisingly do not show adsorption to be a function of the ambient temperature. Indications from the literature are that outgassing temperatures greater than 523K result in surface dehydroxylation whereas outgassing at less than 423K removed only physically adsorbed water from the surface (6,30). The effects of isotherm temperature upon the adsorption isotherms could not be predicted for silica outgassed at 673K since the surface had been dehydroxylated and chemical and physical adsorption of water was involved. On the other hand, adsorption was shown to be a function of temperature for silica which was outgassed at 373K since the surface was not altered and only physical adsorption of water was involved.

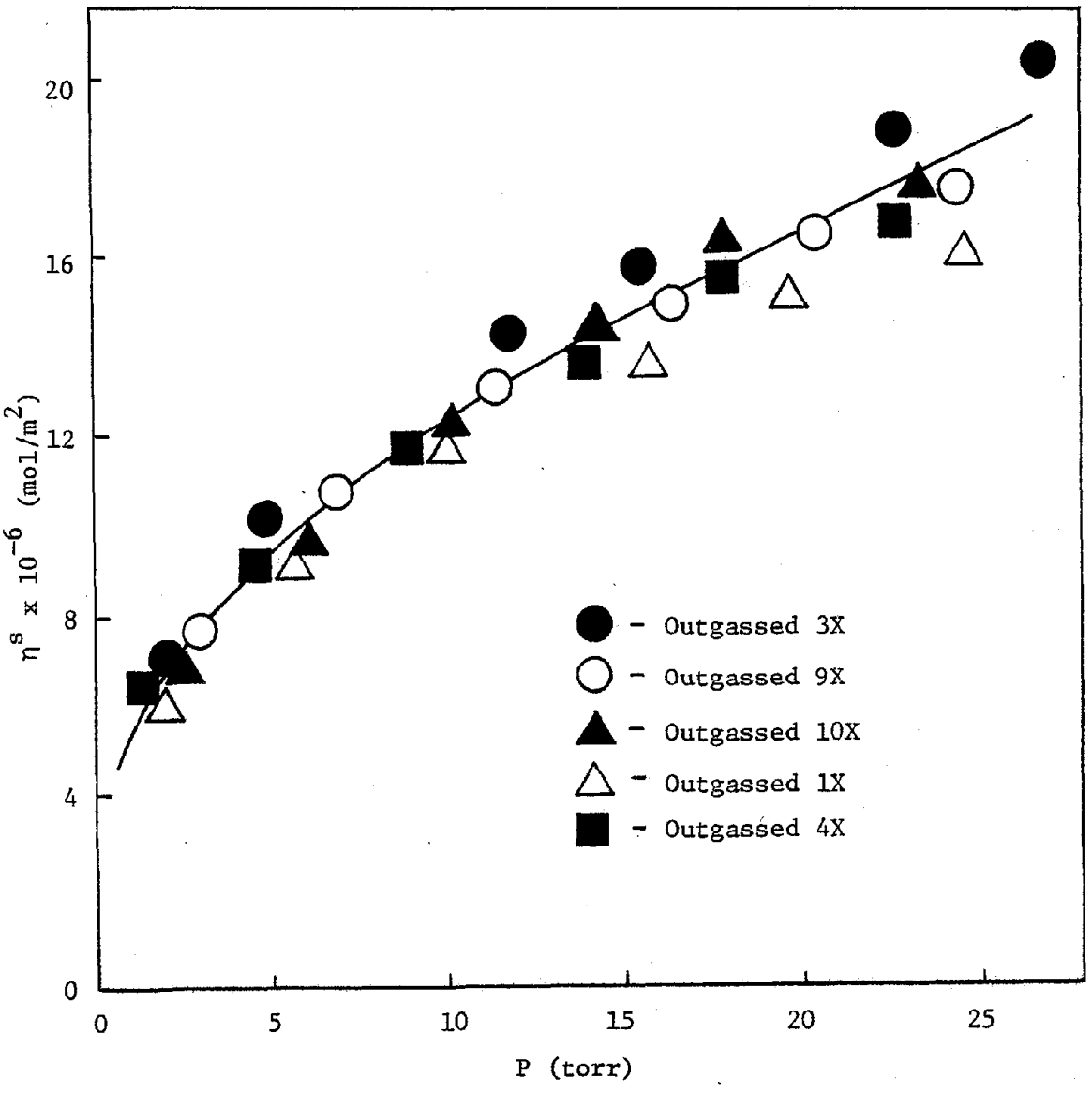

Figure 14. The Effect of Repeated Outgassings of Silica at 373K on Water Adsorption at 302K.

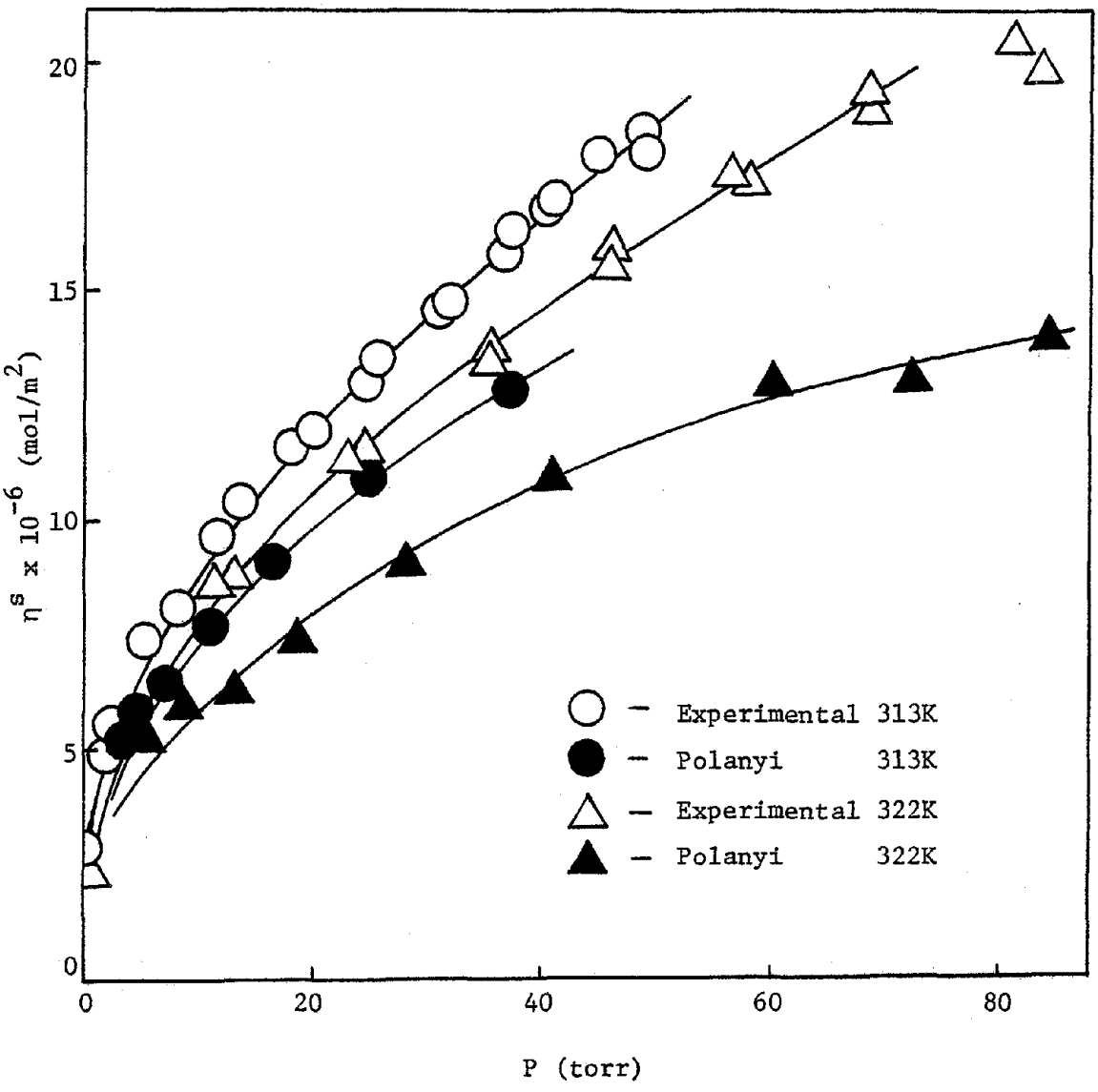

Figure 15. A Comparison of the Polanyi Model and Experimental Results for Water Adsorption at 313K and 322K on Silica Outgassed at 373K.

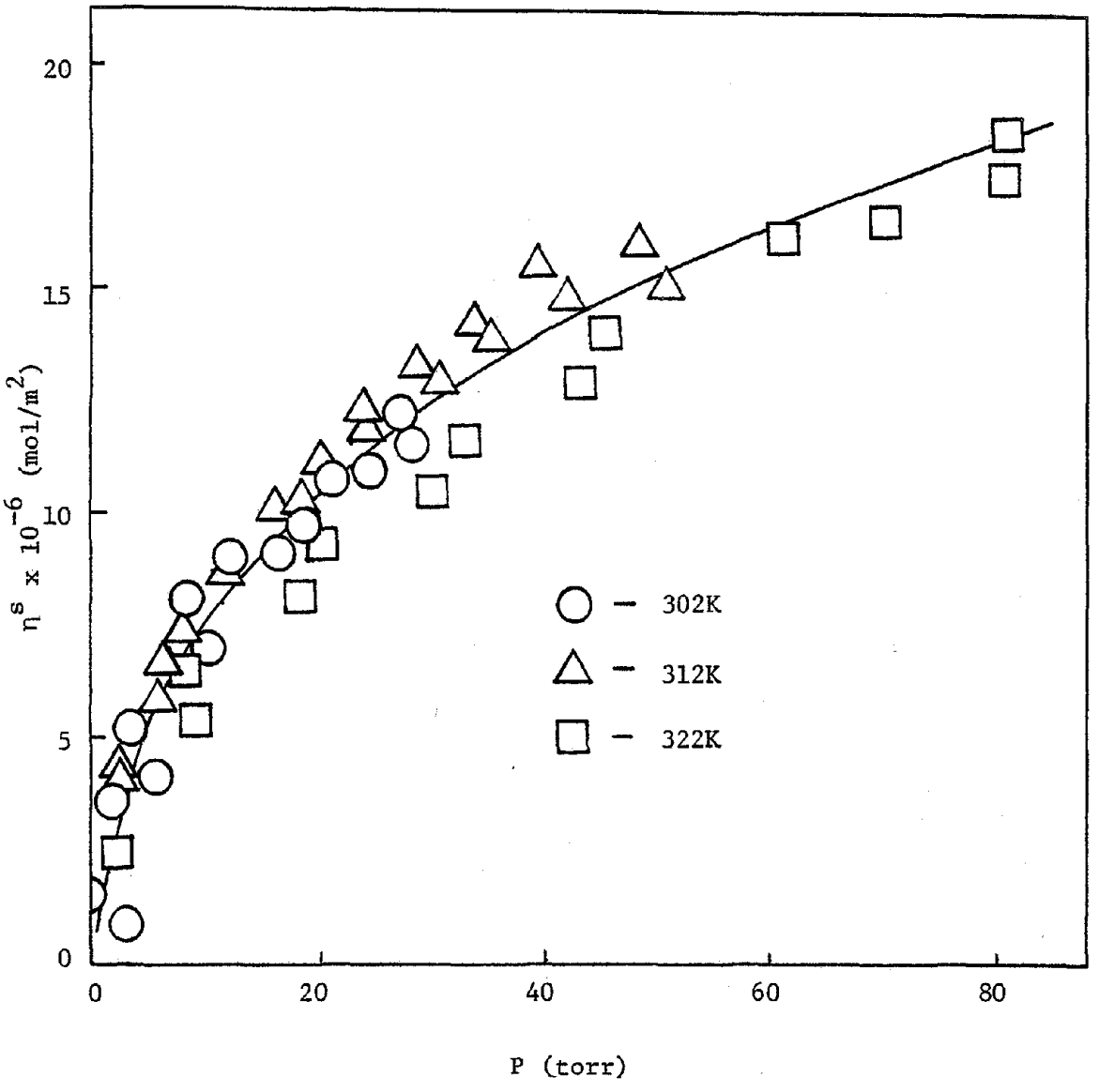

Figure 16. Adsorption Isotherms at 302, 312 and 322K of Water on Silica Outgassed at 673K.

A comparison plot of water adsorption at 302K for silica outgassed at 373K and 673K in Figure 17 has a slope of 0.86 and a y-intercept of 3.7. The slope of 0.86 indicates that the incremental increase in adsorption is less for silica outgassed at 373K than for silica outgassed at 673K. The y-intercept of 3.7 indicates that the adsorption on silica outgassed at 373K is greater than on silica outgassed at 673K at a given pressure.

Reoutgassing silica at 673K decreased the adsorption of water at 302K denoted in Figure 18. There is approximately a 20% decrease in the adsorption of water at a pressure of 20 torr (2666 Pa) after reoutgassing silica at 673K. The irreversibility of water adsorption for silica outgassed at 673K may be attributed to surface dehydroxylation (26,27,30).

To recapitulate, the two sample lots of silica had similar water adsorption characteristics. Water adsorption isotherms for silica outgassed at 373K or reoutgassed at 373K were reproducible and a function of isotherm temperature. Water adsorption predicted by the Polanyi model at 313 and 322K was less than experimentally determined. Water adsorption on silica outgassed at 673K was not a function of isotherm temperature. Reoutgassing silica at 673K decreased water adsorption at 302K. The surface adsorption characteristics of silica were altered by increasing the outgassing temperature from 373 to 673K.

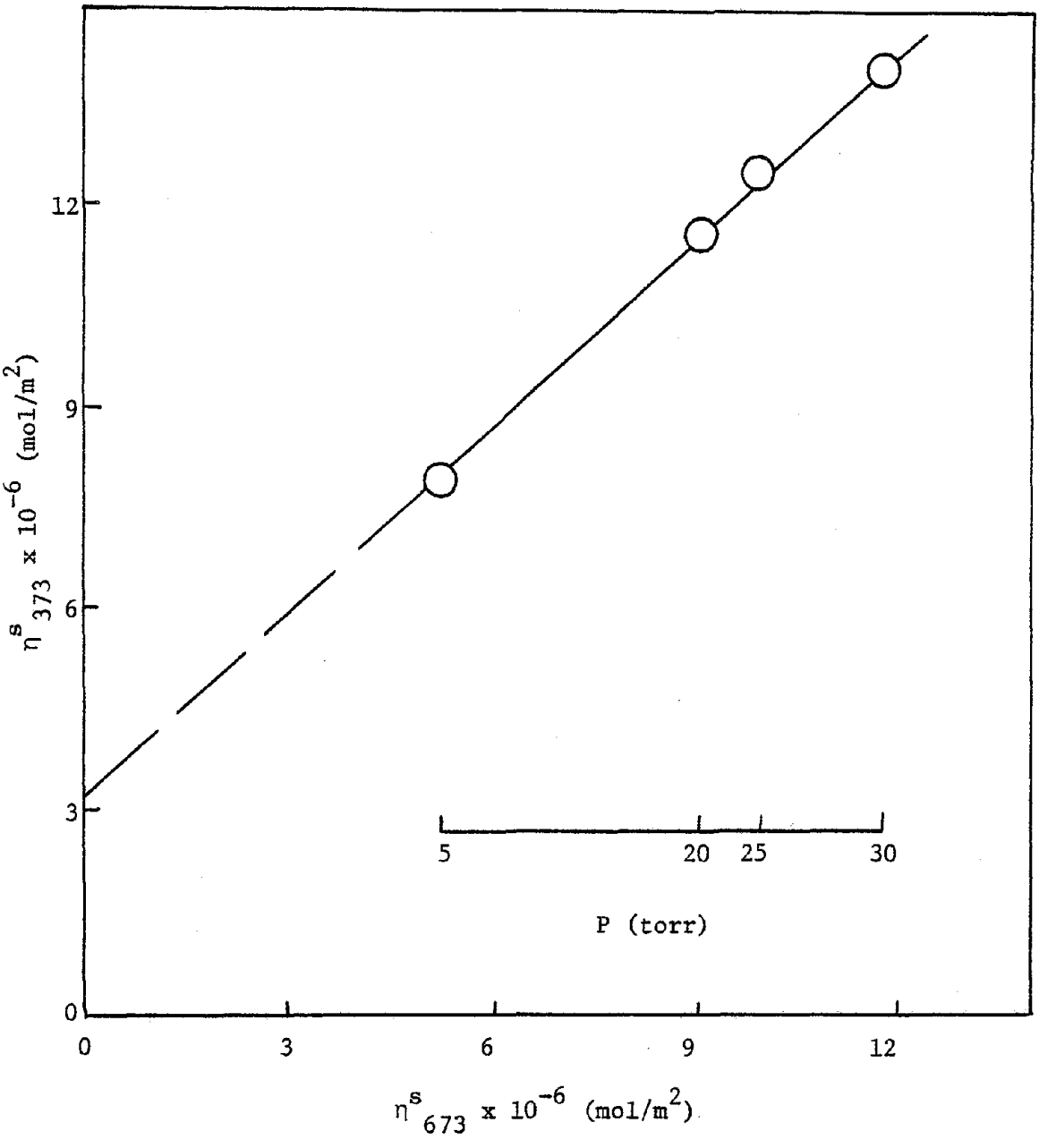

Figure 17. Comparison Plot of Water Adsorption at 302K for Silica Outgassed at 373K and 673K.

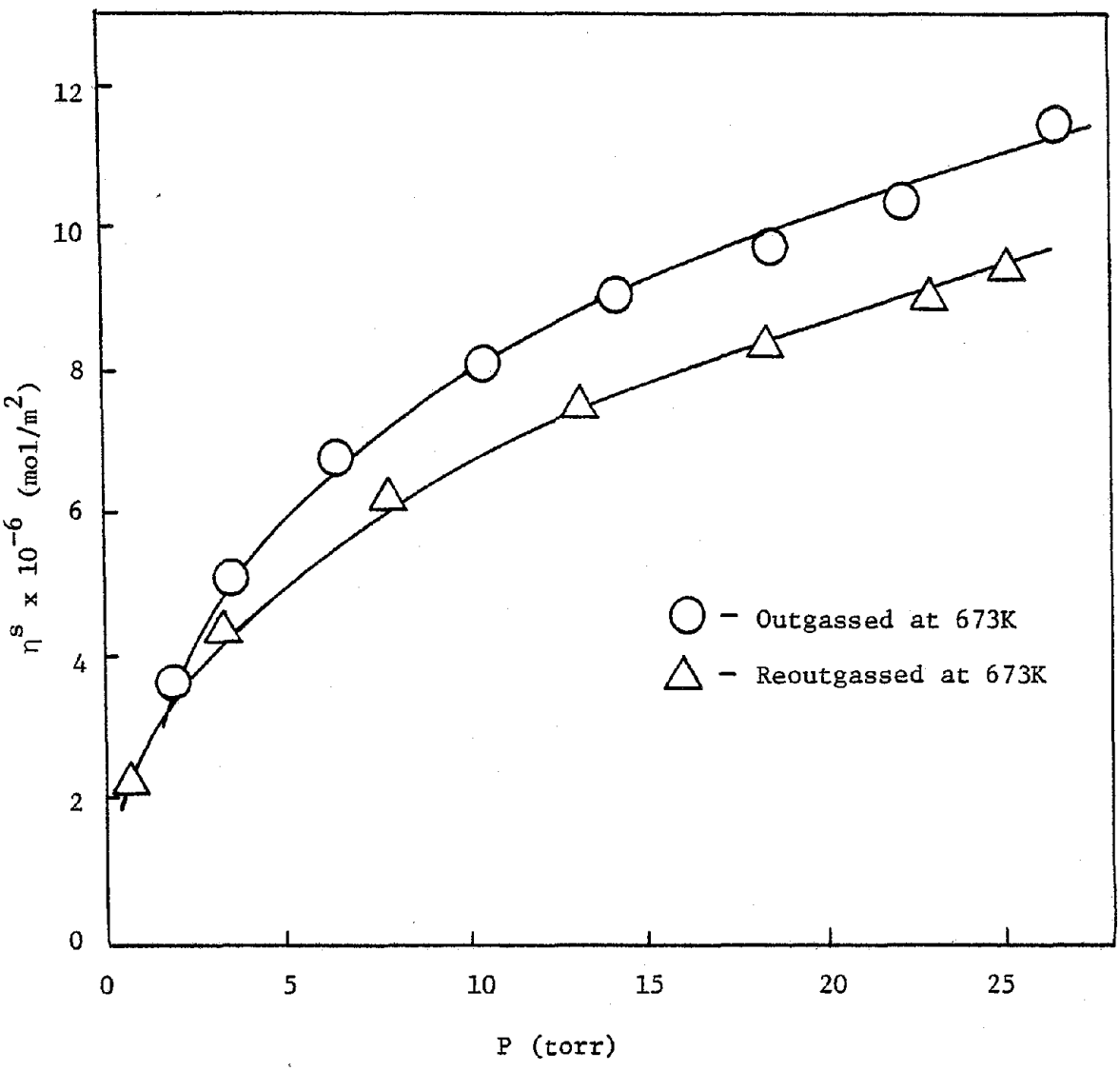

Figure 18. The Effect of Reoutgassing Silica at 673K on the Adsorption of Water at 302K.

F. Water Adsorption on Etched Silica

The adsorption isotherms of water vapor on one etched silica sample reoutgassed several times at 373K and reoutgassed several times at 673K is shown in Figure 19, and the data is shown in Appendix VII. More water was adsorbed on etched silica outgassed at 373K than on the same sample outgassed at 673K which may result from the irreversibility of water adsorption on a dehydroxylated silica surface. It has been determined that the number of sites that could be rehydrated by water vapor decreased upon heating from 673K to 1123K (15). The isotherms were reproducible for etched silica outgassed at 373K and at 673K. Reproducibility of water adsorption on untreated silica reoutgassed at 673K was not obtained as shown in Figure 19. The etched silica surface may rehydroxylate more readily than the untreated silica surface upon outgassing at 673K and reexposure to water vapor.

A further indication of surface reactivity differences between etched and untreated silica outgassed at 373K or 673K is evident from the non-zero intercept in the comparison plot in Figure 20. The comparison plot of untreated silica and etched silica outgassed at 373K had a slope of 1.1 which indicates a 10% greater increase in water adsorption on untreated silica than on etched silica. However, a comparison plot of untreated and etched silica outgassed at 673K had a slope of .73 and indicated a 27% greater increase in water adsorption on the etched silica when compared to untreated silica.

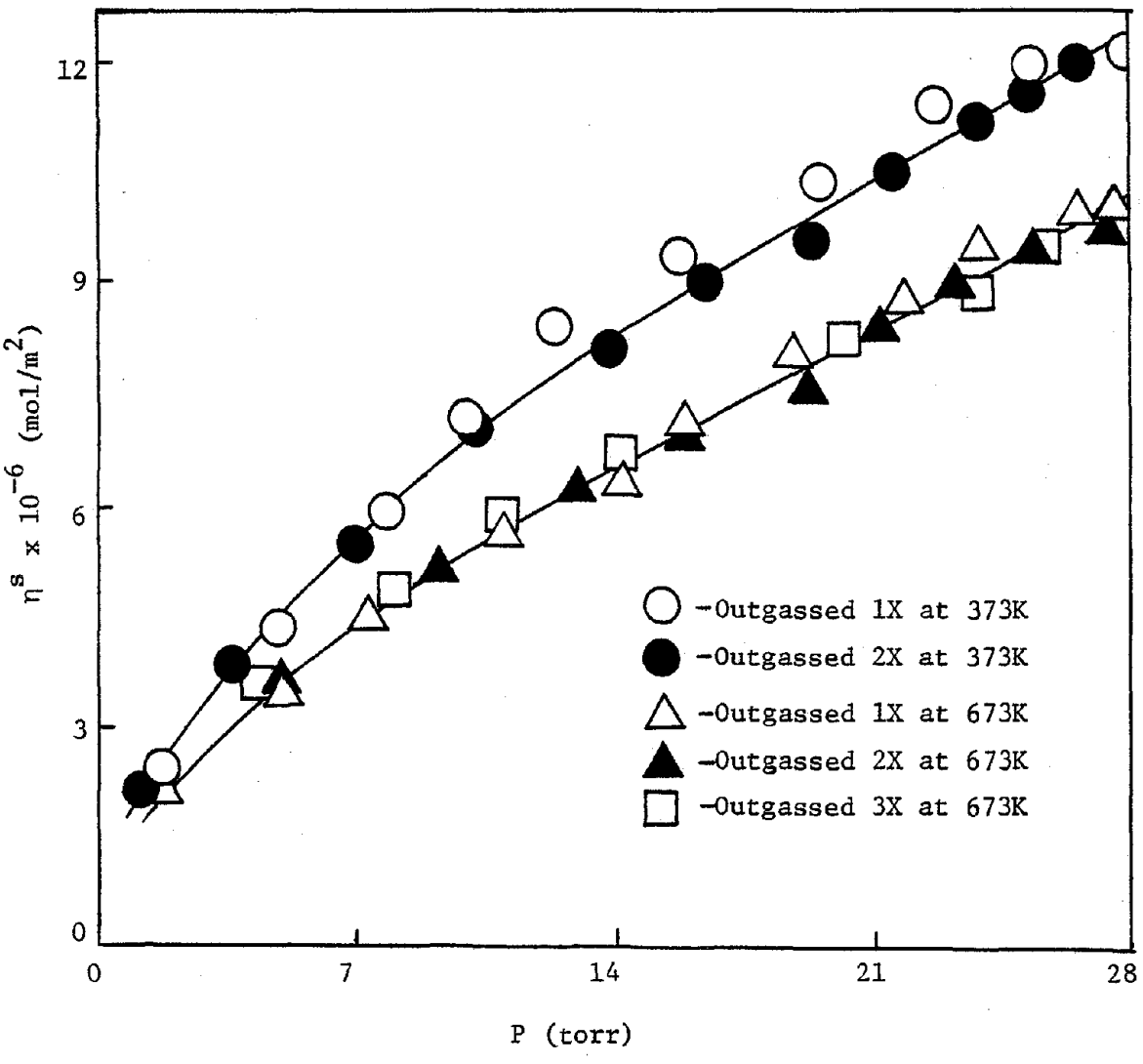

Figure 19. Effect of Repeated Outgassings of Etched Silica at 373K and 673K on Water Adsorption at 302K.

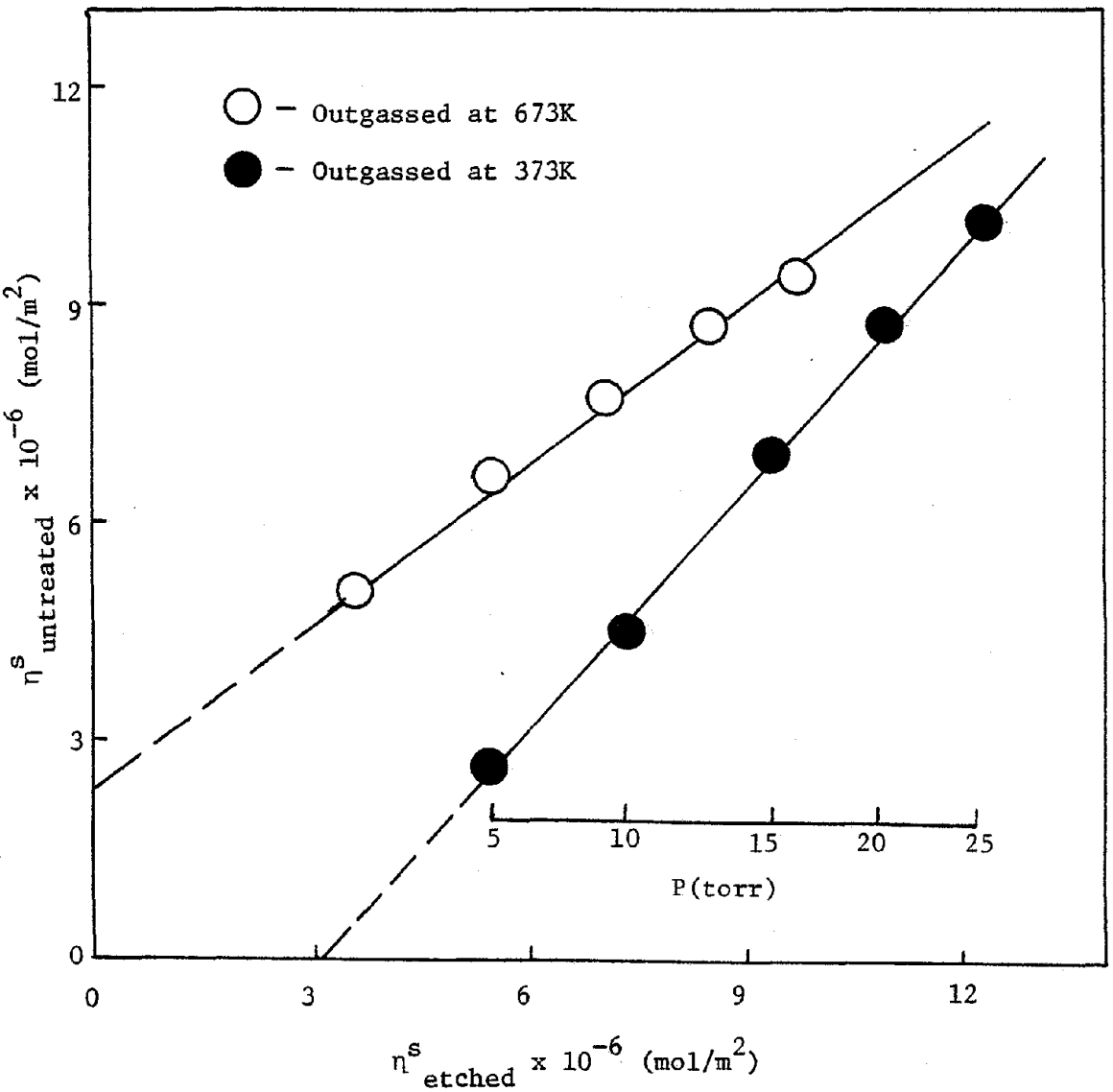

Figure 20. Comparison Plot for Water Adsorption at 302K on Etched and Untreated Silica Outgassed at 373K or 673K.

In conclusion, comparative studies of water adsorption on untreated silica and etched silica indicate that the two silicas have different surfaces, which are affected differently by the outgassing temperature. There is a greater increase in water adsorption on unetched than etched silica outgassed at 373K. Apparently the removal of the amorphous layer of silica by the etching process decreased physical adsorption of water. Conversely there is a greater increase in water adsorption on etched silica than untreated silica outgassed at 673K. Water is adsorbed reversibly on etched silica outgassed at 673K but not on untreated silica outgassed at 673K. The increased water adsorption and reversibility of water adsorption on etched silica compared to untreated silica outgassed at 673K may be due to a greater tendency for rehydroxylation of the etched surface.

G. Heats of Immersion Studies

The heats of immersion at 310K for silica in water are shown in Table II. The number in brackets beside the sample indicates the number of determinations. The heats of empty bulb breaking were determined also and are listed in Appendix XIII. Empty bulb breaking contributed approximately 5.0% to the heat of immersion studies in water for silica outgassed at 373K and at 673K.

Whalen (30) reported a heat of immersion of 340 mJ/m^2 for quartz outgassed at 373K with a surface area of 7.15 m^2/g and < 5 μ particles.

Table II

Heats of Immersion at 310K for Silica in Water

Sample	Outgassing Temperature (K)	Heats of Immersion (mJ/m^2) Corrected for Empty Bulb Breaking
Silica [2]	373	364
Silica [3]	673	447
Etched Silica [4]	373	239
Etched Silica [3]	673	301

He also reported a heat of immersion of 380 mJ/m^2 for the quartz outgassed at 673K. The outgassing time of these samples was dependent upon attainment of a pressure of 10^{-6} torr (1.33×10^{-4} Pa).

The heats of immersion in water of quartz used by Whalen differ from the values determined for silica in this study. The heats of immersion in water for silica outgassed at 373K differed by 7% from Whalen's study. The heats of immersion in water for silica outgassed at 673K differ by 15% from Whalen's study. Quartz in Whalen's study had approximately a 10% increase in the heats of immersion upon increasing the outgassing temperature to 673K whereas there was approximately a 20% increase for silica. Since the purity and history of the samples undoubtedly differ, the differences in the heat of immersion for quartz reported in the literature and values obtained for silica were not surprising.

Silica used in this study and the quartz used in Whalen's study indicate an increase in the heat of immersion in water for the sample upon increasing the outgassing temperature from 373 to 673K. This is an expected trend; removal of physisorbed and chemisorbed water upon outgassing at 673K would result in dehydroxylation of the surface. Wetting of the silica which was outgassed at 673K and is more dehydroxylated may provide a greater heat of immersion than wetting of a silica surface outgassed at 373K which is more fully hydroxylated.

Table II shows that the chemical etching of silica decreases the heat of immersion in water in comparison to untreated silica. The etching process counteracts condensation on the silica surface (35).

Therefore more hydroxyls would be expected on the etched surface and the heat of immersion would be less than for untreated silica.

Etched silica and untreated silica showed a comparable increase of approximately 20% in the heat of immersion in water upon increasing the outgassing temperature to 673K. This indicates that surface dehydroxylation increases the heat of immersion in water for both etched and untreated silica.

In summary, literature values of heats of immersion in water for quartz outgassed at 373 or 673K are approximately 11% greater than values obtained in this work for silica. The difference in heat of immersion values may be attributed to the purity and past history of the samples. Untreated silica had higher heats of immersion in water than etched silica at both outgassing temperatures. Etched silica outgassed at 373K or 673K may have a more hydroxylated surface and hence a decreased heat of wetting. Increasing the outgassing temperature to 673K for both untreated and treated silica increased the heat of immersion by approximately 20%, which may be attributed to the increased surface dehydroxylation upon outgassing at 673K.

H. Water Adsorption on NASA #2 and NASA #4

The water adsorption isotherms at 303K for actual soil samples surrounding a launch complex are shown in Figure 21 and the data is listed in Appendix IX. A comparison plot for water adsorption on NASA #2 and NASA #4 in Figure 22 indicates that surface characteristics

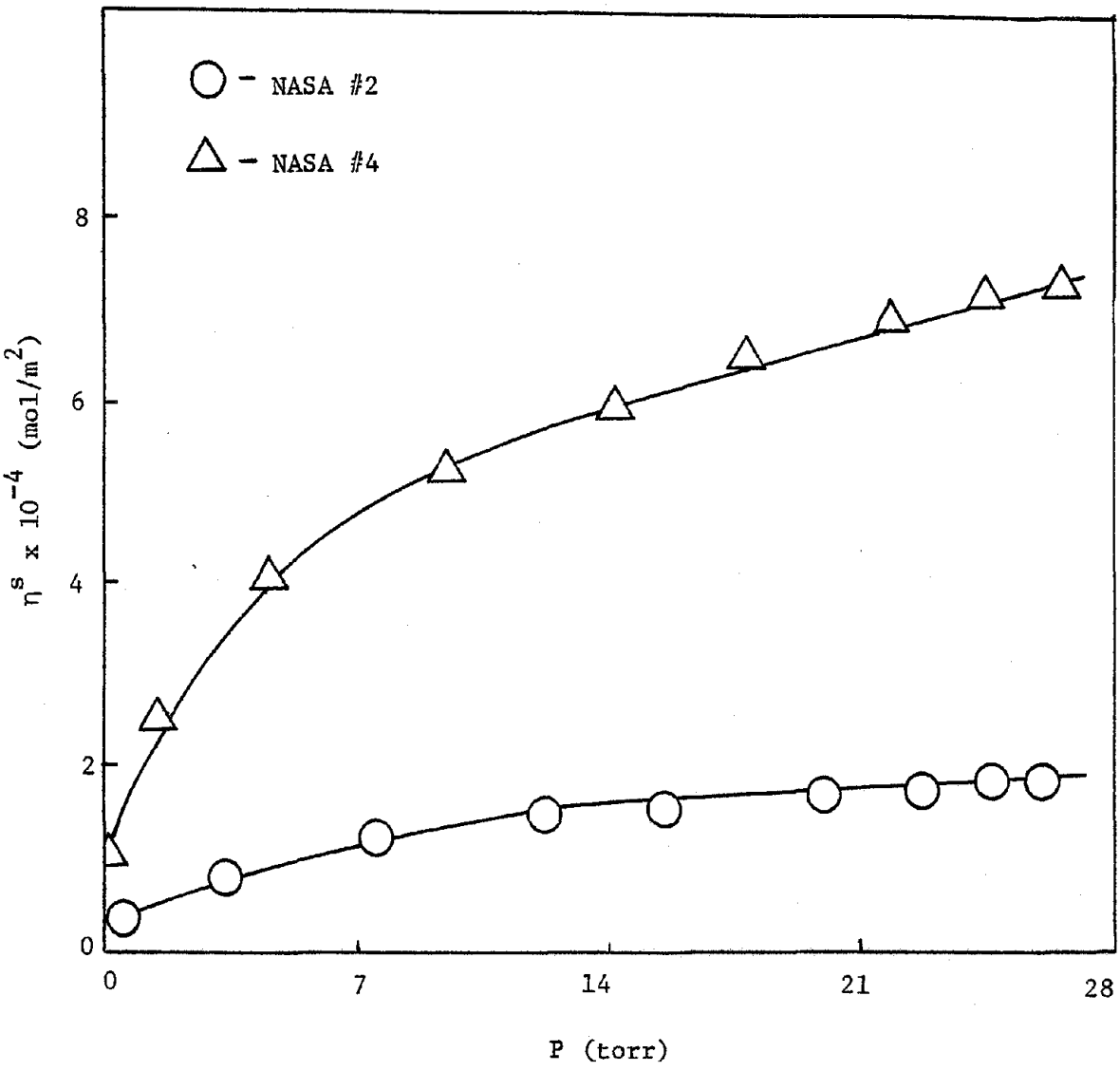

Figure 21. Adsorption Isotherms at 303K for Water on NASA #2 and NASA #4 Outgassed at 373K

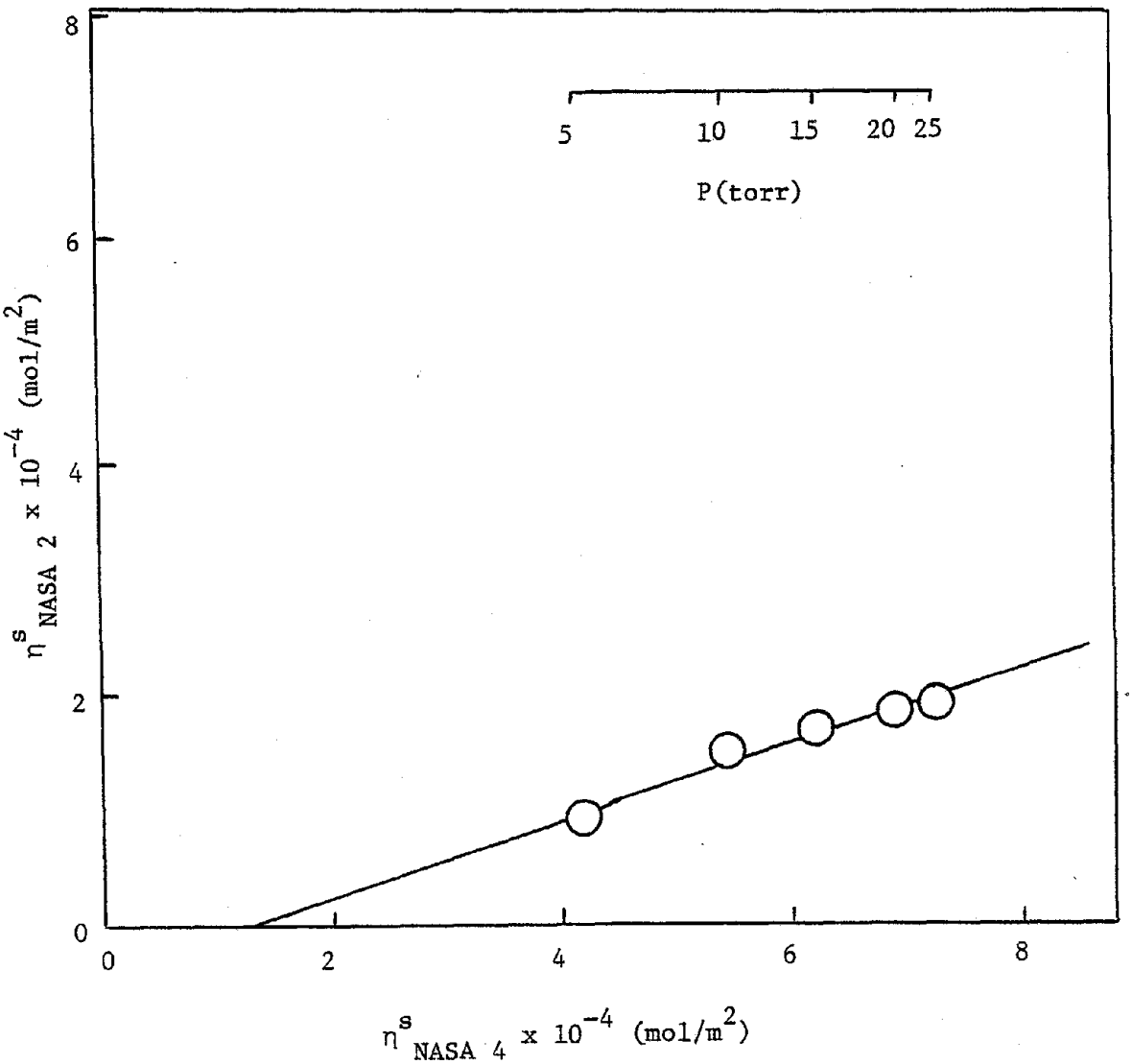

Figure 22. Comparison Plot for Water Adsorption at 303K on NASA #2 and NASA #4 Outgassed at 373K.

of the soil samples differ. A slope of .32 indicates a 68% increase in adsorption on NASA #4 compared to NASA #2. A non-zero y-intercept indicates that the two samples have different water adsorbance capacities. The difference in the water adsorbance characteristics of the two samples may be attributed to the variations in the soil constituents of the two sampling areas.

Table III shows a fractional analysis of NASA #2; a similar analysis was not available for NASA #4. It can be seen that NASA #2 is a heterogeneous sample composed of quartz, mica, heavy minerals, organic matter and clay, and consisting of particle sizes that range from less than 2 μ to greater than 1000 μ. It can be noted that 88% of medium sand, the largest fraction in NASA #2, is quartz.

Figure 23 compares the water adsorption isotherms at 303K for silica, NASA #2 and NASA #4 outgassed at 373K on the basis of moles of water vapor adsorbed per gram of sample. A comparison of water adsorption based upon moles per gram was utilized instead of moles per square meter to eliminate the effects of nitrogen surface area determinations of heterogeneous samples upon the water adsorption calculations. The figure shows that NASA #2 and silica outgassed at 373K have comparable water adsorption at specified water vapor pressures, whereas the adsorption isotherms of silica and NASA #4 are less comparable. The data for water adsorption on NASA #2, NASA #4 and silica is replotted in a comparison plot in Figure 24. A slope of 1.07 indicates that there is a 7% increase in adsorption for silica compared to NASA #2 and a y-intercept of approximately zero for a com-

TABLE III

Fractionation Analysis: NASA #2

Fraction	Size Range	%
Organic Matter		0.53
Clay	< 2 μ	0.04
Silt	50μ - 2μ	1.01
Very Fine Sand	105μ - 50μ	1.79
Fine Sand	250μ - 105μ	32.86
Medium Sand	500μ - 250μ	51.97
Coarse Sand	1000μ - 500μ	11.03
Very Coarse Sand	>1000μ	0.77

Mineralogy of Sand Fraction

500μ - 250μ	Quartz:	88%
	Mica:	5%
	Heavy Minerals:	6%
105μ - 50μ	Quartz:	60%
	Feldspar:	6%
	Mica:	2%
	Heavy Minerals:	32%

Heavy minerals are minerals with specific gravity greater than 2.86. They include Eipdote, Hornblende, Zircon, Apatite, Tourmaline, Magnetite and Ilmenite.

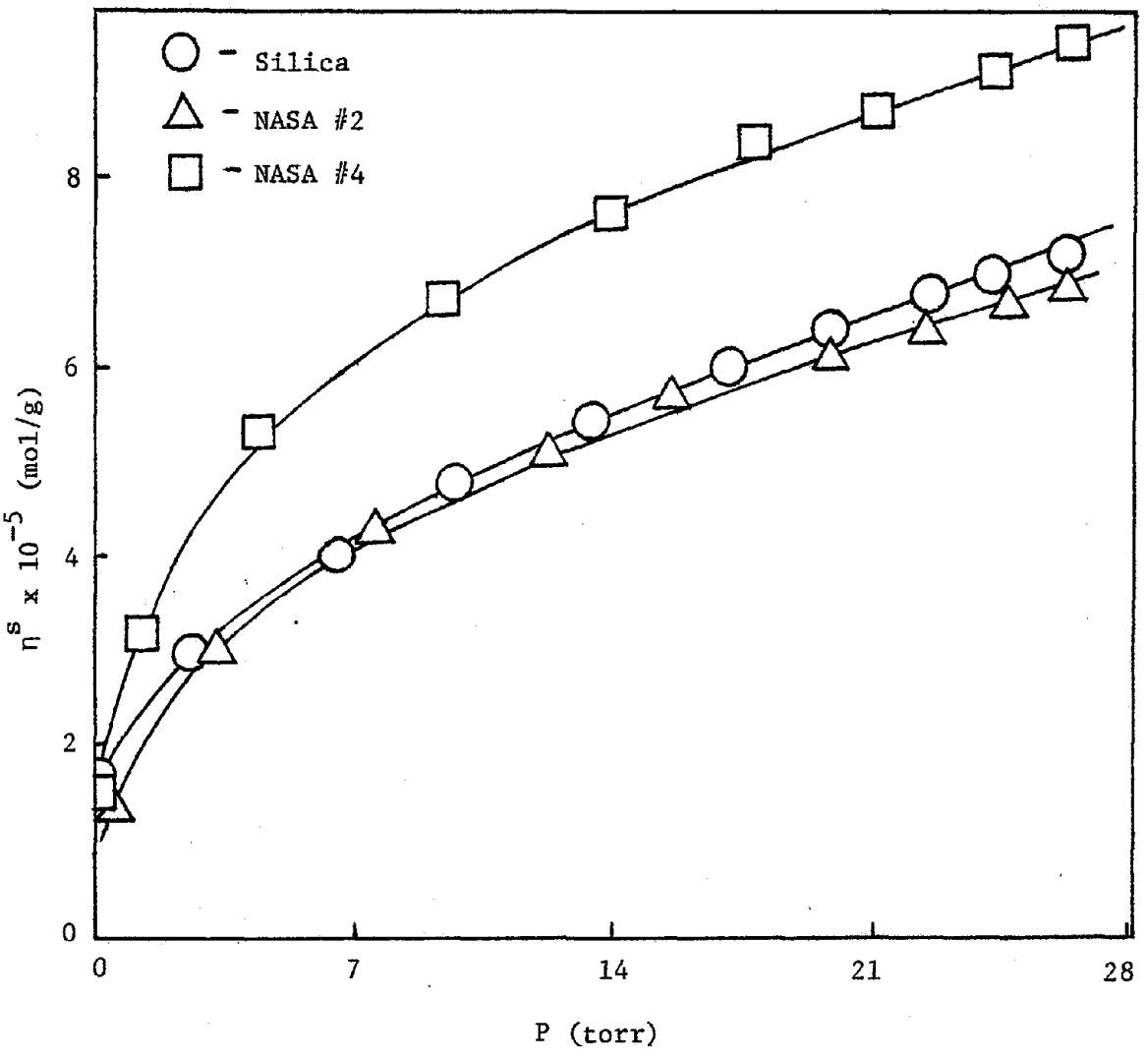

Figure 23. Water adsorption at 303K on Silica, NASA #2, and NASA #4 Outgassed at 373K.

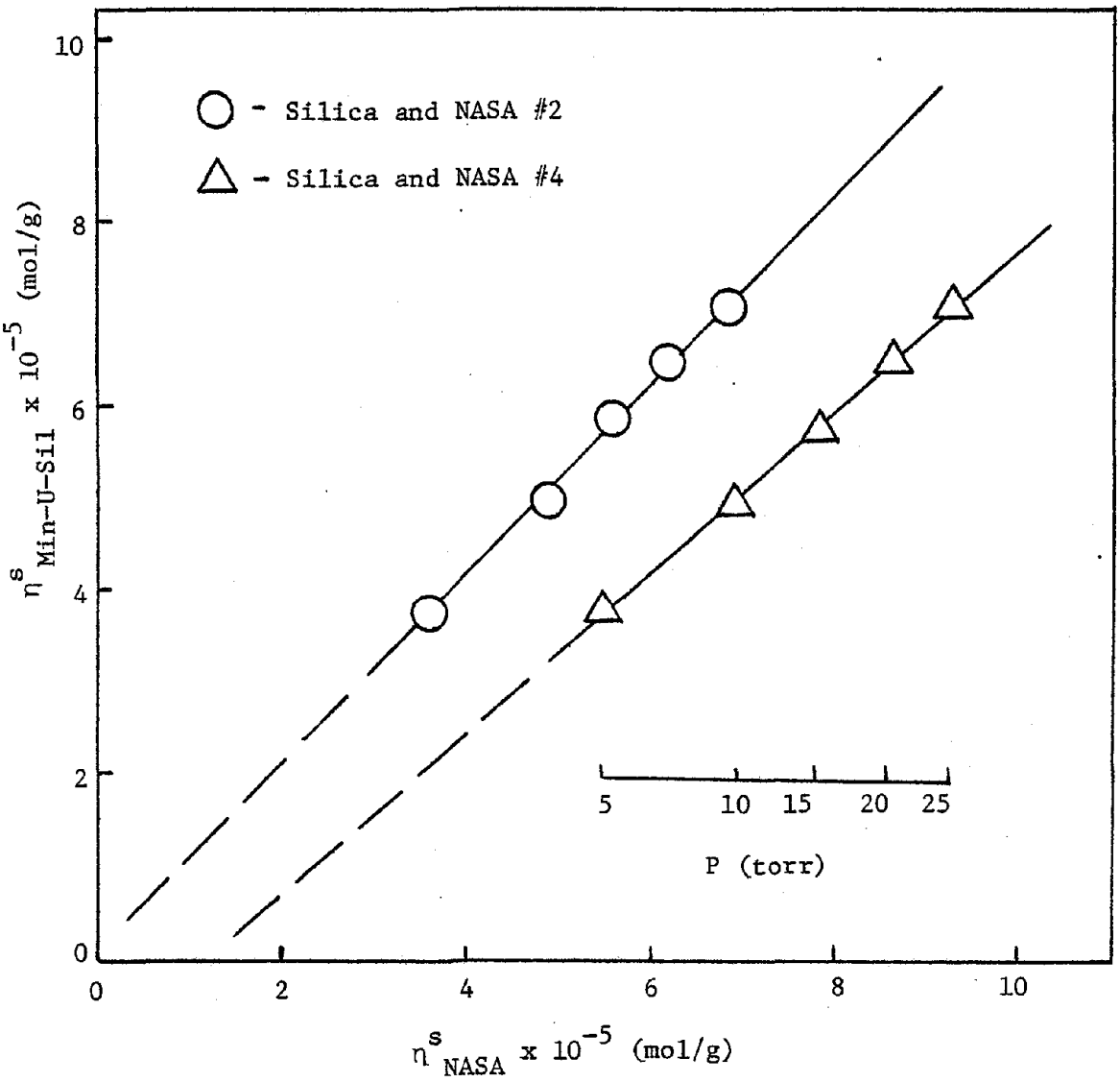

Figure 24. Comparison Plot for Water Adsorption at 303K on Silica and NASA #2 or NASA #4 Outgassed at 373K.

parison plot of silica and NASA #2 indicates that the two samples are similar in adsorption characteristics. Therefore NASA #2 and silica have similar water adsorption characteristics. Conversely a comparison plot of NASA #4 and silica has a slope of 0.89 which indicates an 11% increase in water adsorption for NASA #4 compared to silica. A non-zero intercept indicates that the adsorption capacity at any specified pressure is greater for NASA #4 than silica.

In summary, NASA #2 was shown to be heterogeneous in composition with 88% of the largest fraction composed of quartz. The water adsorption isotherm for NASA #2 at 303K was comparable to the water adsorption isotherm obtained for silica when both samples were outgassed at 373K. The water adsorption isotherm obtained for NASA #4 outgassed at 373K was greater than the isotherm for silica outgassed at 373K. Because a fractional analysis of NASA #4 was not available, the reason for the increased water adsorption on NASA #4 in comparison to silica and NASA #2 cannot be explained. It is evident that the water adsorption characteristics on silica, the model compound, are similar for NASA #2 but dissimilar for NASA #4.

I. Chlorine Adsorption on Untreated Silica

Figure 25 shows the adsorption isotherms at 303K for chlorine gas on silica outgassed at 373K or 673K. Three samples were outgassed at 373K and four samples were outgassed at 673K. Because the adsorption data did not reproduce, an average adsorption of chlorine is plotted and error bars shown. The data is shown in Appendix X.

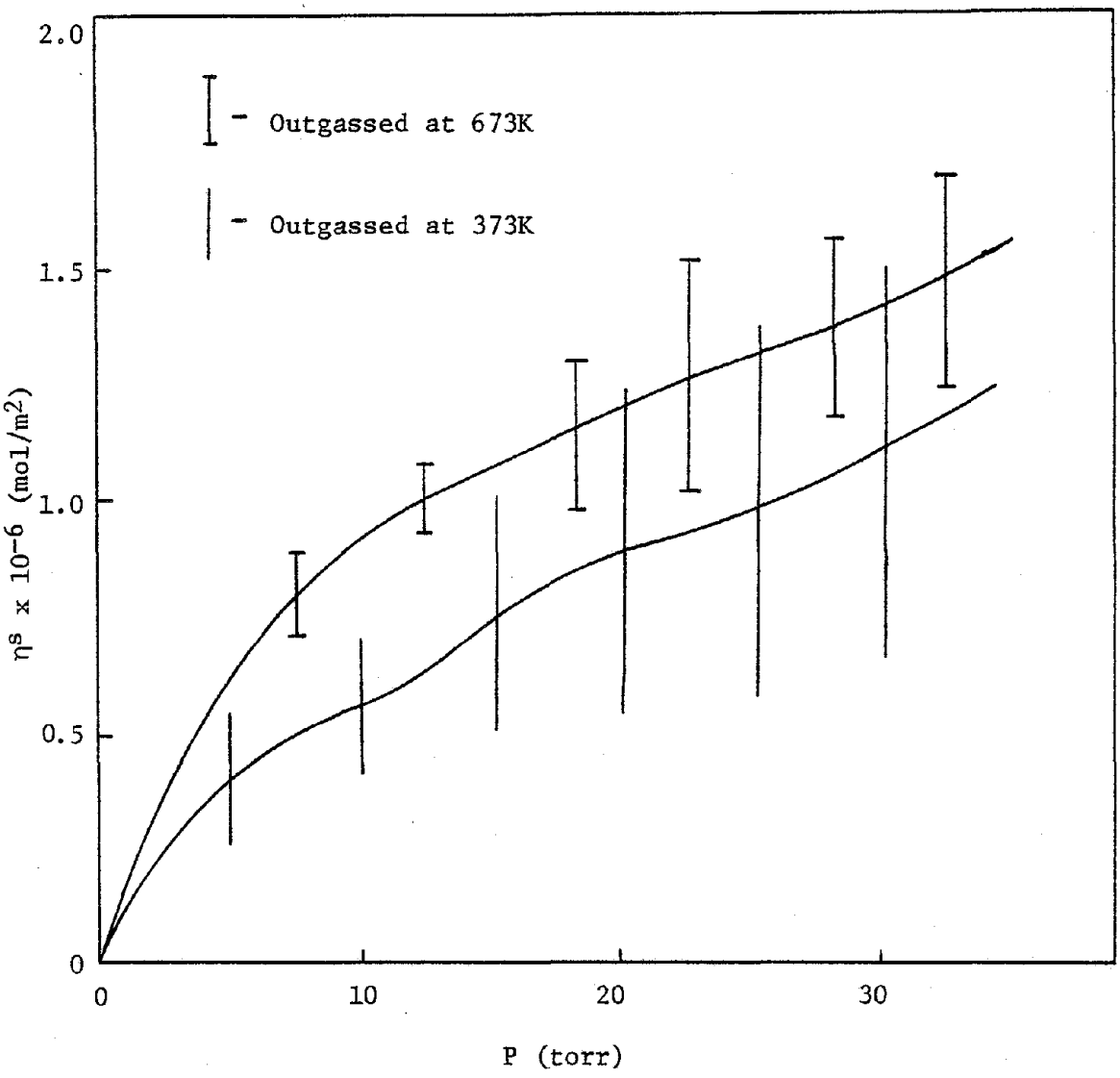

Figure 25. Adsorption Isotherms at 303K for Chlorine on Silica Outgassed at 373K or 673K.

Lack of reproducibility for chlorine adsorption on silica may be attributed to the error in measurements due to the small pressure drops from chlorine adsorption. The reproducibility of chlorine adsorption may also be complicated by hydrolysis of a possible chlorosiloxane species on the sample surface. Hydrolysis produces the halogen halide and a surface silanol (34,35,41). The extent of hydrolysis of the chlorosiloxane would be dependent upon the water vapor present on the glass walls of the adsorption apparatus.

The silica samples were reoutgassed at 373K or 673K to determine the effects of reoutgassing upon chlorine adsorption at 303K. The average adsorption values and associated error bars of chlorine on silica were similar to the values represented by the isotherms in Figure 25. Therefore, reoutgassing silica at 373K and 673K and reexposure to chlorine gas does not alter the chlorine adsorption isotherm. Appendix X contains the adsorption data for these experiments.

Figures 26 and 27 illustrate adsorption of water and chlorine respectively as a function of the relative pressure, (P/P_0), where P_0 is the vapor pressure of the adsorbate at a specified temperature. It can be noted that on silica outgassed at 373K, the chlorine gas adsorption ranged from 0.25 to 1.4 x 10^{-6} mol/m^2 in the P/P_0 ranges from 0.0001 to 0.005. Water adsorption on silica ranges from 2.0 to 14.0 x 10^{-6} mol/m^2 in a P/P_0 range from 0.01 to 0.8. Therefore there is no overlap in the adsorption at any given P/P_0 for chlorine and water vapor, and the two isotherms cannot be compared.

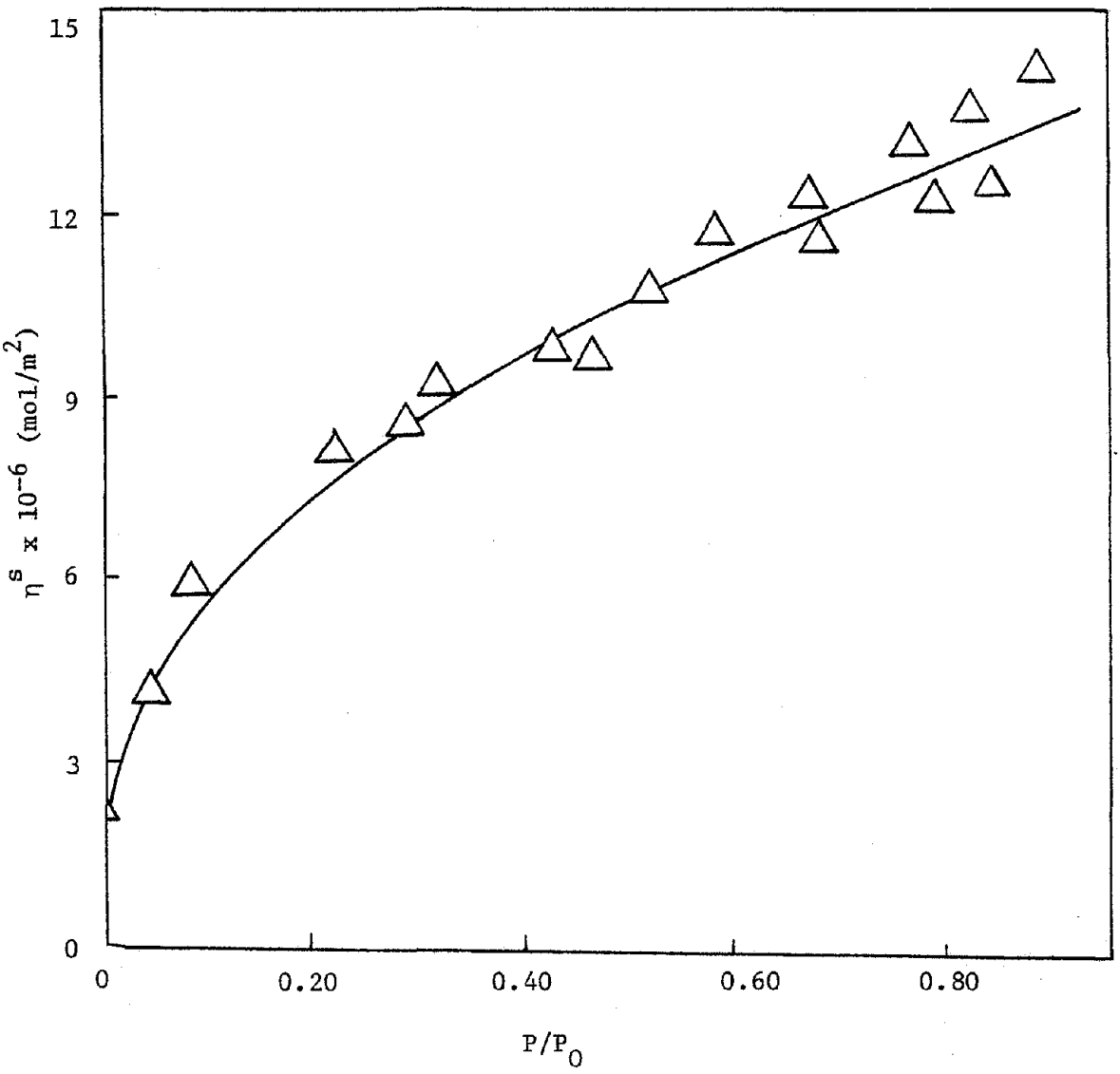

Figure 26. Adsorption Isotherms at 302K for Water on Silica Outgassed at 373K.

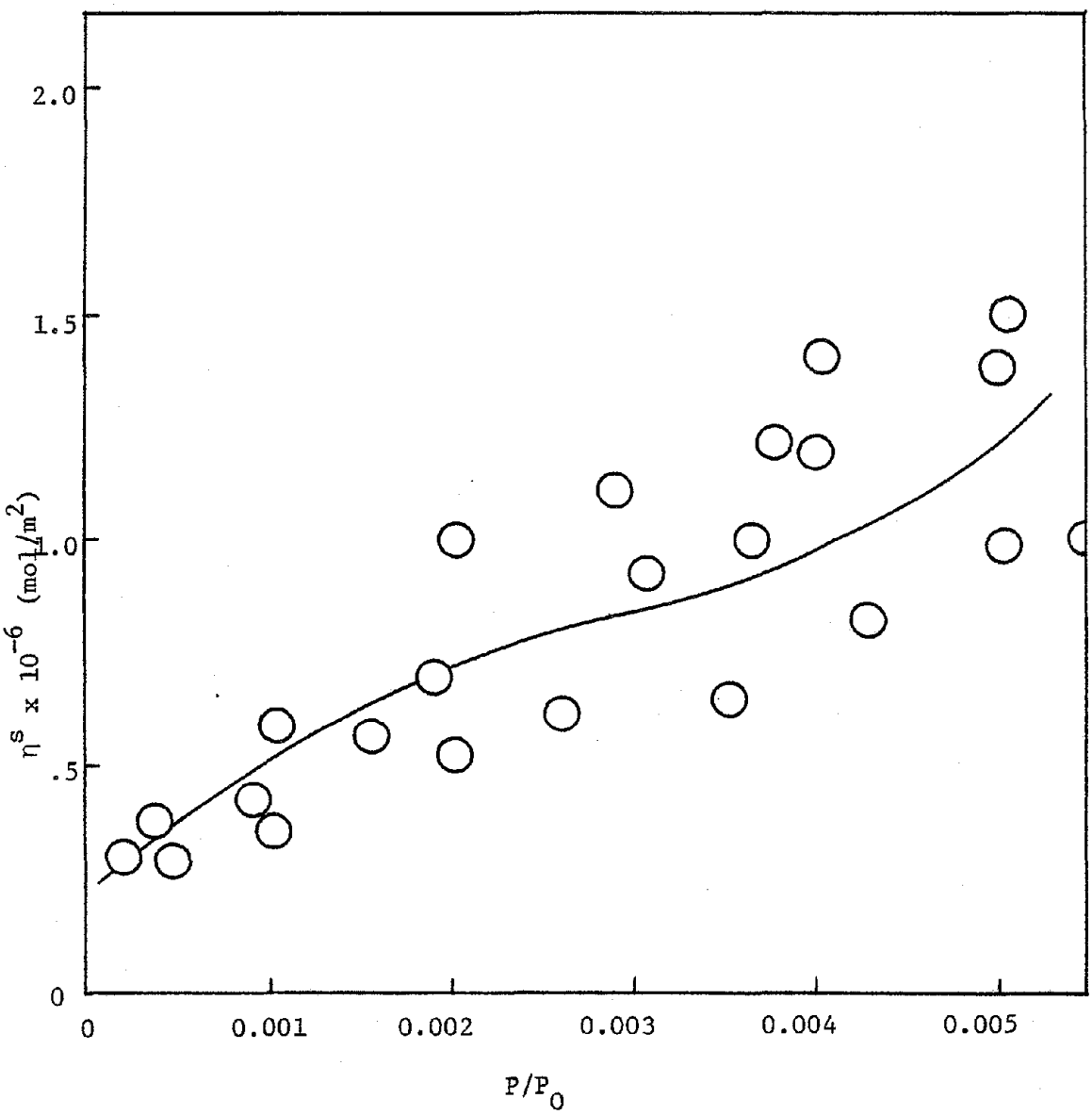

Figure 27. Adsorption Isotherms at 303K for Chlorine on Silica Outgassed at 373K.

The adsorption data and calculations for chlorine adsorption on empty sample bulbs outgassed at 373K or 673K are shown in Appendix XI. Approximately 5% of the chlorine was adsorbed at a chlorine pressure of 14.82 torr (2.0×10^3 Pa) on an empty sample bulb outgassed at 373K whereas approximately 0.7% of the chlorine was adsorbed at a pressure of 1.02 torr (1.4×10^2 Pa) on an empty bulb outgassed at 673K. The greater chlorine adsorption on the sample bulb outgassed at 373K may be attributed to a reaction of chlorine with the residual water on the glass that was not removed by an outgassing temperature of 373K.

In summary, the chlorine adsorption data at 303K for silica outgassed at 373K or 673K was not reproducible. Lack of reproducibility may be due to the error in pressure measurements due to small pressure drops from chlorine adsorption. No comparison of the adsorption of chlorine and water vapor on silica was possible; the P/P_0 range for chlorine adsorption was lower than the P/P_0 range for water adsorption.

J. ESCA Results

The wide scan ESCA spectrum of untreated silica is shown in Figure 28. The narrow scan spectra of carbon, oxygen and silicon are shown in Figure 29 as a, b and c, respectively. The sample surface is relatively free of surface contamination, containing only carbon, oxygen and silicon with atomic fractions of 0.28, 0.55 and 0.17 respectively as shown in Table IV. The value of the oxygen to silicon

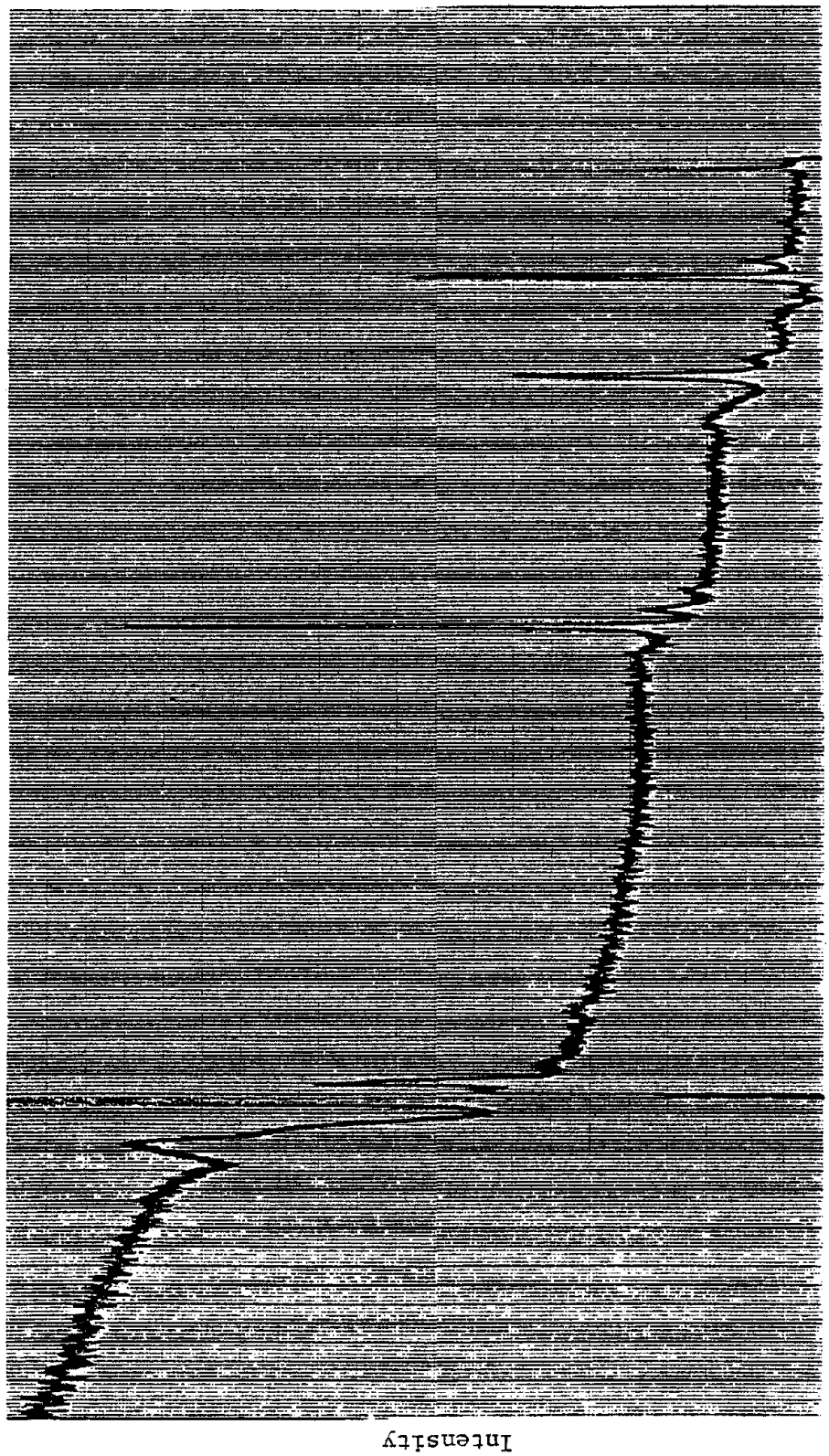

Figure 28. Wide Scan of Silica.

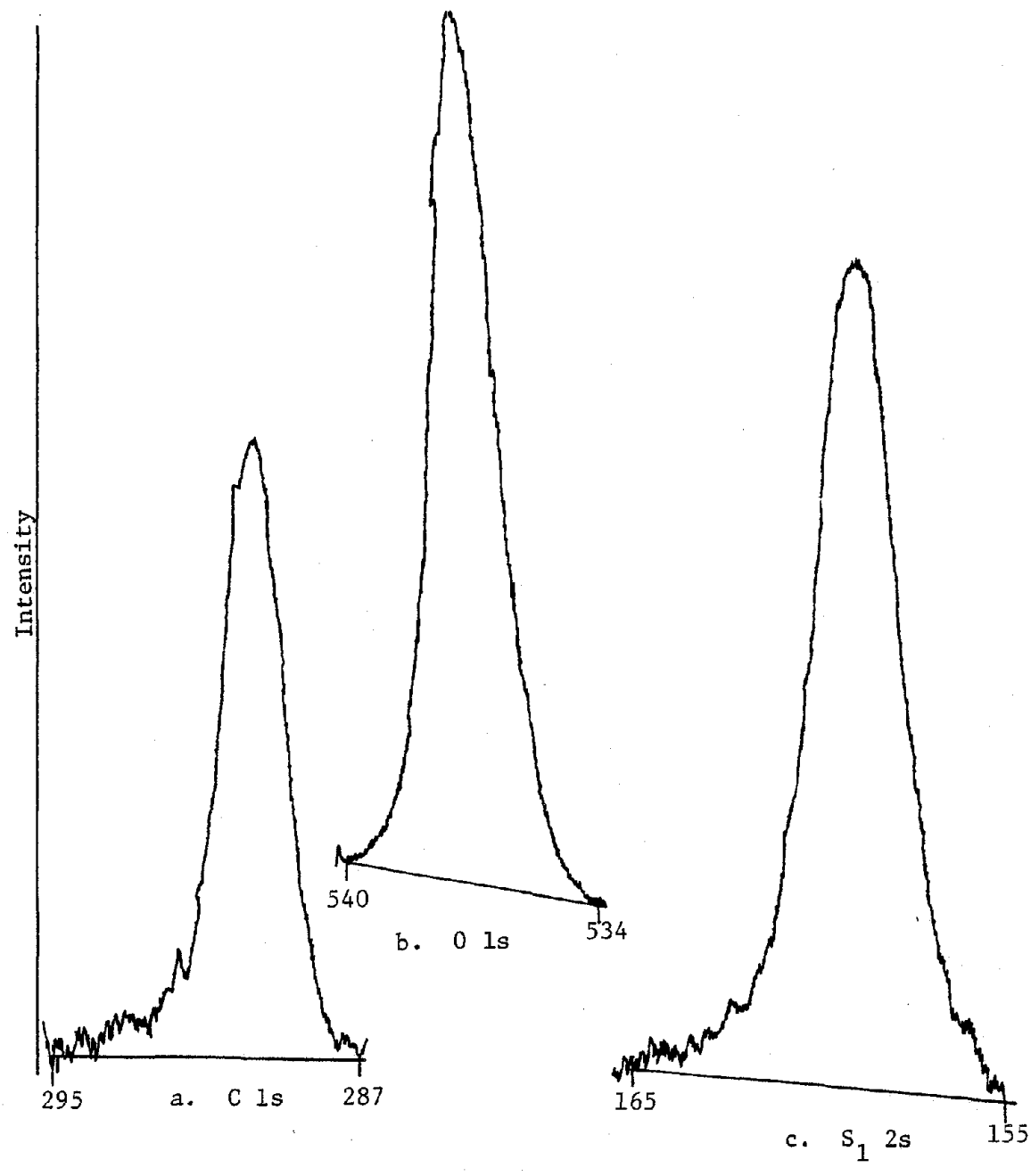

Figure 29. Narrow Scan Spectra of Silica

TABLE IV

ESCA Results for Untreated and Etched Silica

Untreated Silica

Element	Binding Energy (eV)	Atomic Fraction	Atomic Ratio
C 1s	284.0	.28	
O 1s	531.7	.55	
Si 2s	153.0	.17	
Na(A)	—	—	
O/Si			3.2

Etched Silica

C 1s	284.0	.27	
O 1s	531.6	.55	
Si 2s	153.2	.18	
Na(A)	264.2	.0007	
O/Si			3.1

ratio is 3.2 which is greater than the expected value of 2.0. The source of the detected oxygen is unexplained. The binding energies and atomic fractions of carbon, oxygen and silicon were similar for the etched and untreated silica as indicated in Table IV. The ESCA of etched silica indicated no surface fluorine.

ESCA results of silica outgassed at 373K and exposed to 40 torr (5332 Pa) of chlorine gas at 303K are shown in Table V. The binding energies and atomic fractions of carbon, oxygen and silicon are comparable to the ESCA of untreated silica. A small chlorine peak at 198.8 eV as shown in Figure 30 represents a 0.2% surface coverage. Silica outgassed at 673K and exposed to 40 torr (5.3×10^3 Pa) of chlorine gas at 303K had comparable binding energies for C, O and Si and a small chlorine peak at 198.0 eV as shown in Table V. The average binding energy of 198.4 ± 0.4 eV is evidence for the similar chlorine species on silica after outgassing at either 373K or 673K. The small chlorine surface coverage detected on silica may be a result of the small quantity of chlorine vapor adsorbed on silica.

A Na A peak with a surface coverage of approximately 0.1% was detected on silica outgassed at 373K and 673K and on etched silica exposed to chlorine. No Na Auger peak was detected on untreated silica. The source of the sodium may be contamination from the glassware used to contain the sample.

ESCA of compounds with varying chlorine valencies as shown in Table VI were compared with the ESCA of the chlorine species adsorbed from the gas phase on silica outgassed at 373K or 673K. The potassium

TABLE V

ESCA Results for Silica Outgassed at 373K or 673K and Exposed to Chlorine at 303K

Silica Outgassed at 373K

Element	Binding Energy (eV)	Atomic Fraction	Atomic Ratio
C 1s	284.0	.33	
O 1s	532.2	.49	
Si 2s	153.0	.17	
Cl 2p	198.8	.002	
Na(A)	264.0	.001	
O/Si			2.9

Silica Outgassed at 673K

C 1s	284.0	.17	
O 1s	531.6	.62	
Si 2s	153.0	.20	
Cl 2p	198.0	.003	
Na(A)	263.8	.001	
O/Si			3.6

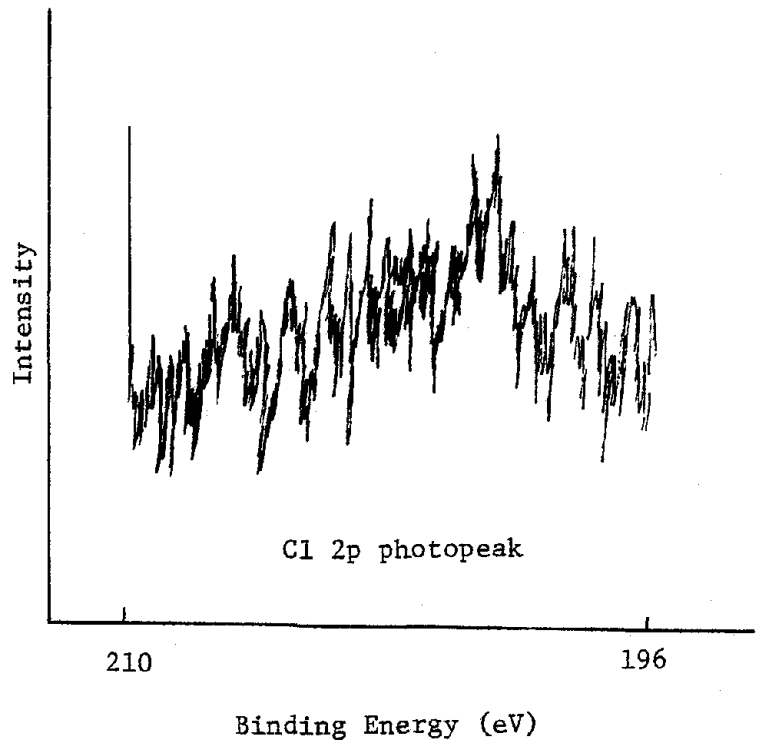

Figure 30. Narrow Scan of Chlorine Detected on Silica Outgassed at 373K and Exposed to Approximately 40 torr (5.3×10^3 Pa) of Chlorine Gas at 303K.

TABLE VI

ESCA Results for Model Chlorine Compounds

Element	Binding Energy (eV)
Potassium Perchlorate	
C 1s	284.0
Cl 2p	207.9
Sodium Chlorate	
C 1s	284.0
Cl 2p	205.0
Sodium Chloride	
C 1s	284.0
Cl 2p	197.4

perchlorate showed a Cl 2p photopeak at 207.9 eV, which is assigned to Cl^{+7}. The Cl 2p peak in sodium chlorate at 205.0 eV was assigned to Cl^{+5}. Likewise, the 197.4 eV peak for sodium chloride was assigned to Cl^{-1}. The binding energy for the chlorine in sodium chloride is similar to the binding energy of the gaseous chlorine species adsorbed onto silica.

The binding energy of chlorine from the pure compound, NACl, may not be the most realistic model to characterize the gaseous chlorine species adsorbed onto silica. Therefore the NaCl (aq) adsorption studies on silica were conducted to try to more accurately simulate Cl_2 (g) adsorption on silica as shown in Table VII. The binding energy of chlorine was 197.8 eV for chlorine adsorbed on silica from a 1M NaCl solution and very closely approximates the binding energy of the gaseous chlorine species adsorbed on silica, and the binding energies of the chloride ion reported in the literature (56). However, more definitive studies are necessary to characterize the gaseous chlorine adsorbed into silica.

The ESCA results of silica exposed to either .01M or 1M NaCl are shown in Table VII. No chlorine was detected on silica exposed to .01M NaCl and there was a 0.3% sodium coverage. Silica exposed to 1M NaCl had a detected sodium surface coverage of 0.4% and a small chlorine signal of 197.8 eV which represented 0.2% surface coverage. The sodium ion preferentially adsorbed onto the silica surface when exposed to the NaCl solutions which possibly indicates that the silica surface is negatively charged. In addition, there

TABLE VII

ESCA Results for Silica Exposed to Chlorine Species

.01M NaCl Solution + 1 g of Silica

Oven Dried at 373K

Element	Binding Energy (eV)	Atomic Fraction
C 1s	284.0	0.30
O 1s	532.0	0.51
Si 2s	153.6	0.18
Na(A)	264.0	0.003
O/Si		2.8

1M NaCl Solution and 1 g of Silica

Oven Dried at 373K

C 1s	284.0	0.17
O 1s	531.6	0.62
Si 2s	153.2	0.20
Na(A)	263.6	0.004
Cl 2p	197.8	0.002
O/Si		3.1

was no significant difference in the amount of chlorine adsorbed from 1M NaCl solution or in the amount of chlorine adsorbed from the vapor state onto silica.

To recapitulate, the atomic fractions of C, O, and Si do not differ for etched and untreated silica, and the surfaces are relatively free from surface contamination. The chlorine species adsorbed onto silica upon exposure to chlorine gas may be the chloride ion. Silica exposed to NaCl aqueous solutions indicate that sodium preferentially adsorbed onto the silica surface. Small quantities of chlorine were detected on silica exposed to chlorine vapor or to a 1M NaCl solution.

CHAPTER V

CONCLUSIONS

The following conclusions are based upon the study of water and chlorine adsorption on Min-U-Sil:

1. Infrared analysis, X-ray diffraction studies and differential scanning calorimetry confirmed that Min-U-Sil was α-quartz. X-ray diffraction analysis indicated that the α-quartz structure of Min-U-Sil was not altered by a chemical etching process. ESCA results indicate that the silica is relatively free of surface contamination containing only C, O, and Si. ESCA results also indicate that the binding energies and atomic fractions of C, O, and Si are similar for etched and untreated silica.

2. The nitrogen BET surface areas of silica outgassed at 373K and 673K were 5.06 m^2g^{-1} and 5.32 m^2g^{-1} respectively. The water surface area determination of silica was 2.8 m^2g^{-1}. The nitrogen BET surface area of etched silica outgassed at 373K and 673K was 2.93 $\pm$ .2 and 3.33 $\pm$ .1 m^2g^{-1} respectively. The nitrogen BET surface areas for NASA #2 and NASA #4 outgassed at 373K were 0.35 and 0.14 m^2g^{-1} respectively.

3. Water adsorption on silica outgassed at 373K decreased with increasing temperature. Water adsorption on silica outgassed at 673K was not a function of temperature. Reoutgassing silica at 373K did not alter the water adsorption isotherm; reoutgassing silica at 673K decreased the amount of water adsorbed.

C.2

LITERATURE CITED

1. Gregory, G. L.; Storey, R. W. NASA, TM-X-3228, Washington, D.C., August, 1975.

2. Solid Propellant Engineering Staff, NASA, TM-33-712, Jet Propulsion Laboratory, Pasadena, California, February, 1975.

3. Gregory, G. L.; Emerson, B. R. Jr.; Hudgins, C. H. NASA Report, TN-78673, Washington, D.C., January 1978.

4. Iler, Ralph K. "The Colloid Chemistry of Silica and Silicates;" Cornell University Press: New York, 1955, pp. 3, 9, 245, 238-39.

5. Keenan, C. W.; Wood, J. H. "General College Chemistry;" Harper and Brothers: New York, 1961; p. 493.

6. Nonaka, A.; Ishizaka, E. J. Colloid Interface Sci. 1977, 63, 381-88.

7. Axelson, J. W.; Piret, E. L. Ind. Eng. Chem. 1950, 42, 665-70.

8. Zettlemoyer, A. C.; Young, G. T.; Chessick, J. J.; Healey, F. H. J. Phys. Chem. 1953, 57, 649-52.

9. Gardner, L. U. Am. Inst. Mining Met. Engrs., Tech. Pubs. 1938, 7, 929.

10. Iler, Ralph K. "The Chemistry of Silica," in press.

11. Kiselev, A. V.; Yashin, Y. I. "Gas-Adsorption Chromatography;" Plenum Press: New York, 1969; pp. 40-44.

12. Lowen, W. K.; Broge, E. C. J. Phys. Chem. 1961, 65, 16.

13. Hair, M. L.; Hertl, W. J. J. Phys. Chem. 1969, 73, 4269-76.

14. Whalen, J. W.; Hu, P. C. J. Colloid Interface Sci. 1978, 65, 460-67.

15. Young, G. L. J. Colloid Interface Sci. 1958, 13, 67-85.

16. Gilpin, R. K.; Burke, M. F. Anal. Chem. 1973, 45, 1383.

17. Scott, R. P. W. in, "Contemporary Liquid Chromatography;" Weissberger, A., Ed.; John Wiley and Sons; New York, 1976; pp. 207-10.

18. Hair, M. L. "Infrared Spectroscopy in Surface Chemistry;" Marcel Dekker, Inc.: New York, pp. 83-84, 90, 134.

19. Weyl, W. A. Research 1950, 3, 230.

20. Novotny, M. in, "Bonded Stationary Phases in Chromatography;" Gruska, E., Ed.; Ann Arbor Science: Ann Arbor, Michigan, 1974; Chapter 10.

21. Cotton, F. A.; Wilkerson, G. "Advanced Inorganic Chemistry, A Comprehensive Text;" John Wiley and Sons: New York, 1962; p. 357.

22. Elmer, T. H.; Nordburg, M. E. U.S. Patent 3,399,043, 1968.

23. Peri, J. B. J. Phys. Chem. 1966, 70, 2937.

24. Unger, K. Angew Chem., Int. Ed. 1962, 11, 267; as cited in Gilpin, R. K.; Burke, M. F. Anal. Chem. 1973, 45, 1385.

25. Kiselev, A. V. Doklady Akad Nauk SSSR 1954, 98, 427, as cited in Whalen, J. W. Adv. in Chem. 1961, 33, 281.

26. Whalen, J. W. J. Phys. Chem. 1961, 65, 1676-81.

27. Zhadanov, S. P. Doklady Akad Nauk SSR (English Translation) 1958, 716.

28. Patrick, W. A., presented in part at the Symposium on Catalysts and Reaction Mechanism, Philadelphia, Pennsylvania, April, 1951, as cited in Iler, R. K. "The Colloid Chemistry of Silica and Silicates," Cornell University Press: New York, 1955; p. 242.

29. Miles, G. A.; Hinden, S. G. J. Am. Chem. Soc. 1950, 72, 5549.

30. Whalen, J. W. in "Advances In Chemistry Series #33;" Gould, R. F., Ed.; American Chemical Society; Washington, D.C., 1961; pp. 281-90.

31. Makrides, A. C.; Hackerman, N. J. Phys. Chem. 1959, 63, 594-98.

32. Hackerman, N.; Hall, A. C. J. Phys. Chem. 1958, 62, 1212.

33. Wade, W. H.; Every, R. L.; Hackerman, N. J. Phys. Chem. 1960, 64, 355-58.

34. Folman, M. Trans. Faraday Soc. 1961, 57, 2000.

35. Trotman, A. F.; Dickerson, A. "Comprehensive Inorganic Chemistry;" Pergamon Press: Ruscutters Bay, Australia, 1973, pp. 1382-85.

36. Weiss, A.; Weiss, A. Z. anorg. allgem. Chem. 1954, 276, 95, as cited in Makrides, A. C.; Hackerman, N. J. Phys. Chem. 1959, 63, 594.

37. Egorov, M. M.; Krasil'nikov, K. G.; Sysoev, E. A. Doklady Akad. Nauk SSSR 1956, 108, 103, as cited in Makrides, A. C.; Hackerman, N. J. Phys. Chem. 1959, 63, 594.

38. Kuznetsov, Y. P.; Petrov, E. S.; Vakhrusheva, A. I. Isv. Sib. Otd. Akad. Nauk SSSR Ser. Khin. Nauk 1972, 3, 42-46; Chem. Abstr. 1972, 77, 156879q.

39. Hair, M. L.; Hertl, W. J. J. Phys. Chem. 1973, 77, 2070-75.

40. Kiselev, A. V.; Ligin, V. I "Infrared Spectra of Surface Compounds;" John Wiley and Sons; New York, 1967, p. 103.

41. Peri, J. B. J. Phys. Chem. 1966, 70, 2937.

42. Chuiko, A. A.; Nemoshkalenoko, V. V.; Ogenko, V. N.; Safro, G. P.; Aleshin, V. G.; Taldenko, Y. D. Tezisy Dokl. Vses. Semin. 1974, 3, 33-34; Chem. Abstr. 1976, 85, 52131t.

43. Salmerón, M.; Baró, A. M. Surface Sci. 1972, 29, 300-2.

44. Chang, C. C. Surface Sci. 1971, 25, 53.

45. Poppa, H.; Elliot, A. G. Surface Sci. 1971, 24, 149.

46. Escard, J.; Pontevianne, B.; Goldsztaub, S.; Carriere, B. C.R. Acad. Sci., Ser B 1973, 277, 519-21; Chem. Abstr. 1974, 80, 42663a.

47. Gregg, S. S.; Sing, K. S. W. "Adsorption Surface ARea and Porosity;" Academic Press: New York, 1967, pp. 36-ff.

48. McClellan, A. L.; Harnsberger, H. F. J. Colloid Interf. Sci. 1967, 23, 577-609.

49. Skiles, J. A.; Wightman, J. P. "Interaction of Chlorine and Hydrogen Chloride with Alumina, Asbestos and Silica;" Semi-Annual Report, NASA Grant NSG-1389, September, 1977.

50. Scofield, J. H. J. of Electron Spectroscopy and Related Phenomena 1976, 8, 129-137.

51. "Select Powder Diffraction Data for Minerals" 2, 1974, published by Joint Committee on Powder Diffraction Standards, 49.

52. Van des Marel, H. W.; Beutelspacher, H. "Atlas of Infrared Spectroscopy of Clay Minerals and their Admixtures;" Elsevier Scientific Publishing Company; Amsterdam, 1976; p. 234.

53. Aristov, B. G.; Kiselev, A. V. Rus. J. Phys. Chem. 1964, 38, 1077-80.

54. Day, R. E.; Parfitt, G. D.; Peacock, J. Progr. Vac. Microbalance Technol. 1973, 2, 61.

55. Polanyi, M. Verh. deut. Physik. Ges 1916, 15, 55, as cited in, Brunauer, S. "The Adsorption of Gases and Vapors"; Princeton University Press; Princeton, N.J., 1943; p. 95.

56. Seals, R. D.; Alexander, R.; Taylor, L. T.; Dillard, J. G. Inorg. Chem. 1973, 12, 2485-87.

APPENDIX I

"BASIC" PROGRAM FOR NITROGEN SURFACE AREA DETERMINATIONS

OS/8 FILE NAME PGM .BA DATE 01/03/70

```
5 DIM X(30),Y(30),E1(30),A(30)
10 DIM W(30),P1(30),P2(30)
15 DIM V(30)
20 READ S
25 LET I1=1
30 READ C1,W1,W2,H1,H2,T1,X1,X2,V1,P4,A1,S1
35 LET W4=W1-W2
40 LET V(1)=0.0
45 LET P2(1)=0.0
50 LET T5=(307.2+T1)/2
55 LET V2=(T1/H2)*((V1*(H1-H2)/307.2)-(3.65*H2/T5))
60 LET I=2
65 READ N
70 READ W(I),P(I),P2(I)
75 IF W(I)-1<0.0 THEN 100
80 LET Z9=1
85 IF W(I)-1=0.0 THEN 110
90 LET Z9=1
95 IF W(I)-1>0.0 THEN 120
100 LET X3=0.0
105 GO to 125
110 LET X3=X1
115 GO to 125
120 LET X3=X2
125 LET A(I)=0.001169*(VI+X3)/W4
130 LET B=((0.3593+V2)/(T1*W4))+(1.311/T5*W4))
135 LET C=(0.3593*V2*A1)/(W4*T1)
140 LET P5=P2(I-1)
145 LET D=P1(I)-P2(I)
150 LET E=P2(I)-P5
155 LET F=P2(I)**2-P5**2
160 LET G=A(I)*D
165 LET H=B*E
170 LET D1=C*F
175 LET D2=G-H-D1
180 LET V(I)=V(I-1)+D2
185 LET X(I)=P2(I)/P4
190 LET Y(I)=X(I)/(V(I)*(1.0-X(I)))
195 IF N-I+1<0.0 THEN 230
200 Z9=1
205 IF N-I+1=0.0 THEN 230
210 Z9=1
215 IF N-I+1>0.0 THEN 220
```

```
220 I=I+1
225 GO TO 30
230 LET S2=0.0
235 LET S3=0.0
240 LET S4=0.0
245 LET S5=0.0
250 FOR I=2 TO N+1
255 LET S2=S2+X(I)
260 LET S3=S3+ç(I)
265 LET S4=S4+X(I)*Y(I)
270 LET S5=S5+X(I)**2
275 NEXT I
280 LET I5=((N*S4)-(S2*S4))/((N*S5)-(S2**2))
285 LET L=((N*S4)-(S2*S3))/((N*S5)-(S2**2))
290 LET S6=(0.2687*S1)/(L+15)
295 LET S7=0.0
300 FOR I=2 TO N+1
305 LET E(I)=Y(I)-(15+L*X(I))
310 LET S7=S7+E(I)**2
315 LET S8=SQR(S7/N)
320 NEXT I
325 PRINT "SAMPLE IDENTIFICATION NO.=";C1,TAB(30);"W1=";W1
326 PRINT "H1=";H1,TAB(15);"X1=";X1,TAB(30);"W1=";W1
327 PRINT "W2=";W2,TAB(15);"H2=";H2,TAB(30);"PS=";P4
328 PRINT "ALPHA=";A1.TAB(15);"WS=";W4,TAB(30);"TS=";T1
329 PRINT "VD=";V1,TAB(15);"S=";S1,TAB(30);"B=";B
330 PRINT "C=";C,TAB(15);"VS=";V2
331 PRINT
332 PRINT
333 PRINT "ITERATION, WHICH X, A, P1, P2, V, X, Y"
334 FOR I=2 TO N+1
335 LET J=I+1
340 PRINT, J,TAB(10),W(I),TAB(20),A(I),TAB(30),P1(I)
341 PRINT TAB (5),P2(1),TAB(15),V(I),TAB(25),X(I)
342 PRINT TAB (10),Y(I)
343 PRINT
344 PRINT
345 NEXT I
350 PRINT "SW=";S6
351 PRINT "STANDARD ERROR OF LEAST SQ. LINE=";S8
355 IF S-I1=0.0 THEN 9999
360 L9=1
365 IF S-I1=0.0 THEN 9999
370 LET L9=1
375 IF S-11>0.0 THEN 380
380 LET I1=I1+1
385 GO TO 30
1000 DATA 1
1001 DATA 111, 24.34627,23.04928,513,143.93,77
1002 DATA 132.2,0.0,28.77,729.4,.000066,16.2
```

```
1003 DATA 9
1004 DATA 1,88.83,47.32
9998 STOP
9999 END
```

APPENDIX II

"BASIC" PROGRAM USED FOR GAS ADSORPTION

```
1 REM - THE PURPOSE OF THIS PROGRAM IS TO CALCULATE
2 REM - THE SURFACE ADSORPTION OF A GAS
5 LET V3=13.34
10 LET V4=25.24
15 LET V5=50.35
20 LET V6=93.05
25 LET R=62360.
30 LET N=0
35 LET L=0
40 LET N7=0
45 LET X=1
50 PRINT "ENTER V-D";
55 INPUT B9
60 PRINT "ENTER TEMPERATURE";
65 INPUT T
70 PRINT "ENTER SAMPLE BULB VOLUME".
75 INPUT V
80 PRINT "ENTER SAMPLE WEIGHT, IN GRAMS";
85 INPUT W
90 PRINT "ENTER AREA, IN SQUARE METERS PER GRAM";
95 INPUT A
100 PRINT "ENTER BULB VOLUME";
105 INPUT V9
110 PRINT
115 PRINT TAB (23);"SUMMARY TABLE"
116 LET Z9=1
120 PRINT
125 PRINT TAB (12);"PRESSURE";TAB(30);"M PER MTR SQ";
    TAB(50);"M PER G"
130 PRINT
135 PRINT
140 READ P1,P2
145 IF X=1 THEN 165
150 LET Y=1
155 IF P1=9999 THEN 215
160 LET N7=(L*V)/(R*T)
165 LET N9=(P1*(V9+B9))/(R*T)
170 LET N1=(P2*(V9+B9+V))/(R*T)
180 LET L=P2
185 LET X=X+1
190 LET N=N+(N7+N9-N1)/(W*A)
195 LET N8=N*A
200 PRINT
205 PRINT TAB(10);P2;TAB(30);N;TAB(50);N8
```

```
210 GO TO 140
215 PRINT "CHANGE BULB VOLUME? (YES OR NO)"
220 INPUT A$
221 IF A$="YES" THEN 100
235 PRINT "THEN WE SHALL GO TO THE SECOND SET OF CALCULATIONS"
240 PRINT
245 PRINT "ENTER BEGINNING BULB LEVEL (5,4,3, OR 0)";
250 INPUT B
255 IF B=5 THEN 290
260 LET Y=1
265 IF B=4 THEN 320
270 LET Y=1
275 IF B=3 THEN 350
276 LET Y=1
280 IF B=0 THEN 380
281 LET Y=1
290 READ P5
295 LET C=(P5*(V5+B9+V)/(R*T)
300 LET N5=N+(N1-C)/(W*A)
305 LET Q5=N5*A
310 PRINT TAB(10);P5;TAB(30);N5;TAB(50);Q5
320 READ 4
325 LET C=(P4*(V4+B9+V))/(R*T)
330 LET N4=N+(N1-C)/(W*A)
335 LET Q4=N4*A
340 PRINT
345 PRINT TAB(10);P4;TAB(30);N4;TAB(50);Q4
350 READ P3
355 LET C=(P3*(V3+B9+V))/(R*T)
360 LET N3=N+(N1-C)/(W*A)
365 LET Q3=N3*A
370 PRINT
375 PRINT TAB(10);P3;TAB(30);N3;TAB(50);Q3
380 READ E1
385 LET C=(E1*(B9+V))/(R*T)
390 LET E8=N+ (N1-C)/(W*A)
395 LET E9=E8*A
400 PRINT
405 PRINT TAB(10);E1;TAB(30);E8;TAB(50);E9
406 READ P3
407 LET E=(P3*(V3+B9+V))/(R*T)
408 LET N3=E8+(C-E)/(W*A)
409 LET Q3=N3*A
410 PRINT
411 PRINT TAB (10);P3;TAB(30);N3;TAB(50);Q3
412 READ P4
415 LET E=(P4*(V4+B9+V))/(R*T)
420 LET N4=E8+(C-E)/(W*A)
425 LET Q4=N4*A
430 PRINT
```

```
435 PRINT TAB (10);P4;TAB(30);N4;TAB(50);Q4
440 READ P5
445 LET E=(P5*(V5+B9+V))/(R*T)
450 LET N5=E8+(C-E)/(W*A)
455 LET Q5=N5*A
460 PRINT
465 PRINT TAB (10);P5;TAB(30);N5;TAB(50);Q5
470 READ P6
475 LET E=(P6*(V6+B9+V))/(R*T)
480 LET N6=E8+(C-E)/(W*A)
485 LET Q6=N6*A
490 PRINT
495 PRINT TAB(10);P6;TAB(30);N6;TAB(50);Q6
9990 END
```

APPENDIX III

DATA FOR WATER ADSORPTION ON UNTREATED SILICA

All samples were outgassed at a specified temperature for 2 hours. All weights are expressed in grams.

Run #20A

Sample: Min-U-Sil

Weight: 1.9783

Outgassing Temperature: 373K

Isotherm Temperature: 302K

Pressure torr	$Mol/m^2 \times 10^{-6}$
0.29	2.1
1.14	4.26
4.04	6.81
8.51	8.51
12.66	9.91
15.73	10.8
19.99	11.7
22.99	12.5
25.09	13.0

Run #30A

Sample: Min-U-Sil

Weight: 1.9758

Outgassing Temperature: 373K

Isotherm Temperature: 302K

Pressure torr	$Mol/m^2 \times 10^{-6}$
0.56	3.13
2.64	5.78
6.52	7.97
9.92	9.58
13.26	10.7
17.09	11.8
19.82	12.7
22.72	13.4
24.25	14.0
26.15	14.4

Run #22A

Sample: Min-U-Sil

Weight: 2.2915

Outgassing Temperature: 373K

Isotherm Temperature: 313K

Pressure torr	$Mol/m^2 \times 10^{-6}$
0.4	2.26
2.26	4.83
5.84	7.32
12.4	9.78
18.82	11.5
24.72	13.2
31.72	14.6
37.88	15.8
41.98	16.9
45.08	17.8
49.07	18.5

Run #23A

Sample: Min-U-Sil

Weight: 2.1779

Outgassing Temperature: 373K

Isotherm Temperature: 313K

Pressure torr	$Mol/m^2 \times 10^{-6}$
0.61	2.77
3.08	5.54
8.01	8.21
14.39	10.4
20.86	12.0
26.45	13.5
32.62	14.8
37.56	16.1
41.71	17.1
45.29	17.9
49.39	18.4

Run #24A

Sample: Min-U-Sil

Weight: 2.1487

Outgassing Temperature: 373K

Isotherm Temperature: 322K

Pressure torr	$Mol/m^2 \times 10^{-6}$
0.66	2.36
4.94	5.64
13.73	8.81
24.45	11.4
35.98	13.6
46.44	15.7
58.12	17.5
69.11	19.5
81.38	20.4

Run #25A

Sample: Min-U-Sil

Weight: 2.2382

Outgassing Temperature: 373K

Isotherm Temperature: 322K

Pressure torr	$Mol/m^2 \times 10^{-6}$
0.47	2.08
4.23	5.31
12.89	8.54
23.82	11.3
35.56	13.4
46.24	15.4
57.07	17.4
69.48	19.3
84.6899	19.7

Run #26

Sample: Min-U-Sil Outgassed 1X

Weight: 2.0405

Outgassing Temperature: 373K

Isotherm Temperature: 302K

Pressure torr	$Mol/m^2 \times 10^{-6}$
0.05	1.32
0.44	3.44
2.12	6.3
5.52	9.11
10.19	11.6
15.38	13.5

Run #12

Sample: Min-U-Sil Outgassed 3X

Weight: 2.0396

Outgassing Temperature: 373K

Isotherm Temperature: 302K

Pressure torr	$Mol/m^2 \times 10^{-6}$
0.31	3.84
2.01	7.13
5.12	10.0
8.77	12.3
11.82	14.2
15.27	15.7
18.54	16.7
20.76	17.8
22.41	18.7
25.94	19.5
26.67	20.2

Run #29

Sample: Min-U-Sil Outgassed 4X

Weight: 2.0405

Outgassing Temperature: 373K

Isotherm Temperature: 302K

Pressure torr	$Mol/m^2 \times 10^{-6}$
0.02	1.31
0.34	3.44
1.77	6.34
4.67	8.99
9.24	11.7
13.84	13.8
17.82	15.4
22.57	16.8

Run #18

Sample: Min-U-Sil Outgassed 9X

Weight: 2.0396

Outgassing Temperature: 373K

Isotherm Temperature: 302K

Pressure torr	$Mol/m^2 \times 10^{-6}$
0.42	3.11
2.6	6.69
6.24	9.76
9.97	12.3
14.32	14.5
17.82	16.3
22.99	17.7

Run #19

Sample: Min-U-Sil Outgassed 10X

Weight: 2.0396

Outgassing Temperature: 373K

Isotherm Temperature: 302K

Pressure torr	$Mol/m^2 \times 10^{-6}$
0.5	3.93
3.06	7.58
7.32	10.6
11.57	12.9
16.32	14.8
20.36	16.3
24.25	17.4

Run #27

Sample: Min-U-Sil Outgassed 2X

Weight: 2.0405

Outgassing Temperature: 373K

Isotherm Temperature: 312K

Pressure torr	Mol/m^2 x 10^{-6}
0.19	2.11
1.38	4.69
4.57	7.24
8.72	9.46
13.5	11.4
17.25	12.9
20.09	14.4
23.99	16.1
28.57	17.9
33.25	19.5
37.56	21.1
39.98	22.6
43.14	24.1
45.4	25.0

Run #23

Sample: Min-U-Sil Outgassed 3X

Weight: 2.0411

Outgassing Temperature: 373K

Isotherm Temperature: 312K

Pressure torr	$Mol/m^2 \times 10^{-6}$
0.09	1.03
0.92	3.49
3.34	6.03
7.02	8.26
11.57	10.3
16.07	12.2
22.57	14.8
28.99	17.0
33.4	18.7
36.98	20.0
40.03	21.6
42.98	23.0
44.56	24.1

Run #13

Sample: Min-U-Sil Outgassed 4X

Weight: 2.0396

Outgassing Temperature: 373K

Isotherm Temperature: 312K

Pressure torr	$Mol/m^2 \times 10^{-6}$
0.0969999	2.11
0.844	4.51
3.315	7.17
6.302	9.30
10.48	11.4
16.442	13.9
21.406	15.9
25.8	17.4
28.277	18.7
31.767	19.7
34.116	20.6
36.565	21.7
39.98	22.9
42.978	24.1
45.794	24.9
48.142	25.8

Run #24

Sample: Min-U-Sil Outgassed 5X

Weight: 2.0411

Outgassing Temperature: 373K

Isotherm Temperature: 312K

Pressure torr	$Mol/m^2 \times 10^{-6}$
0.19	1.81
1.32	4.19
3.8	6.43
7.8	8.74
12.5	10.8
16.26	12.6
20.09	14.1
24.4	15.7
28.98	17.4
33.4	19.2
36.15	20.8
39.56	22.1
43.81	23.5
48.81	23.9

Run #14

Sample: Min-U-Sil Outgassed 5X

Weight: 2.0396

Outgassing Temperature: 373K

Isotherm Temperature: 312 K

Pressure torr	$Mol/m^2 \times 10^{-6}$
0.11	2.30
1.41	5.39
4.78	8.28
8.48	10.5
12.29	12.4
16.4	14.2
22.34	16.4
29.07	18.2
35.65	20.1
39.98	21.7
44.98	22.9

Run #25

Sample Min-U-Sil Outgassed 6X

Weight: 2.0411

Outgassing Temperature: 373K

Isotherm Temperature: 312 K

Pressure torr	$Mol/m^2 \times 10^{-6}$
0.22	2.10
1.58	4.59
4.55	7.05
8.35	9.16
12.12	11.0
15.89	12.5
19.74	14.1
23.4	15.6
27.24	17.2
30.98	18.7
34.67	20.2
37.71	21.7
41.23	23.0
43.81	24.2

Run #19A

Sample: Min-U-Sil

Weight: 1.7025

Outgassing Temperature: 673K

Isotherm Temperature: 302K

Pressure torr	$Mol/m^2 \times 10^{-6}$
2.67	1.05
3.9	2.57
5.79	4.24
7.88	5.73
10.02	7.12
12.99	8.35
15.99	9.23
17.87	10.1
20.41	10.9
23.82	11.6
26.4	12.2

Run #13A

Sample: Min-U-Sil

Weight: 2.0530

Outgassing Temperature: 673K

Isotherm Temperature: 302K

Pressure torr	$Mol/m^2 \times 10^{-6}$
0.34	1.72
1.9	3.66
3.79	5.16
6.6	6.68
10.67	8.03
14.34	9.01
18.41	9.74
21.77	10.4
24.1	11.0
26.4	11.4
27.82	11.6

Run #13B

Sample: Min-U-Sil Outgassed 2X

Weight: 2.0530

Outgassing Temperature: 673K

Isotherm Temperature: 302K

Pressure torr	$Mol/m^2 \times 10^{-6}$
0.88	2.24
3.4	4.34
8.13	6.14
13.19	7.46
18.41	8.43
22.99	9.02
25.4	9.42
28.25	9.62

Run #14A

Sample: Min-U-Sil

Weight: 1.8284

Outgassing Temperature: 673K

Isotherm Temperature: 312K

Pressure torr	$Mol/m^2 \times 10^{-6}$
0.63	2.05
2.62	4.11
5.17	5.81
8.25	7.34
12.26	8.71
15.99	10.1
19.72	11.2
23.72	12.3
27.82	13.3
33.72	14.4
38.98	15.6
47.76	16.0

Run #15A

Sample: Min-U-Sil

Weight: 1.8874

Outgassing Temperature: 673K

Isotherm Temperature: 312 K

Pressure torr	$Mol/m^2 \times 10^{-6}$
1.73	1.88
4.75	3.39
8.52	4.64
11.99	5.73
15.77	6.86
19.41	7.89
23.09	8.87
27.09	9.63
31.98	10.4
37.56	11.3
43.76	12.1

Run #28A

Sample: Min-U-Sil

Weight: 2.0075

Outgassing Temperature: 673K

Isotherm Temperature: 312K

Pressure torr	$Mol/m^2 \times 10^{-6}$
0.79	2.19
3.12	4.44
6.79	6.59
11.83	8.55
17.82	10.3
24.35	11.9
29.98	13.1
35.52	14.0
41.71	14.9
50.54	14.6

Run #17A

Sample: Min-U-Sil

Weight: 1.9972

Outgassing Temperature: 673K

Isotherm Temperature: 322K

Pressure torr	$Mol/m^2 \times 10^{-6}$
2.32	2.53
8.63	5.53
18.24	8.17
30.5	10.6
43.39	13.0
57.39	14.7
69.8	16.5
80.06	17.4

Run #18A

Sample: Min-U-Sil

Weight: 1.7946

Outgassing Temperature: 673K

Isotherm Temperature: 322K

Pressure torr	$Mol/m^2 \times 10^{-6}$
2.22	3.4
9.58	6.63
19.99	9.52
32.57	11.7
45.24	14.0
60.7	16.1
72.23	17.7
80.79	18.4

APPENDIX IV

DATA FOR WATER ADSORPTION ON EMPTY SAMPLE BULBS

Sample Bulb Outgassed at 373K

P	Moles of H_2O Adsorbed	($\times 10^{+6}$)
5.38		0.79
9.59	1.3×10^{-6}	1.30
13.20	6.4×10^{-7}	0.64
18.62	5.2×10^{-7}	0.52
23.34	1.7×10^{-6}	1.70
26.40	4.4×10^{-7}	0.44

At P = 5.38 torr, 0.79×10^{-6} moles of H_2O was adsorbed on the empty bulb. At P = 5.52 torr, $.50 \times 10^{-4}$ mol/g or 1.0×10^{-4} moles of H_2O was adsorbed on Min-U-Sil outgassed at 373K, in run #26.

$$\frac{7.9 \times 10^{-7}}{1.0 \times 10^{-4}} \times 100 = .8\% \text{ of } H_2O \text{ adsorbs to the glass sample flask}$$

Sample Bulb Outgassed at 673K

P	Moles of Water Adsorbed	x 10^{+6}
6.33	3.0	0.30
17.09	3.4	3.40

At P = 6.33 torr, 3.0 x 10^{-7} moles of water was adsorbed on the sample bulb. At P = 6.66 torr, 7.4 x 10^{-5} moles of water was adsorbed on Min-U-Sil outgassed at 673K in run #13A.

$$\frac{3.0 \times 10^{-7}}{7.4 \times 10^{-5}} \times 100 = .40\%$$ of H_2O adsorbs to the glass sample bulb.

APPENDIX V

SAMPLE CALCULATION OF THE F-TEST

$n^s \times 10^{-5}$ (mol/m^2)

Run #20A	Run #30A
0.21	0.31
0.43	0.58
0.68	0.80
0.85	0.96
0.99	1.07
1.08	1.18
1.17	1.28
1.25	1.34
1.30	1.40
	1.44
Average ($\bar{\chi}$) 0.88×10^{-5}	1.04×10^{-5}
Standard Deviation (σ) 0.38×10^{-5}	0.38×10^{-5}

1) Compute the overall average of all samples (μ)

$$\mu = \frac{0.88 \times 10^{-5} + 1.04 \times 10^{-5}}{2} = .96 \times 10^{-5}$$

2) Compute $(\bar{\chi}-\mu)$ and $(\bar{\chi}-\mu)^2$

Run	$(\bar{\chi}-\mu)$	$(\bar{\chi}-\mu)^2$
20A	$-8. \times 10^{-7}$	6.4×10^{-13}
30A	$8. \times 10^{-7}$	6.4×10^{-13}

3) Compute: $\frac{1}{\#\ \text{Points}} \Sigma\ (\bar{\chi}-\mu)^2$

$$\frac{1}{19}\ (6.4 \times 10^{-13} + 6.4 \times 10^{-13}) = 6.74 \times 10^{-14}$$

4) Compute the variance for all points (by calculator)

$$\text{Variance} = 1.32 \times 10^{-11}$$

5) Compute: $\sigma^2 = \frac{1}{\#\ \text{Points}} \cdot \text{Variance}$

$$\sigma^2 = \frac{1}{19} \cdot 1.32 \times 10^{-11} = 6.94 \times 10^{-13}$$

6) Divide 3) by 5)

$$\frac{6.74 \times 10^{-14}}{6.94 \times 10^{-13}} = 9.71 \times 10^{-2}$$

and take 9.71×10^{-2} to the following power:

$$\frac{\#\ \text{Points}}{\#\ \text{Runs}-1} = \frac{19}{2-1} = 19$$

$$9.71 \times 10^{-2}\ \text{Exp.}\ 19 = 5.71 \times 10^{-20}$$

7) Compare 5.71 with value in F-Test Table.[1]

8) For Run #20A, which has 9 data points, and Run #30A, which has 10 data points, the F-distribution table gives a value of 2.42 for the 95% confidence level.

9) Since the calculated value of $5.71 \times 10^{-20} < 2.42$, the two runs are determined to come from the same population.

---

[1] Breiman, L. "Statistics: With a View Towards Applications;" Houghton Mifflin Company:Boston, 1973; pp. 153-58, 383-84.

APPENDIX VI

CALCULATIONS BASED UPON THE POLANYI MODEL FOR WATER ADSORPTION AT 313 AND 323K

1. A plot of ε vs ϕ was based upon data in run #20A and 30A for water adsorption at 303K on Min-U-Sil outgassed at 373K

P(torr)	moles/gram x 10^{+5}	χi = g H_2O/g SiO_2 x 10^{4}	$\phi = \chi i/P_o$ x 10^{+4}	$\varepsilon = RT \ln \frac{P_o}{P}$ (J/mol)
2	2.7	.3	4.9	6778
4	3.4	6.1	6.1	5046
6	3.9	7.0	7.0	4029
8	4.4	8.0	8.0	3310
10	4.8	8.6	8.6	2753
12	5.2	9.4	9.4	2297
14	5.4	9.7	9.7	1912
16	5.7	10.0	10.0	1577
18	6.0	11.0	11.0	1280
22	6.5	12.0	12.0	778
24	6.8	12.0	12.0	561

P_o is the vapor pressure of water at 303K

2. Based upon the ε vs ϕ curve for water adsorption at 303K, the predicted isotherms for water adsorption at 313 and 323K can be calculated as follows:

   a. determine ϕ values for ε values from the E vs ϕ curve for water adsorption at 303K.

b. Determine the water adsorption in moles/g at 313 or 323K from:

$$n_s = \frac{\phi \times P_o}{18 \text{ g/mole of } H_2O}$$

c. Determine the pressure associated with the water adsorption from:

$$\ell n\ P = \ell n\ P_o - \frac{\varepsilon}{RT}$$

where P_o is the vapor pressure of water at either 313 or 323K.

APPENDIX VII

DATA FOR WATER ADSORPTION ON ETCHED SILICA

All samples were outgassed at a specified temperature for 2 hours.

All weights are expressed in grams.

Run #12A

Sample: Etched Min-U-Sil Outgassed 1X

Weight: 2.0943

Outgassing Temperature: 373K

Isotherm Temperature: 302K

Pressure torr	$Mol/m^2 \times 10^{-6}$
1.78	2.42
4.74	4.32
7.73	5.89
9.97	7.15
12.21	8.42
15.36	9.36
19.09	10.4
22.25	11.4
24.82	12.0
27.97	12.1

Run #12B

Sample: Etched Min-U-Sil Outgassed 2X

Weight: 2.0943

Outgassing Temperature: 373K

Isotherm Temperature: 302K

Pressure torr	$Mol/m^2 \times 10^{-6}$
1.08	2.07
3.55	3.84
6.84	5.53
10.2	7.09
13.57	8.09
16.14	9.02
18.99	9.59
21.24	10.5
23.55	11.2
25.09	11.6
26.25	12.1
27.4	12.2

Run #12C

Sample: Etched Min-U-Sil Outgassed 1X

Weight: 2.0943

Outgassing Temperature: 673K

Isotherm Temperature: 302K

Pressure torr	$Mol/m^2 \times 10^{-6}$
1.78	2.02
4.81	3.42
7.23	4.48
10.76	5.57
13.79	6.38
15.77	7.12
18.62	8.02
21.41	8.75
23.72	9.95
27.4	10.1

Run #12D

Sample: Etched Min-U-Sil Outgassed 2X

Weight: 2.0943

Outgassing Temperature: 673K

Isotherm Temperature: 302K

Pressure torr	$Mol/m^2 \times 10^{-6}$
2	2.25
5.14	3.71
9.12	5.25
13.21	6.18
15.67	6.96
18.99	7.64
20.82	8.36
22.99	8.91
24.82	9.50
26.82	9.83

Run #12E

Sample: Etched Min-U-Sil Outgassed 3X

Weight: 2.0943

Outgassing Temperature: 673K

Isotherm Temperature: 302K

Pressure torr	$Mol/m^2 \times 10^{-6}$
1.48	2.13
4.46	3.49
8.02	4.78
10.94	5.85
14.33	6.70
17.14	7.54
20.09	8.28
23.4	9.03
25.09	9.48
27.08	9.71
27.99	9.96

APPENDIX VIII

HEAT OF EMPTY BULB BREAKING IN WATER

Bulb outgassed at 373K [2]	109 mJ
Bulb outgassed at 673K [2]	117 mJ

APPENDIX IX

DATA FOR WATER ADSORPTION ON NASA #2 AND NASA #4

All samples were outgassed at 373K for 2 hours. All weights are expressed in grams.

Run #26A

Sample: NASA #2

Weight: 1.5520

Outgassing Temperature: 373K

Isotherm Temperature: 303K

Pressure torr	$Mol/m^2 \times 10^{-5}$
0.52	3.74
3.39	8.41
7.62	12.1
12.21	14.6
15.54	16.2
19.99	17.3
22.72	18.0
24.72	18.8
26.25	19.1

Run #27A

Sample: NASA #4

Weight: 1.5819

Outgassing Temperature: 373K

Isotherm Temperature: 303K

Pressure torr	$Mol/m^2 \times 10^{-4}$
0.22	1.15
1.28	2.52
4.58	4.14
9.53	5.32
14.04	6.01
17.82	6.63
21.41	9.79
24.4	7.20
26.45	7.37

APPENDIX X

DATA FOR CHLORINE ADSORPTION ON UNTREATED SILICA

All samples were outgassed at the specified temperature for 2 hours. All weights are expressed in grams. All isotherm temperatures were 303K.

Run #4A

Sample: Min-U-Sil

Weight: 1.9206

Outgassing Temperature: 373K

Pressure torr	$Mol/m^2 \times 10^{-6}$
1.15	.250
6.59	.410
11.17	.549
15.24	1.04
21.24	1.15
28.08	1.23
33.6	1.40
40.4	1.55

Run #3A

Sample: Min-U-Sil

Weight: 2.1481

Outgassing Temperature 373K

Pressure torr	$Mol/m^2 \times 10^{-6}$
2.6	.369
8.26	.586
14.82	.713
20.86	.934
27.77	1.07
33.4	1.23
38.15	1.40

Run #2A

Sample: Min-U-Sil

Weight: 2.0907

Outgassing Temperature: 373K

Pressure torr	$Mol/m^2 \times 10^{-6}$
3.55	.393
13.06	.863
16.71	1.10
19.53	1.32
27.55	1.45
32.78	1.69
37.89	1.90

Run #1B

Sample: Min-U-Sil Outgassed 2X

Weight: 2.0388

Outgassing Temperature 373K

Pressure torr	$Mol/m^2 \times 10^{-6}$
2.42	.456
5.95	.595
13.02	.863
19.7	.962
25.99	1.16
29.15	1.19
33.4	1.34
37.71	1.45
40.81	1.60

Run #4B

Sample: Min-U-Sil Outgassed 2X

Weight: 1.9206

Outgassing Temperature: 373K

Pressure torr	$Mol/m^2 \times 10^{-6}$
0.4	.112
3.55	.257
8.47	.407
13.02	.470
23.94	.568
29.82	.718
33.34	.938

Run #6A

Sample: Min-U-Sil

Weight: 2.0289

Outgassing Temperature 673K

Pressure torr	$Mol/m^2 \times 10^{-6}$
0.56	.103
1.37	.408
7.53	.727
14.34	.935
21.62	1.09
27.35	1.35
32.83	1.41
38.56	1.53
40.03	1.68

Run #7A

Sample: Min-U-Sil

Weight: 1.8447

Outgassing Temperature 673K

Pressure torr	$Mol/m^2 \times 10^{-6}$
0.68	.098
1.8	.211
2.48	.436
7.8	.820
14.82	1.01
21.99	1.18
26.72	1.28
31.98	1.42
35.56	1.45
37.4	1.65
39.98	1.78

Run #10A

Sample: Min-U-Sil

Weight: 2.2705

Outgassing Temperature 673K

Pressure torr	$Mol/m^2 \times 10^{-6}$
1.02	.120
2.22	.207
3.25	.324
7.23	.790
12.41	1.02
19.98	1.11
26.77	1.21
31.4	1.31
37.98	1.41
43.39	1.56

Run #5A

Sample: Min-U-Sil

Weight: 1.9206

Outgassing Temperature 673K

Pressure torr	$Mol/m^2 \times 10^{-6}$
0.4	.162
3.04	.565
9.86	1.02
15.92	1.28
21.82	1.66
25.72	1.66
29.35	1.75
34.56	1.95
38.15	2.1
42.56	2.19

Run #6B

Sample: Min-U-Sil Outgassed 2X

Weight: 2.0289

Outgassing Temperature 673K

Pressure torr	Mol/m^2 X 10^{-6}
0.64	.103
1.32	.227
3	.537
9.67	.767
17.51	.877
21.51	1.01
25.99	1.09
29.08	11.6
31.98	13.2
33.25	14.3
37.98	16.5

Run #7B

Sample: Min-U-Sil Outgassed 2X

Weight: 1.8447

Outgassing Temperature 673K

Pressure torr	Mol/m^2 x 10^{-6}
1.23	.167
6.03	.575
12.94	.669
18.41	1.02
24.72	1.10
28.09	13.2
34.08	15.2
36.56	16.7
39.4	17.5

Run #5B

Sample: Min-U-Sil Outgassed 2X

Weight: 1.9206

Outgassing Temperature 673K

Pressure torr	$Mol/m^2 \times 10^{-6}$
0.47	.166
1.8	.403
6.56	.791
12.41	1.06
21.09	1.18
25.99	1.26
29.98	1.45
34.88	1.58
38.25	1.78

APPENDIX XI

DATA FOR CHLORINE ADSORPTION ON EMPTY SAMPLE BULBS

Sample Bulb Outgassed at 373K

P	Moles of Chlorine Adsorbed ($\times 10^{+7}$)
1.32	3.80
2.70	0.63
6.47	6.70
14.82	4.0
24.25	12.0

At P = 14.82 torr, 4.0×10^{-7} moles of chlorine was adsorbed on the empty bulb. In run #3A at P = 14.82 torr, 3.6×10^{-6} moles/g or 7.8×10^{-6} moles of chlorine was adsorbed on Min-U-sil outgassed at 373K

$$\frac{4.0 \times 10^{-7}}{7.7 \times 10^{-6}} \times 100 = 5.1\%$$ of chlorine adsorbed on the glass walls

Sample Bulb Outgassed at 673K

P	Moles of chlorine Adsorbed ($\times 10^{+7}$)
1.02	0.30
2.10	0.13
4.32	6.50
13.19	6.90
20.94	4.40
27.72	7.00

At P = 1.02 torr, 0.30×10^{-7} moles of chlorine was adsorbed on the empty bulb. In run #6A at P = 1.32 torr, 2.14×10^{-6} moles/g or 4.34×10^{-6} moles of chlorine was adsorbed on Min-U-Sil outgassed at 673K

$$\frac{3.0 \times 10^{-8}}{4.3 \times 10^{-6}} \times 100 = .70\% \text{ of chlorine adsorbed on the glass walls.}$$